GROUND-WATER RECHARGE IN THE PLANT, SOIL AND ATMOSPHERE CONTINUUM

by

Yüksel K. Birsoy

Submitted in Partial Fulfillment
of the Requirements for the Degree of
Doctor of Philosophy

NEW MEXICO INSTITUTE OF MINING AND TECHNOLOGY

Socorro, New Mexico

December, 1977

BENİ BÜTÜN ÇALIŞMALARIMDA İNSAN ÜSTÜ
BİR FERAGATLA DESTEKLEYEN
ANNEM EMİNE VE BABAM İBRAHİM BİRSOY'A.

THIS STUDY IS DEDICATED TO
MY MOTHER EMİNE AND FATHER İBRAHİM BİRSOY

ACKNOWLEDGMENTS

I would like to express my sincere gratitude to my thesis advisor, Professor Lynn W. Gelhar, for his invaluable suggestions, guidance and moral support throughout this study. The author depended heavily on his encouragement and help during this research.

I would like to extend my appreciation to the members of my committee, Drs. Vijay P. Singh, Vernon LeFebre, and P. Huyakorn, for their continued interest.

My special thanks go to my friends, Mr. Göksel Övül and Lawyer Sahir Güven. The impact of their moral support, at the times when it was needed, is inexpressible.

Financial support of New Mexico Institute of Mining and Technology is sincerely appreciated.

I am indebted to the State Hydraulic Works, Groundwater Division, Ankara, Turkey, for granting me a study leave.

The author is indebted to Candace Merillat and his colleagues, Adel A. Bakr, and Richard L. Naff, for editing, Karen Patterson and Cookie Valencia for typing the manuscript, and Catherine Lucero for drafting the figures.

Above all, without the understanding, encouragement and love of my wife, Rezan, this dissertation would not have been possible.

ABSTRACT

The primary objective of this investigation is the study of the effects of various environmental factors on the ground-water recharge process. To this end, a sink function representing water uptake of plant roots is developed such that it varies with potential evapotranspiration and moisture conditions in the soil. This model is compared and contrasted with existing root extraction models in literature. The parameters of the sink function are estimated from the data of Denmead and Shaw (1962). By adding the sink function to the continuity equation, the equation describing the flow in a physically continuous saturated and unsaturated domain with the effect of plant transpiration is obtained. The equation for one-dimensional vertical flow is solved with the aid of the backward implicit finite difference scheme. The developed flow model is tested with the actual field data of Nimah (1972). The differences between the model prediction and the observations are discussed. In the final part of the report, the effects of various environmental factors on the recharge process are studied. Two major conclusions of this study are a) initial moisture conditions are the decisive factor in the generation of ground-water recharge, and b) diurnally varying potential evapotranspiration tends to increase ground-water recharge.

ABSTRACT

The primary objective of this investigation is the study of the effects of various environmental factors on the ground-water recharge process. To this end, a sink function representing water uptake of plant roots is developed such that it varies with potential evapotranspiration and moisture conditions in the soil. This model is compared and contrasted with existing root extraction models in literature. The parameters of the sink function are estimated from the data of Denmead and Shaw (1962). By adding the sink function to the continuity equation, the equation describing the flow in a physically continuous saturated and unsaturated domain with the effect of plant transpiration is obtained. The equation for one-dimensional vertical flow is solved with the aid of the backward implicit finite difference scheme. The developed flow model is tested with the actual field data of Nimah (1972). The differences between the model prediction and the observations are discussed. In the final part of the report, the effects of various environmental factors on the recharge process are studied. Two major conclusions of this study are a) initial moisture conditions are the decisive factor in the generation of ground-water recharge, and b) diurnally varying potential evapotranspiration tends to increase ground-water recharge.

TABLE OF CONTENTS

LIST OF FIGURES

LIST OF TABLES

LIST OF SYMBOLS

The following list covers the symbols which are widely used herein.

Symbol	Definition
A	volume of water extracted by plant roots per unit volume of soil per unit time
A_{max}	maximum value of A
B	applied water
C	soil water capacity
C_p	specific heat of air
C_r	recharge parameter
D	diffusivity
D_s	discharge rate from the basin
E_t	actual evapotranspiration rate
E^*_t	potential evapotranspiration rate
E_v	actual soil evaporation rate
E^*_v	potential soil evaporation rate
E^*_{td}	diurnally varying potential evapotranspiration rate
G	heat flux into the soil
H	total potential
I	first kind modified Bessel function
J	second kind modified Bessel function
J^*	hydraulic gradient
K	hydraulic conductivity
K_o	saturated hydraulic conductivity
K_m	melting constant
L	depth to water table

Symbol	Definition
L_r	total length of roots in unit volume of soil
L_a	leaf area index
L_{sa}	leaf surface area
L_e	latent heat of evaporation
L_t	light intensity
M	molecular weight of water
P	precipitation
$\overline{P}$	average precipitation
$\overline{P}_N$	effective rate of precipitation
Q_m	snow melt
R	recharge
R_n	net radiation
R_w	gas constant for water vapor
R_u	universal gas constant
S	saturation
S_n	normalized saturation
T_r	actual transpiration rate
T_r^*	potential transpiration rate
T_{so}	soil surface temperature in °Kelvin
T_ℓ	leaf temperature
T*	air temperature in °F
~~V~~	volume
V_r	volume of soil per unit length of roots
Z	normalized depth
a	root radius
a_r	root resistance

Symbol	Definition
b	soil parameter
d	rooting depth
e_z	actual vapor pressure
e_z^*	saturation vapor pressure
e_{so}	soil surface actual vapor pressure
f	relative humidity
f_{so}	soil surface relative humidity
g	acceleration of gravity
h	water potential
h_b	soil parameter
h_d	soil parameter
h_r	water potential at the root surface
h_{ro}	water potential at the root surface when $z = 0$
h_s	water potential in the soil
h_{so}	water potential at the soil surface
h_w	wilting point
ℓ	thickness of the soil column
n	number of the nodal points
$\vec{n}$	normal vector
p	pressure
q	specific discharge
$\vec{q}$	specific discharge vector
q_o	soil surface flux
q^*	rate of water uptake by plants roots
q_b	bottom flux
r	radial distance

Symbol	Definition
r_1	root radius
t	time
α	root water extraction parameter
$\beta_f(\theta)$	dimensionless sink function
γ_e	Euler's constant
γ	pyschrometric constant
ε	soil parameter
ζ	recharge parameter
θ	moisture content
θ_r	residual saturation
ρ	density
ρ_a	air density
σ	area element
ϕ	porosity
ω	angular velocity
Ω	phase angle

CHAPTER 1: INTRODUCTION

Human technological activities and developments are largely dependent on water resources. Ground water is by far the most abundant water resource and, fortunately, it is a fastly renewable natural resource as compared with most others. In areas where surface waters are insufficient, it is the only source of water available to satisfy continuously growing needs. For optimal utilization of that source, it is important to accurately estimate quantities available from ground-water reservoirs. Since precipitation is the only source of recharge, the relationship between precipitation and recharge is also vital, particularly in arid and semi-arid environments. For an in-depth knowledge of this recharge-precipitation relation, the phase changes of water along its path from atmosphere to water table and vice versa need to be investigated.

Ground-water recharge has been studied extensively by several researchers (Jacob, 1943; Werner, 1957; Hantush, 1967; Maasland, 1959 and Dagan, 1967), most of whom treated the water in the saturated zone as a separable (discontinuous) phase in the hydrologic cycle. Freeze (1967 and 1971) emphasized the importance of an unsaturated soil column lying above the saturated zone and studied recharge by taking into account the fact that the water in the saturated and unsaturated zones is a physical continuum.

Relatively little research has been concerned with how vegetative cover, one of the major pathways for water transfer from soil to atmosphere, affects ground-water recharge, though quite a few models (Molz and Remson, 1970; Nimah, 1972; Warrick, 1974; Feddes et al., 1975 and Neuman et al. 1974) describing plant root extraction from the soil are present in the literature.

This study is an investigation of how the recharge process is affected by various types of soils, plant communities, and atmospheric conditions, utilizing the premise that water in the saturated and unsaturated zones is a continuum.

CHAPTER 2: LITERATURE REVIEW

2.1 Basic Concepts and Definitions in Unsaturated Flow Through Porous Media

The mass of liquid flowing through the interconnected pore spaces of a porous medium may consist of more than a single fluid phase (i.e., oil, water, and gas). If only two fluid phases are present and if these two fluid phases are chemically inactive with respect both to each other and to the soil, the flow is called two-phase flow. In the case of air and water flow through a porous medium, the effect of the air flow may be ignored for a viable simplification of the problem (Corey, 1969). This flow model, which is a special case of two-phase flow where pressure in the air is assumed to be constant, is known as either partially saturated or unsaturated flow. Water saturation, S, refers to the amount of water in a porous medium defined as

$$S = \frac{\text{Volume of water within a REV}}{\text{Volume of pore space within a REV}} , \tag{2.1}$$

where REV is a representative elementary volume of the soil, as described by Bear (1972).

Another widely used concept to express the amount of water in a porous material is its moisture content, θ, which is defined as

$$\theta = \frac{\text{Volume of water within a REV}}{\text{Bulk volume of REV}} . \tag{2.2}$$

Thus, the relation between moisture content and water saturation is

$$\theta = \phi S \tag{2.3}$$

where ϕ is the porosity of the soil.

2.2 Basic Principles and Equations

2.2.1 Continuity Equation

In this section, the general conservation of mass equation (or continuity equation) is derived by considering an arbitrary elementary volume in a porous medium. Consider a volume $\forall$, defined as the interior of surface σ, which is large enough to ignore microscopic inhomogeneities of moisture content or solid structure that may take place over very small distances, and it is fixed in time and space, but doesn't necessarily have a certain geometric shape (Fig. 2.1). The total mass of the fluid in the volume is

$$\int_{\forall} \rho\phi S d\forall ,$$

where ρ is the density of the fluid and $d\forall$ is a volume element, and the integration is taken over the volume. The mass of the liquid flowing outward from the volume per unit time is

$$\oint \rho \vec{q} \cdot \vec{n} d\sigma ,$$

where $\vec{q}$ is the specific discharge vector and $\vec{n}$ is the outward normal vector to the surface area element $d\sigma$ of the volume under consideration. In the case of a sink within the volume, the total extracted fluid per unit time is given as $\int_{\forall} \rho A d\forall$, where A is the volume of the fluid extracted from the soil per unit volume of the soil per unit time. Since volume is constant in time, the decrease of the mass of the liquid per unit time can be written as

$$-\frac{\partial}{\partial t} \int_{\forall} \rho\phi S d\forall = -\int_{\forall} \frac{\partial}{\partial t} (\rho\phi S) d\forall . \qquad (2.4)$$

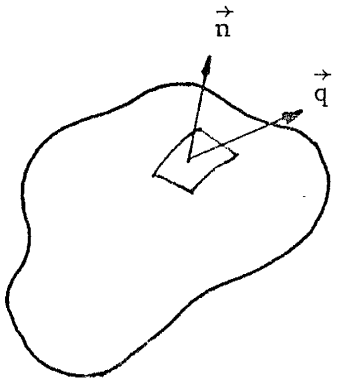

Figure 2.1 The Elementary Control Volume

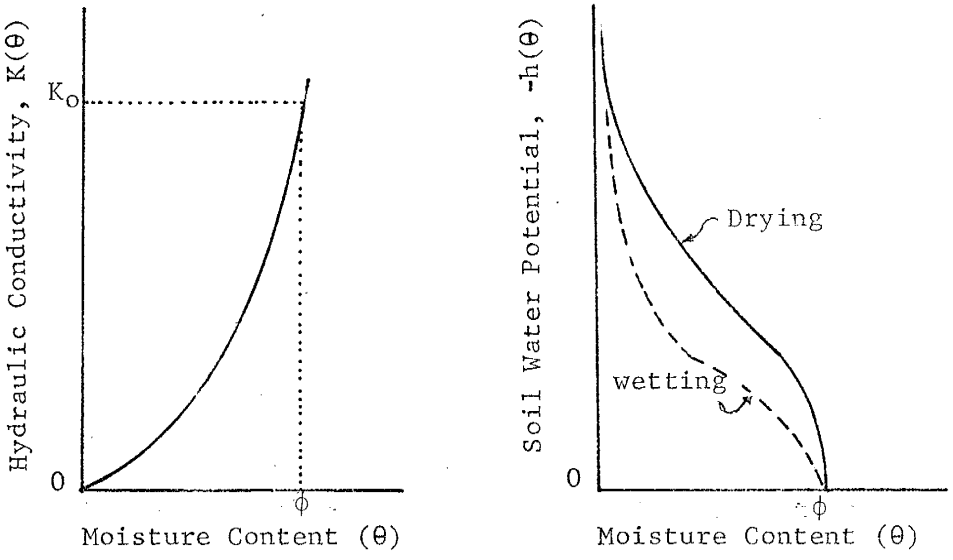

Figure 2.2 Typical water potential and unsaturated hydraulic conductivity curves, as functions of moisture content θ. K_o is the saturated hydraulic conductivity and ϕ is the porosity.

Also, since the rate of decrease of the mass of the liquid should equate the algebraic sum of the mass of the fluid flowing out from the volume and that extracted by the sinks, the conservation of mass equation takes the form

$$-\int_{\forall} \frac{\partial}{\partial t}(\rho\phi S)d\forall = \oint \rho\vec{q}\cdot\vec{n}d\sigma + \int_{\forall} \rho A d\forall. \tag{2.5}$$

The surface integral, which is the first term on the right-hand side of Eq. (2.5), can be transformed to a volume integral by Green's formula as

$$\oint \rho\vec{q}\cdot\vec{n}d\sigma = \int_{\forall} \nabla\cdot(\rho\vec{q})d\forall$$

and thus

$$\int_{\forall}\left[\frac{\partial}{\partial t}(\rho\phi S) + \nabla\cdot(\rho\vec{q}) + \rho A\right]d\forall = 0.$$

Because the above equation holds for any volume, one can deduce

$$\frac{\partial}{\partial t}(\rho\phi S) + \nabla\cdot(\rho\vec{q}) + \rho A = 0.$$

If the fluid is assumed to be incompressible (ρ is constant) then substitution of Eq. (2.3) into the above equation yields

$$\frac{\partial\theta}{\partial t} + \nabla\cdot\vec{q} + A = 0. \tag{2.6}$$

The three components (q_x, q_y, q_z in the cartesian coordinate system) of the specific discharge vector $\vec{q}$, the moisture content θ, and sink term A represent five unknowns in Eq. (2.6). Thus, four more equations are

necessary to obtain the basic equation governing fluid motion through a saturated and/or unsaturated medium, when sink effects are included within the medium. Darcy's equation, stated by Henry Darcy in 1856, is the tool that enables us to obtain three more equations to replace the specific discharge vector $\vec{q}$ in Eq. (2.6). In the following section the generalized Darcy equation for a fully saturated medium, its application to unsaturated media, and its limitations will be discussed. A discussion of the sink term A will be given in later sections.

2.2.2 Generalized Darcy's Law

Darcy's law states that the amount of flow through a fully saturated medium of a fluid chemically inactive with the porous material is directly proportional to the total potential gradient at the point under consideration. The proportionality constant $\underline{K}$, which is a symmetric second-rank tensor in an anisotropic medium, is called hydraulic conductivity. The generalized Darcy's equation as stated for a fully saturated medium is

$$\vec{q} = - \underline{K}\nabla(h - z), \tag{2.7}$$

where

h is the pressure head (or soil-water potential in the unsaturated zone) and given as $h = p/g$,

p is pressure,

g is the acceleration of gravity, and

z is the elevation head (+ downward).

Swartzendruber (1962a, 1962b, and 1963) brought attention to non-linear flow behavior at low hydraulic gradients and proposed the flow equation:

$$q = \eta[J^* - \eta_1 (1 - \exp (- \eta_2 J^*))] \tag{2.8}$$

where

q is the specific discharge,

J^* is hydraulic gradient, and

η, η_1 and η_2 are constants.

Notice that if η_1 or η_2 or both are equal to zero, Eq. (2.8) reduces to $q = \eta J^*$, which is Darcy's equation in a given principal direction. Although supporting experimental evidence and theoretical arguments (see Bolt and Groenevelt, 1969) are given for Swartzendruber's proposal, the validity of the linear form of Darcy's equation for a saturated medium in the region below a Reynolds number between 1 and 10 is generally accepted, and Eq. (2.7) is most widely used by ground-water hydrologists.

It is reported (Corey and Rathjens, 1956) that anisotropic conductivity exists in unsaturated media. However, the little work (Corey and Rathjens, 1956 and Cisler, 1972) that has been published to date does not clarify the nature of the phenomenon. Thus, it has become customary to assume an isotropic porous medium, as in this study, if unsaturated flow is involved. With the isotropy assumption, Darcy's equation becomes

$$\vec{q} = - K\nabla(h - z) \tag{2.9}$$

where K is hydraulic conductivity.

After the above simplification of Darcy's equation with an isotropic medium assumption, the first modification of Eq. (2.9) for unsaturated flow may be made by recognizing that air occupying pore spaces reduces the effective area and increases the tortuosity of flow for the remaining fluid (water). Therefore, hydraulic conductivity K varies with moisture

content θ; $K(\theta)$ is called unsaturated hydraulic conductivity. A second modification of Darcy's equation involves the soil water potential h which may also be expressed as a function of the water content of the soil (the gravitational potential z remains unchanged). Thus, Darcy's equation for saturated and unsaturated flow takes the form

$$\vec{q} = - K(\theta) [h(\theta) - z]. \tag{2.10}$$

A detailed discussion of the Darcy's equation in the form of Eq. (2.10) can be found in Bear (1972), Kirkham and Powers (1972), and Swartzendruber (1969).

Swartzendruber (1963) indicated that Eq. (2.10) may not be valid at low-moisture contents ($\theta \leq 0.30$), and further experimental research is needed to specify its range of validity in unsaturated media. Nevertheless, for practical purposes, Eq. (2.10) has been widely employed in unsaturated flow problems.

Typical water potential and unsaturated hydraulic conductivity curves, as a function of moisture content, are shown in Fig. (2.2). As seen in the figure, water potential $h(\theta)$ shows a hysteresis effect depending on drying or wetting of the soil, while hydraulic conductivity does not. There is good reason to believe that the hysteresis effect of hydraulic conductivity is relatively small, and is generally considered negligible for most practical applications (see data of Nielsen and Biggar, 1961; and Elric and Bowman, 1964).

Equation (2.10) together with the curves in Fig. (2.2) reduces the number of unknowns of Eq. (2.6) from five to two. Another equation involving the sink term A must be found without introducing any other unknowns, in order to obtain a complete dynamic equation of flow. The

sink term A may physically represent the extraction of water from the soil by the plant roots. Since plants have low resistance to water flow and little storage capacity (Baver et al. 1972), storage change of plant body may be assumed negligible. In this case, the value of the integral $\int_o^d Adz$, where d is the rooting depth, will give the actual rate of transpiration. Meteorological factors (wind, net radiation, air temperature, relative humidity, etc.) determine the demand for transpiration. The plant supplies this transpiration demand by using the available moisture in the soil. Therefore, the sink term A and the value of the integral $\int_o^d Adz$ are strictly governed by plant, soil, and atmosphere relations. In the next section the current practice with soil, plant, and atmosphere interrelations is outlined.

2.3 Relationships Between Plant, Soil, and Atmosphere

The existing models depicting plant, soil, and atmosphere relations can be classified as follows:

1. Canopy model
2. Root models
   - 2.1 Single root models
   - 2.2 Integrated root models

2.3.1 Canopy Model

The canopy model (e.g., Lemon et al, 1973; Stewart and Lemon, 1969; Shawcroft, 1971; and Lemon et al., 1971) is schematically represented in Fig. (2.3) and is known as SPAM (Soil, Plant-Atmosphere Model) in the literature. In this model, the plant body is considered as a horizontal

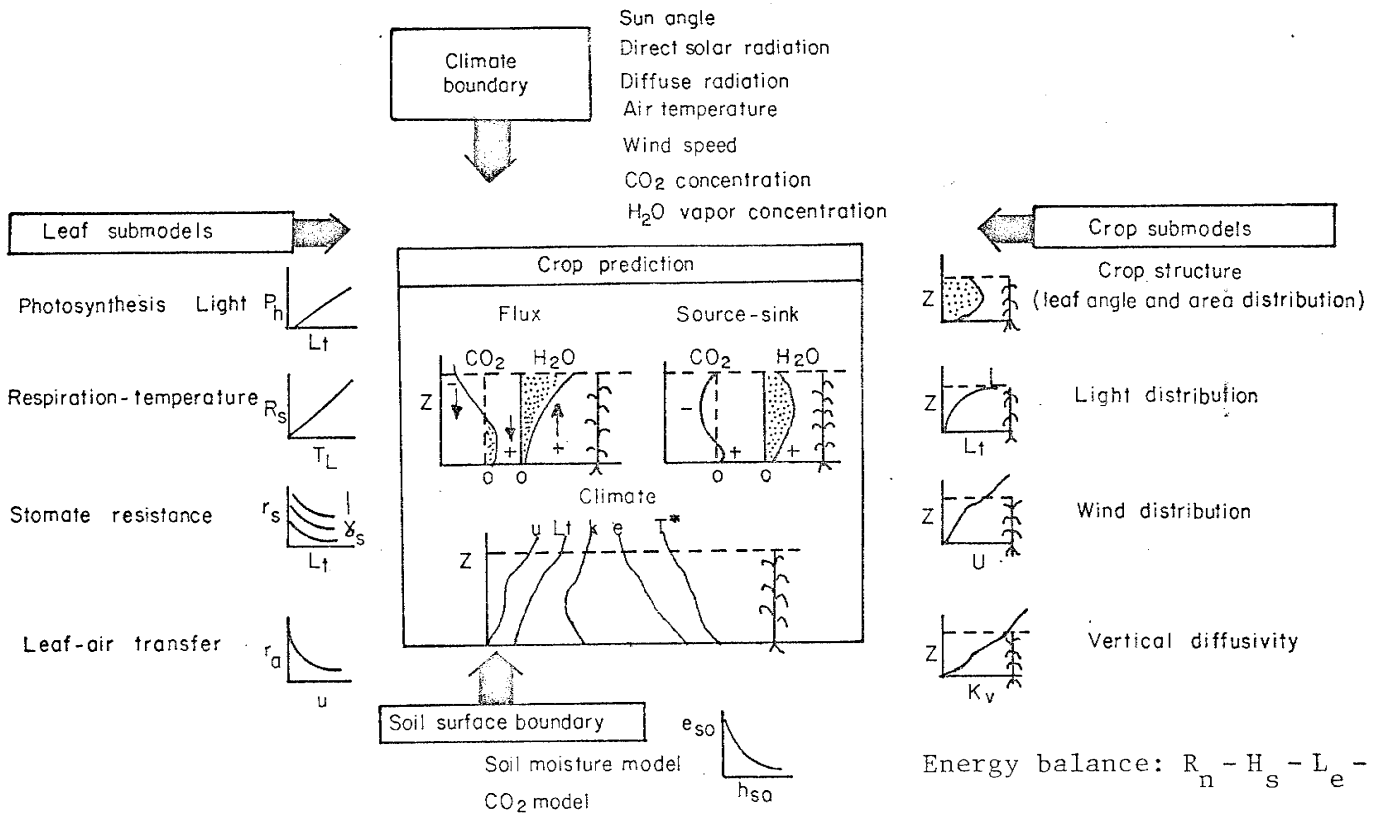

Figure 2.3 Schematic summary of a mathematicsl soil-plant-atmosphere model (SPAM) giving required inputs, submodels, and representative daytime predictions of climate and community activity (that is, water vapor and carbon dioxide exchange). Abbreviations: height (z), wind (u), light (Lt), concentration of carbon dioxide (χ), water vapor (e), air temperature (T*), surface vapor pressure (e_{so}), surface soil moisture or water potential (h_{so}), photosynthesis (P_h), respiration (R_S), leaf temperature (T_l), stomate resistance (r_s), minimum stomate resistance at high light intensities (γ_s), gas diffusion resistance (r_a), leaf surface area (L_{sa}), vertical diffusivity (K_v), net radiation (R_n), sensible heat (H_s), latent heat (L_e), photochemical energy equivalent (P_e), and soil heat storage (S_h) (after Lemon et al., 1971).

slab. The upper boundary of this slab is the atmosphere, and the bottom boundary is the soil. At the top, the external climate is defined by solar radiation, wind speed, temperature, CO_2 concentration, and humidity. These climatic variables, measured 2-3 meters above the crop, provide upper boundary values needed for mathematical calculations. The bottom boundary (the soil surface) is defined in terms of heat flux into the soil, CO_2 flux from the soil, and soil moisture tension at the soil surface. Heat flux is measured directly using soil heat flux plates near the surface. Soil-surface moisture tension is estimated from soil-moisture tension measurements made at various depths in the soil. This soil-surface moisture tension value is used to calculate the actual vapor pressure at the soil surface by the thermodynamic relation,

$$e_{so} = e(T_{so}) \exp\left(\frac{S_M}{R_u T_{so}}\right), \qquad (2.11)$$

where

e_{so} is the actual vapor pressure at the soil surface,

$e(T_{so})$ is the saturation vapor pressure at the temperature T_{so},

R_u is the universal gas constant, and

S_M is the soil moisture tension at the soil surface.

The CO_2 flux from the soil surface was estimated from the measurements of Moss (1959; reported in Stewart and Lemon, 1969). These upper and lower inputs of SPAM are shown at the top and bottom of Fig. (2.3), respectively.

To construct the model, the diffusion of external climate into the canopy is needed. This is done by the aid of a) a complete description of plant structure in height (-z), in terms of leaf size, leaf angle,

and azimuth; and b) the crop submodels to simulate light, wind, and vertical-turbulence diffusivity distribution in the plant community. The description of the plant structure and the crop submodels are shown on the right of Fig. (2.3).

Once the diffusion of external climate into the crop system is known, the response of each individual leaf to its immediate climate can be simulated with the leaf submodels shown on the left of Fig. (2.3). These leaf submodels are to simulate a) photosynthesis response to incident light, b) respiration response to temperature, c) stomato response to light, and d) gas-diffusion resistance response to wind speed.

Since leaf responses and properties of the air stream surroundings each of the individual leaves are interdependent, the equations describing plant responses and properties of air flow are solved simultaneously with successive approximations. By integrating the response of each individual leaf over the crop cover, the energy balance equation is also checked.

The model predictions are shown in the center of Fig. (2.3). A comparison between model forecasting and the actual data is also shown in Fig. (2.4).

2.3.2 Root Models

2.3.2.1 Single Root Models

Gardner (1960) and Cowan (1965)[1] considered a single root as an indefinitely long cylinder in an infinite two-dimensional medium and assumed that flow takes place in a radial direction only. The root,

[1] Because of the similarities between the root extraction model of Cowan (1965) and single root model of Gardner (1960), the model of Cowan (1965) is classified as a single root model.

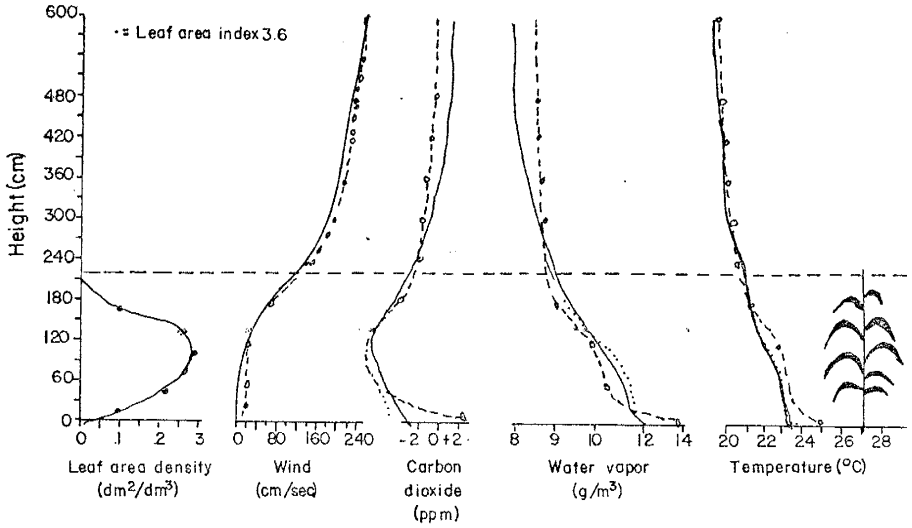

Figure 2.4 Measured (circles and dashed lines) and predicted (solid and dotted lines) profiles of climate factors in and above a cornfield, with the field's vertical leaf area density shown. Profiles are half-hour mean values. (18 August 1968; 11:45 a.m. to 12:15 p.m., Eastern Standard Time.) (after Lemon et al., 1971).

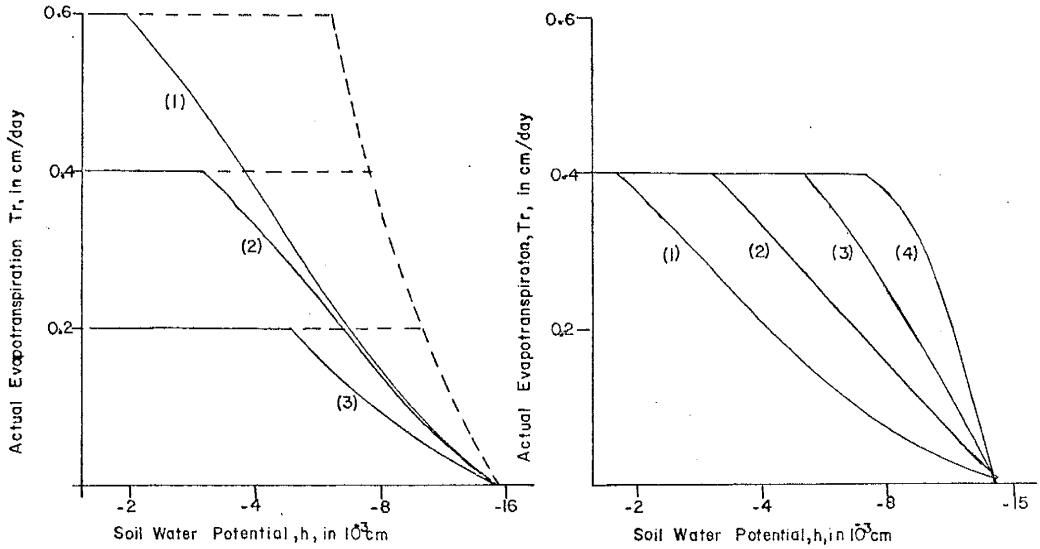

Figure 2.5 Relation between daily transpiration, T_r, and soil water potential, h_s. The full curves are for a periodic diurnal fluctuation of the potential transpiration rate E_t^* while the broken curves relate to steady values of T_r. (1) $T_r^* = 0.75$ cm day^{-1}; (2) $T_r^* = 0.50$ cm day^{-1}; (3) $T_r^* = 0.25$ cm day^{-1}.

Figure 2.6 Relation between daily transpiration, T_r, and soil water potential, h_s, for crops with different densities of rooting. (1) $V_r = 8$ cm^2, $V_r = 4$ cm^2; (3) $V_r = 2$ cm^2; (4) very dense rooting. (after Cowan, 1965).

mathematically speaking, represents a line sink. Thus, plant root extraction in these models is handled as a boundary condition, and the sink term A in Eq. (2.6) need not be considered. The flow equation in cylindrical coordinates is obtained by substituting Eq. (2.10) into Eq. (2.6).

$$\frac{\partial \theta}{\partial t} = \frac{1}{r} \frac{\partial}{\partial r} \left(rK \frac{\partial h}{\partial r} \right) \qquad (2.12a)$$

or

$$\frac{\partial \theta}{\partial t} = \frac{1}{r} \frac{\partial}{\partial r} \left(rD \frac{\partial \theta}{\partial r} \right) \qquad (2.12b)$$

where

r is the radial distance from the root axis,

D is the soil water diffusivity which is defined as

$D = K \frac{dh}{d\theta}$.

By assuming the soil water diffusivity D is constant and applying the following initial and boundary conditions

$$\theta = \theta_o \qquad h = h_o \qquad r \geq a \qquad t = 0$$

$$q^* = 2\pi a K \frac{\partial h}{\partial r} = 2\pi a D \frac{\partial \theta}{\partial r} \qquad r = a \qquad t > 0$$

Gardner (1960) obtained the solution of Eq. (2.12), for large t, as

$$h - h_o = \frac{q^*}{2\pi K} \ln \left(\frac{4Dt}{a^2} - \gamma e \right) \qquad (2.13)$$

where

a is the root radius,

q* is the rate of water uptake by the root or flux at the root surface, expressed as the volume of water per unit length of root per unit time, and

γe is Euler's constant (0.57722).

For the solution of Eq. (2.12), the water uptake q* is also assumed to be constant.

Cowan (1965) applied the Kirchhoff transformation

$$\Theta = \int Kdh \tag{2.14}$$

to Eq. (2.12) and obtained

$$\frac{\partial \Theta}{\partial t} = \frac{D}{r} \frac{\partial}{\partial r} \left(r \frac{\partial \Theta}{\partial r} \right) . \tag{2.15}$$

By treating the extraction of moisture as though it were from a cylinder of soil $r_2 > r > r_1$ with the conditions

$$\frac{\partial \Theta}{\partial r} = Q \frac{r_2^2 - r_1^2}{2r_1} \quad \text{at} \quad r = r_1$$

$$\frac{\partial \Theta}{\partial r} = 0 \quad \text{at} \quad r = r_2$$

and also taking into account the diurnal fluctuations of Q for constant D and neglecting transient terms dependent on initial conditions, the solution of Eq. (2.15) is given by the real part of

$$\Theta_r = \Theta_s - \overline{Q} \text{ Real } [\alpha_c + \beta \exp(i\omega t - i\Omega)] \tag{2.16}$$

where

Q is the rate of extraction (cm^3 dy^{-1} per cm^3 of soil),

$\overline{Q}$ is the average value of Q during a day,

ω is angular velocity (radians per day),

Ω is phase angle,

Θ_r is volume average of Θ,

Θ_s is the value of Θ at the root surface,

$$\alpha_c = \frac{r_2^4}{2(r_2^2 - r_1^2)} \ln \frac{r_2}{r_1} - \frac{3r_2^2 - r_1^2}{8},$$

$$\beta \exp(-i\Omega) = \frac{D(R_2^2 - R_1^2)}{2 R_1 i^{1/2}} \left[\frac{Jo(R_1 i^{1/2}) I_1(R_2 i^{1/2}) + I_o(R_i^{1/2}) J_1(R_2 i^{1/2})}{J_1(R_1 i^{1/2}) I_1(R_2 i^{1/2}) - J_1(R_1^{1/2}) J_1(R_2 i^{1/2})} \right] + \frac{iD}{w}$$

$$R_1 = (\omega/D)^{1/2} r_1,$$

$$R_2 = (\omega/D)^{1/2} r_2,$$

I and J are modified Bessel functions of the first and second kind, respectively,

r_1 = root radius,

$r_2 = (1/\pi L_r)^{1/2}$, and

L_r is the total length of roots in the unit volume of the soil.

Cowan (1965) indicated in his study that $\beta \to \alpha_c$ and $\Omega \to o$ for large values of D/r_1^2 and small values of r_2^2/r_1^2. For fairly dry soils with sparse rooting, β differs from α_c by less than 10% when the time lag is less than 1.25 hours. Therefore, he approximated Eq. (2.16) by

$$\Theta_r = \Theta_s - \alpha_c Q. \tag{2.17}$$

Cowan (1965) also obtained the relation, shown in Fig. (2.5) and Fig. (2.6), between the potential evapotranspiration rate defined by Penman (1948) and the actual transpiration rate. This was done by making use of Eq. (2.17) and by introducing plant resistance to flow and water availability in the soil.

2.3.2.2 Integrated Root Models

In this approach, root extraction (volume of water per unit volume of soil per unit time) at a single point in the soil is considered and is averaged by integrating over a volume of the soil. This averaged value of the root extraction is represented by the sink term A in Eq. (2.6). This integrated approach was the basis of the study of transpiring plants for several authors (Molz and Remson, 1970; Nimah and Hanks, 1973a-b; and Feddes et al. 1974).

A steady-state solution of Eq. (2.12) was given by Gardner (1960) as

$$h - h_o = \frac{q^*}{4\pi K} \ln \frac{b^2}{a^2} \tag{2.18a}$$

or

$$q^* = \frac{K}{\ln(b^2/a^2)/4\pi} \quad (h - h_o) \tag{2.18b}$$

where

b is the outer radius of the cylinder,

h is the water potential at b, and

h_o is the water potential at a.

Eq. (2.18b) suggests that root-water extraction by plant roots may be expressed as

$$A = -\frac{K(h_r - h_s)}{g(z)} \tag{2.19}$$

where

h_r is the water potential at the root surface,

h_s is the water potential in the soil, and

$g(z)$ is an empirical quantity.

Equation (2.19) simply states that the flow into a root system is directly proportional to the potential difference between the root surface

and the soil. The same proportionality was also deduced by Honert (1948) with an analogy to electrical systems. Similar equations and a detailed discussion of the flow of water through the plant (roots, xylem, and leaves) from soil to atmosphere can be found in Hendricks and Hansen (1962).

Though Eq. (2.19) seems reasonable to work with, the value of the variable g(z) and its physical meaning pose many questions. Feddes et al. (1974) pointed out the possibility that 1/g(z) may be directly proportional to the specific area of the soil-root interface (total surface area of roots per unit bulk volume of soil) and inversely proportional to the impedance (thickness divided by the hydraulic conductivity) of the soil-root interface.

Root surface potential h_r, unlike g(z), is a physically meaningful and well defined variable. It is, however, very hard (if not impossible) to measure. In order to overcome this difficulty, Nimah (1972) defined root potential h_r as

$$h_r = h_{ro} + a_r z \tag{2.20}$$

where

h_{ro} is root potential when z = 0,

z is the vertical distance from the soil surface, and

a_r is root resistance (which was assumed to be 1.05).

Because the value of the integral $\int_o^d Adz$ should equate to the plant transpiration rate T_r, the value of h_{ro} can be calculated in terms of plant transpiration and soil water potential from the equation

$$h_{ro} = -\left[T_r + \int_o^d K(a_r z - h_s)\, dz/g(z)\right] \Big/ \int_o^d Kdz/g(z). \tag{2.21}$$

Note that if h_r, calculated with the aid of Eq. (2.20) and Eq. (2.21), is greater than h_s at any point in the root zone, then A becomes a source term at this point instead of a sink. Therefore, an iterative solution of h_{ro}, created by setting A = 0 at points where $h_r > h_s$, may be necessary to maintain A as a sink term. Also note that in order to calculate h_{ro} from Eq. (2.21), the actual transpiration rate T_r should be known beforehand. Nimah (1972) used lysimetric data to utilize the sink term defined by Eq. (2.19) and Eq. (2.20). The ratio $1/g(z)$ was given in his study as

$$\frac{1}{g(z)} = \frac{RDF(z)}{\Delta x \cdot \Delta z}$$

where

Δz and Δx are space increments, and

RDF(z) is the portion of total active roots in the depth increment z.

Feddes et al. (1974) and Neuman et al. (1974) assumed the root surface potential h_r, in Nimah's (1972) model, to be constant throughout the root zone. In other words, root resistance a_r in Eq. (2.20), was assumed to be equal to zero. They also handled the empirical quantity $1/g(z)$ in a different way than Nimah (1972). A regression analysis was performed on relative root weight distribution to determine the regression coefficient of the equation

$$\frac{1}{g(z)} = \frac{e^{-\lambda_r z}}{g(0)} \quad . \tag{2.22}$$

The results of the regression analyses of Feddes et al. (1974) are summarized in Table (2.1). A detailed discussion of the subject can be found in their paper. The regression coefficients, tabulated in Table (2.1), were used to express g(z) in Eq. (2.19).

TABLE 2.1 Results of Linear Regression Analysis of the Equation $\ell n \frac{1}{g(z)} = \ell n \frac{1}{g(0)} - \lambda_r z$ for Red Cabbage for the Various Water Balance Periods Involved (after Feddes et al., 1974).

Line	Period	Number of 1/g(z) Data	Slope λr	Intercept ℓn 1/g(0)	1/g(0)	Correlation Coefficient	Standard Deviation From Regression
1	June 21 to June 27	5	0.1379	-2.5392	0.0789	0.999	0.039
2	June 27 to July 4	5	0.1267	-2.4903	0.0829	0.998	0.075
3	July 4 to July 11	6	0.1363	-2.1268	0.1192	0.992	0.056
4	July 11 to July 18	8	0.1313	-1.4139	0.2432	0.992	0.222
5	July 18 to July 25	11	0.0992	-1.0936	0.3350	0.986	0.297
6	July 25 to Aug. 2	12	0.0869	-0.8851	0.4170	0.955	0.511
7.	Aug. 2 to Aug. 9	16	0.0696	-1.1162	0.3275	0.956	0.524

Both Feddes et al. (1974) and Neuman et al. (1974) maximized plant transpiration rate T_r subject to the constraints

$$|T_r| \geq |T_{rmax}| \quad \text{and} \quad h_r \geq h_w$$

where

T_{rmax} is maximum possible transpiration rate, and

h_w is the wilting point.

The maximum possible transpiration rate is calculated with the aid of the maximum possible evapotranspiration rate, E_{tmax}, given by Feddes (1971, reported in Feddes et al. 1974)

$$E_{tmax} = \frac{\Delta(R_n - G)/L_e + \rho_a C_p (e_z^* - e_z)/r_a}{\Delta + \gamma} \tag{2.23}$$

where

R_n is the net radiation above the canopy,

G is the heat flux into the soil,

L_e is the latent heat of vaporization of water,

ρ_a is the density of moist air,

C_p is the specific heat of air at constant pressure,

Δ is the slope of saturation vapor pressure curve,

γ is the pyschometric constant, and

e_z, e_z^* are the actual and saturation vapor pressure in the air at height $-z$ and temperature T_z, respectively.

The maximum possible soil evaporation rate, E_{vmax}, is given by Ritchie (1972)

$$E_{vmax} = \frac{\Delta}{(\Delta + \gamma)L_e} R_n \, e^{-.39L_a} \tag{2.24}$$

where

L_a is the leaf-area index defined as leaf surface area per unit surface area of soil surface.

Then the maximum possible transpiration rate is calculated from

$$T_{rmax} = E_{tmax} - E_{vmax}. \tag{2.25}$$

Feddes et al. (1974) and Neuman et al. (1974) differ from each other in terms of actual soil evaporation. The former maximized soil evaporation subject to the constraints

$$|E_v| \leq |E_{vmax}| \quad \text{and} \quad h_r \geq h_d$$

where the subscript d refers to dry soil moisture conditions, while the latter used the thermodynamic relation (another form of Eq. (2.11))

$$h_{so} = \frac{R_w T_{so}}{Mg} \ln f_{so} \tag{2.26}$$

where

h_{so} is soil water potential at the soil surface,

R_w is the universal gas constant,

M is the molecular weight of water,

T_{so} is soil surface temperature (in °K), and

f_{so} is relative humidity of the soil surface

to predict soil-surface water potentials as a function of time. The predicted soil-surface potentials were used as a boundary condition in the numerical solutions. However, soil-surface temperature and soil-surface relative humidity in the above equation were approximated by the air temperature and air relative humidity, respectively.

The integrated root-extraction models outlined so far are applications of Eq. (2.19) with slight modifications. Feddes et al. (1975) derived a sink function quite different from Eq. (2.19) by making use of the anaerobiosis and wilting-point concepts. The anaerobiosis point may be defined as the moisture content above which, due to lack of free oxygen in the soil, oxygen demand of the plants is not met. Fully saturated conditions are an example of anaerobic conditions. The wilting point is defined, in the same sense, as the soil moisture content below which plants cannot extract water from soil. In other words outside the range between the anaerobiosis point and the wilting point, plant life is endangered, and plant transpiration ceases. Feddes et al. (1975) noted that there exists a moisture content, between the anaerobisis point and the wilting point, below which plant growth is limited and the plant transpiration rate decreases. With this information, Feddes et al. (1975) made the following assumptions:

Plant root extraction:

a) is zero above the moisture content producing anaerobiosis and below the wilting point,

b) is constant in time and takes place at a maximum rate for moisture contents between the anaerobiosis limit and the moisture content below which plant growth is limited, and

c) varies linearly with moisture content between the wilting point and the lower end of the constant rate of root extraction.

The sink term in the model of Feddes et al. (1975) for a clay soil is shown in Fig. (2.7). These investigators also introduced a dimensionless sink function as

$$\beta_f(\theta) = A(\theta)/A_{max}$$

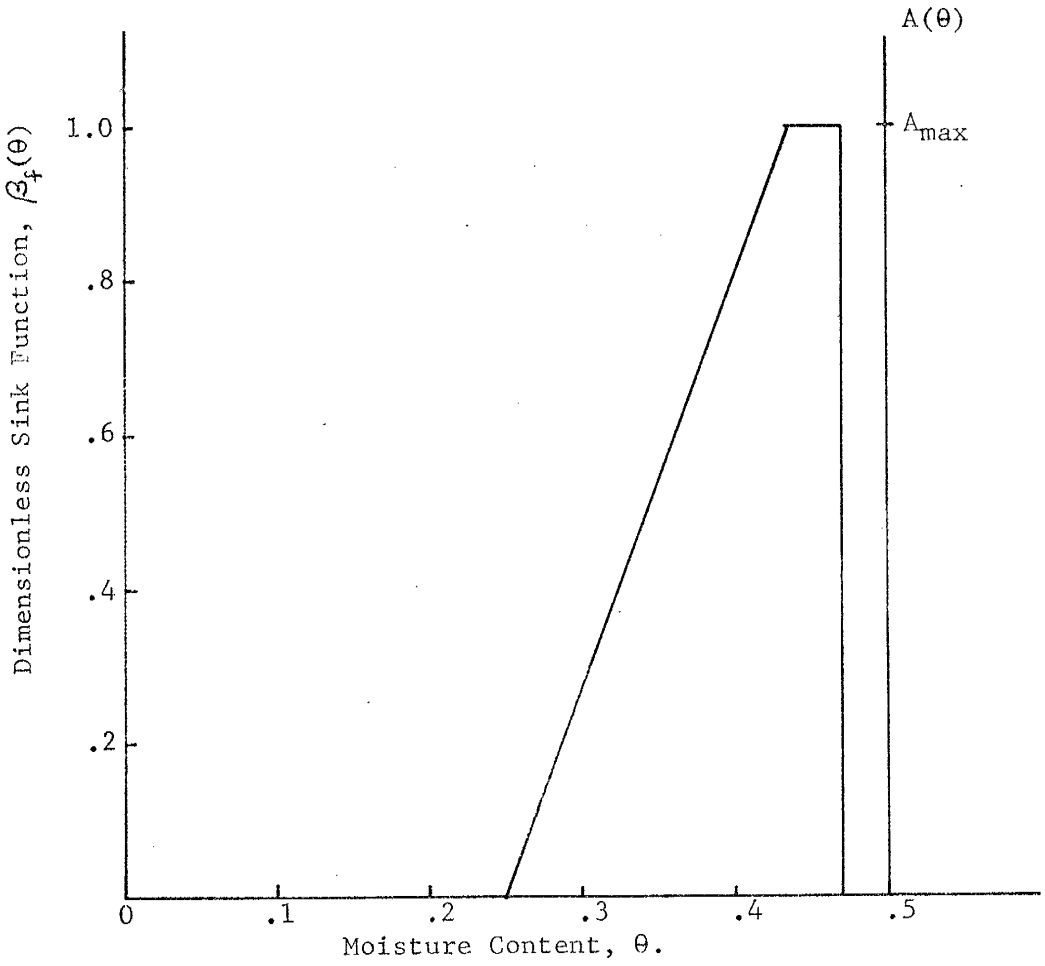

Figure 2.7: Relation of the sink function, $A(\theta)$, and the dimensionless sink function, $\beta_f(\theta)$, both as a function of moisture content (after Feddes et al., 1975)

where

A_{max} is maximum value of $A(\theta)$ and is given as

$$A_{max} = 2.\ T_r/d.$$

Then the expression for $A(\theta)$ becomes

$$A(\theta) = 2\beta_f(\theta)\ T_r/d. \tag{2.27}$$

Equation (2.27) is used as a sink term by Feddes et al. (1975). Maximum possible evapotranspiration, transpiration, and soil evaporation defined by the equations Eq. (2.23), Eq. (2.25), and Eq. (2.24), respectively, were also incorporated. The value of $\beta_f(\theta)$ for their clay soil is also shown in Fig. (2.7). Soil surface evaporation was calculated from Eq. (2.26) following Neuman et al. (1974).

Molz and Remson (1970) devised another type of sink function by making use of an empirical rule given by Danielson (1967), stating that 40, 30, 20, and 10 percent of the total transpiration requirements come from successively deeper layers of the root zone. A sink function which meets the above percentage requirements is

$$A(z) = -\frac{1.6(T_r^2)}{d^2}z + \frac{1.8\ T_r}{d}\ . \tag{2.28}$$

The empirical rule utilized in Eq. (2.28) was discussed by Van Bavel et al. (1968), who pointed out that in dry conditions most transpiration requirements come from deeper roots in moister soil. Therefore, because of functional and percentage behavior, Molz and Remson (1970) regarded Eq. (2.28) as a reasonable equation for steady-state and moist soil conditions only.

Molz and Remson (1970) also proposed for transient flow problems the sink term

$$A(z,\theta) = T_r^* \frac{R(z)\ D(\theta)}{\int_o^d R(z)\ D(\theta)dz} \tag{2.29a}$$

or

$$A(z,\theta) = E.R(z)\ D(\theta) \tag{2.29b}$$

where

$R(z)$ is effective root density, and

$$E = T_r^* \Big/ \int_o^d R(z)\ D(\theta)dz.$$

For steady-state flow E is constant. Thus, E.R(z) in Eq. (2.29b) can be calculated for steady-state flow with the aid of Eq. (2.28). Gardner and Ehling's (1962) data were used to calculate steady-state E.R(z) values; these values were then employed in transient flow problems. These steady-state E.R(z) values are tabulated in Table (2.2).

Warrick (1974) gave an analytical solution to Eq. (2.6) for one-dimensional vertical steady-state flow by assuming that the sink term A is a function of z only. This assumption is considered reasonable for steady-state flow problems (Molz and Remson, 1970). Substitution of Eq. (2.10) in Eq. (2.6) yields (for one-dimensional vertical steady-state flow):

$$\frac{d}{dz}\left(K \frac{dh}{dz}\right) - \frac{dK}{dz} = A(z). \tag{2.30}$$

If the hydraulic conductivity varies with soil water potential as

$$K = K_o \exp(bh)$$

TABLE 2.2 Corresponding Values of Dimensionless Depth Z (= z/d) and Effective Root Density E.R(z) (after Molz and Remson, 1970).

Z	E.R(z)	Z	E.R(z)
0.06	3.90	0.55	0.112
0.05	3.14	0.60	0.0856
0.10	2.15	0.65	0.0640
0.15	1.31	0.70	0.0460
0.20	0.920	0.75	0.0323
0.25	0.635	0.80	0.0210
0.30	0.450	0.85	0.0123
0.35	0.329	0.90	0.00600
0.40	0.250	0.95	0.00200
0.45	0.193	1.00	0.00
0.50	0.150		

where

K_o is saturated hydraulic conductivity, and

b is a soil parameter.

Application of the Kirchhoff transformation

$$\Theta = \int_{-\infty}^{h} K(h)dh = K/b$$

to Eq. (2.30) yields

$$\frac{d^2\Theta}{dz^2} - b\frac{d\Theta}{dz} = A(z). \qquad (2.31)$$

The solution of the above equation, subject to the boundary conditions

$$\frac{d\Theta}{dz} - b\Theta = -q_o \quad \text{at} \quad z = 0$$

$$\Theta = K_o/b \quad \text{at} \quad z = L,$$

is given as (Warrick, 1974)

$$\Theta = \frac{q_o}{b} + \frac{1}{b}(K_o - q_o)\exp[-b(L - z)] - \exp(bz)\int_z^L \exp(bz)\int_o^z A(\xi)d\xi dz$$

where

q_o is upward soil surface flux,

L is depth to water table, and

ξ is a dummy variable.

Soil-Plant-Atmosphere models discussed in this section are summarized in Table (2.3).

TABLE 2.3 Soil-Plant, and Atmosphere Models

Type or Model	Reference	Form of the Sink Function	Remarks
Canopy	Lemon et al. (1971, 1973) Shawcroft (1971)	N.A.	Soil moisture conditions should be known a priori
Single Root Models	Gardner (1960)	Root is considered to be an infinitely long cylinder, and flow takes place in radial direction only. Total root extraction of water is equal to evapotranspiration rate.	Actual transpiration rate should be known. Does not consider vertical movement of soil moisture.
	Cowan (1965)	Root is considered to be an infinitely long cylinder, and flow takes place in radial direction only.	Does not consider vertical movement of soil moisture.
Integrated Root Models	Molz et al. (1970)	$A(z,\theta) = T_r \frac{R(z) \cdot D(\theta)}{\int_o^d R(z)\, D(\theta) dz}$	Actual transpiration rate, and the value of $T_r \cdot R(z) / \int_o^d R(z) D(\theta) dz$ should be known a priori
	Nimah et al. (1973a,b) Nimah (1972)	$A(z,h) = -K(h_r - h_s)/g(z)$ where $h_r = h_{ro} + a_r z$ and $T_r = \int_o^d A(z,h) dz$.	Lysimetric data is necessary to determine h_r.
	Feddes et al. (1974) Neuman et al. (1974)	$A(z,h) = K(h_r - h_s)/g(z)$ where h_r = constant and T_r is maximized subject to the constraints $\lvert T_r \rvert \leq \lvert T_r^* \rvert$ & $h_r \geq h_w$.	Plants are forced to transpire at potential rate.
	Feddes et al. (1975)	$A(\theta) = \beta_f(\theta)$ Amax	It is possible to estimate actual evapotranspiration rates more than potential rates if $\beta(\theta) > 0.5$.
	Warrick (1974)	$A = A(z)$	An analytical solution applicable only steady-state problems
	Present study	$A(h) = f(z) T_r^* e^{-T_r^* h^2/\alpha}$	The change of parameter α with plant and soil characteristics is not known. A function having more parameters may be appropriate.

2.4 Ground-Water Recharge

The existence of ground-water reservoirs can always be related directly or indirectly to precipitation. Other processes encountered in the formation of ground-water reservoirs are a) interception, b) stemflow, c) surface storage and surface runoff, d) infiltration, e) percolation, f) evaporation, g) transpiration, and h) recharge. Precipitated water might go through all or some of these processes to form ground-water reservoirs or it might return back to the atmosphere by evaporation and transpiration from any point of its journey to the water table without producing ground-water recharge. Precipitated water which reaches lakes or oceans by surface runoff or ground-water discharge is not the focus of this study. Possible paths of precipitated water in this restricted portion of hydrologic cycle, for one-dimensional vertical flow, is schematically shown in Fig. (2.8).

Recharge, which is the final process of precipitation in the formation of ground-water reservoirs, is one of the most difficult and important problems of hydrology; therefore, early methods for estimating recharge are attempts at direct measurement with extensive field observations, rather than understanding the physics involved in the process. The early methods are outlined by Meinzer (1949) as a) using a lysimeter, b) determining the amount of precipitation on a drainage basin and deducting runoff and precipitation losses, c) making periodic determination of soil moisture at different depths, d) observing the fluctuations of the water table and applying a factor for specific yield, and e) determining the decrease in flow of influent streams between gauging stations. A summary of a few field applications of these methods can be found in Walton (1970).

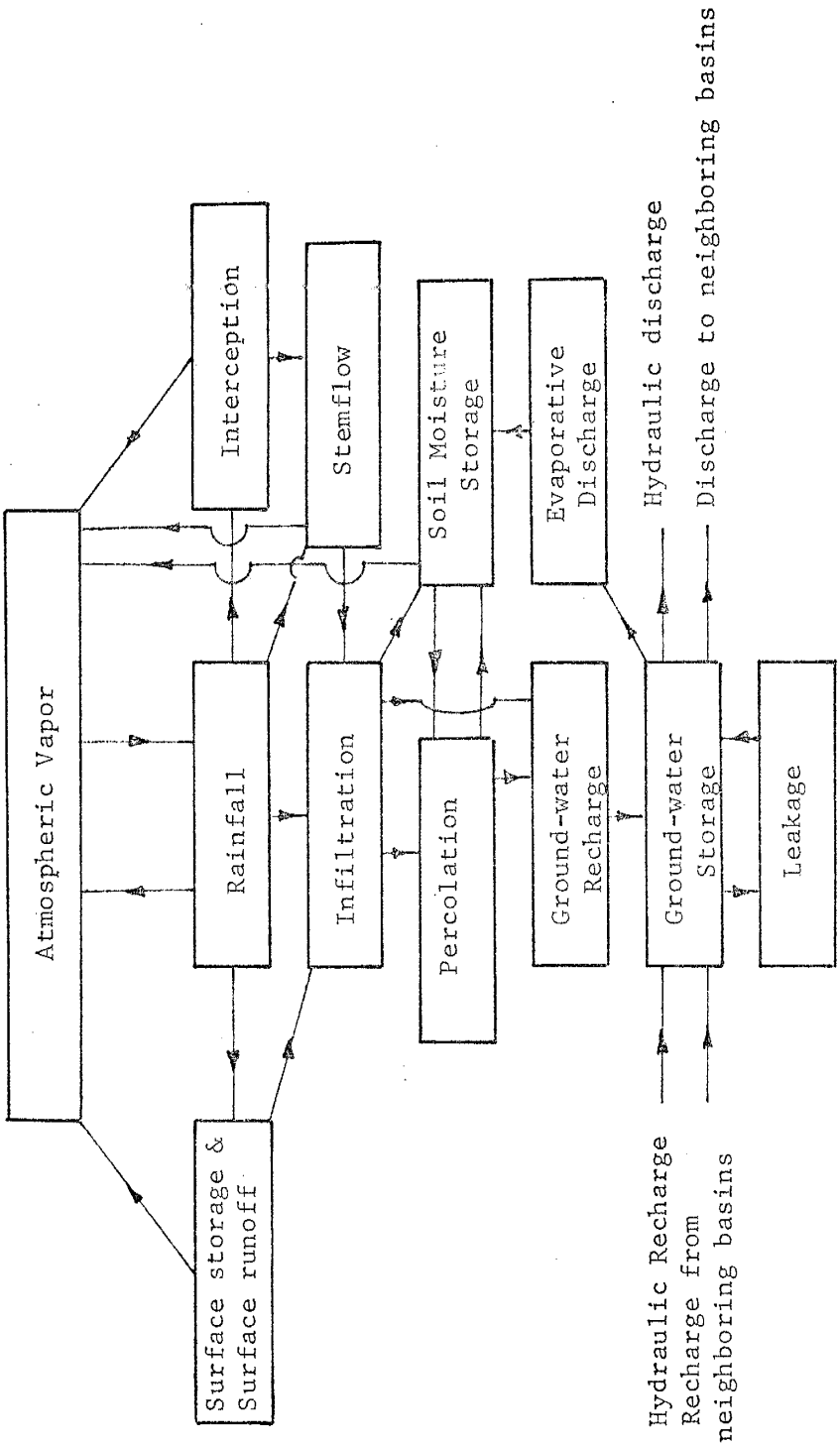

Figure 2.8 Schematic representation of the processes involved in the formation of ground-water reservoirs.

Hantush (1957) examined 30 years of water level and pumpage records of Roswell Basin in New Mexico and concluded that the system was in dynamic equilibrium two times during the 30-year period. From these data, Hantush arrived at a recharge estimate assuming a linear relationship between recharge and precipitation.

$$R = C_r \overline{P}_n = Q_p + D_s$$

where

R is the annual recharge,

$\overline{P}_n$ is the effective average rate of precipitation at the end of n^{th} year,

Q_p is the annual pumpage,

D_s is the annual discharge from the basin, and

C_r is a coefficient.

Effective average rate of precipitation is defined by Jacob (1943) as "the rate of precipitation which, had it been maintained uninterruptedly throughout the past, would have produced the same water-table profile actually existed at that particular time" and is given by the formula

$$\overline{P}_n = \sum_{i=1}^{k} \frac{2(k + 1 - i)}{k(k + 1)} P_{n+1-i}$$

where

k is the number of years the rainfall of a given year is effective, and

P_{n+1-i} is the precipitation at the $(n + 1 - i)^{th}$ year.

With the knowledge of the rate of pumpage and effective average rate of precipitation during those particular years when the system was in dynamic

equilibrium, Hantush (1957) arrived at the following equation for Roswell Basin in New Mexico:

$$21{,}000 \text{ (acre-feet/inch)}\overline{P}_n = Q_p + 8{,}000 \text{ (acre feet)}.$$

Thus, if the system is in dynamic equilibrium, his equation for recharge has the form:

$$R = C_r \overline{P}_n.$$

Luckey (in Konikow and Bredehoeft, 1974) derived a recharge equation assuming the following conditions:

a) that when total applied water exceeds the potential evapotranspiration, the ratio of an increment of recharge to an increment of applied water equals 1,

b) that this same ratio is less than 1 when the total applied water is less than the potential evapotranspiration, and

c) that when the total applied water is less than the potential evapotranspiration, recharge increases as the total applied water approaches the potential evapotranspiration.

Luckey suggested the following relationship:

$$R_f = 1 - \frac{E_t}{B} \cdot \frac{\zeta}{\zeta + 1} \qquad E_t/B \leq 1$$

$$R_f = \left(\frac{B}{E_t}\right)^{\zeta} \cdot \frac{1}{\zeta + 1} \qquad E_t/B \geq 1$$

where

R_f is recharge fraction which is defined as $R_f = R/B$,

B is total applied water (irrigation plus precipitation), and

ζ is a parameter.

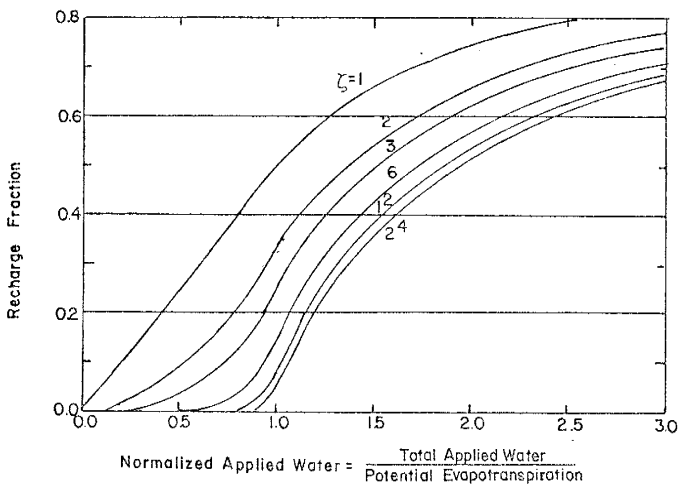

Figure 2.9 Relationship between recharge fraction (fraction of total applied water that is recharged) and ratio of total applied water to potential evapotranspiration for selected values of the recharge parameter ζ (after R.R. Luckey, in Konikow and Bredehoeft, 1974).

Recharge fraction R_f as a function of normalized applied water and the parameter ζ is given in Fig. (2.9). As seen in the figure the recharge fraction is insensitive to parameter ζ above a value of 12 (Konikow and Bredehoeft, 1974). The value of ζ for different climates, soil, and plants is not yet known.

Studies of saturated flow produced by localized recharge, undertaken by Werner (1957), Maasland (1959), Hantush (1967, and Dagan (1967), are primarily different applications of the Bousinesq equation. By assuming a constant specific yield in all of these studies, the flow in the partially saturated zone was neglected. Freeze (1967) incorporated the continuity between ground water and soil moisture. He studied the effects of soil type, duration of rainfall, antecedent soil-moisture conditions, and depth of ponding on the recharge process for bare soils. Pikul et al. (1974) were able to predict water levels in the Hulsart well near Old Bridge, New Jersey, by utilizing soil-moisture surpluses obtained from evapotranspiration tables prepared by Thornthwaite and Mather (1957). The model of Pikul et al. (1974) which is schematically shown in Fig. (2.10), has two distinct submodels, saturated and unsaturated. In the unsaturated zone, the flow is assumed to be strictly vertical. The bottom of the unsaturated column is kept at saturation and soil-moisture surpluses obtained from Thornthwaite and Mather (1957) are used as a boundary condition at the top of the soil column. In the saturated submodel, the Bousinesq equation is used, in which vertical flow effect in the saturated zone is neglected. Both submodels were linked to each other by adjusting the lower boundary of each unsaturated column at the end of each time step with the shape of the water table obtained from Bousinesq equation. Recharge into the saturated zone is obtained with a

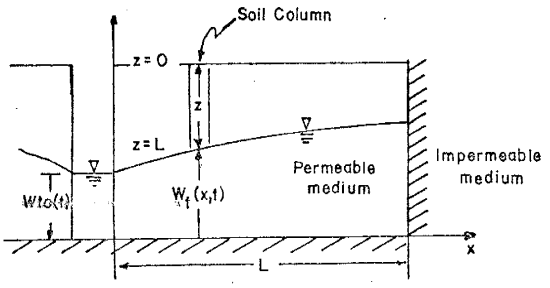

Figure 2.10 Idealization of the unsaturated-saturated subsurface flow problem (after Pikul et al., 1974).

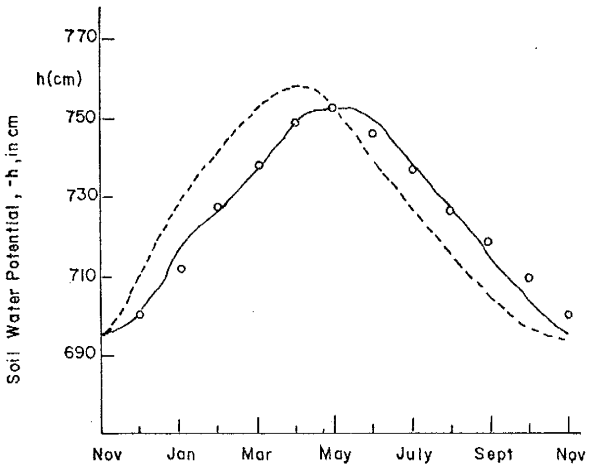

Figure 2.11 Hulsart hydrograph: the actual hydrograph (solid line) was simulated by using a linked model (circles). The hydrograph obtained by using a saturated model without input from unsaturated models (dashed line) is also shown (after Pikul et al., 1974).

material balance for each unsaturated column and for each time step. Recharge obtained in this way is used as a recharge term in the Bousinesq equation in the following time step.

The simulated hydrograph with the model of Pikul et al. (1974) and an actual hydrograph of Hulsart Well, New Jersey, is given in Fig. (2.11). As seen in the figure, simulation results agree very well with the actual hydrograph. However, soil-moisture surpluses obtained from evapotranspiration tables of Thornthwaite and Mather (1957) were prepared for the calculation of potential evapotranspiration, which, by definition, depends on the assumption that there is always moisture in the soil to evaporate at a maximum rate. Ward (1967) has indicated that the amount of discrepancy between actual and potential evapotranspiration rates increases as rainfall diminishes. In New Jersey, where the model of Pikul et al. (1974) was applied, the discrepancy between actual and potential evapotranspiration rates can be considered negligible. It is doubtful that the good agreement obtained in this instance between actual and predicted hydrograph readings could be obtained in an arid or semi-arid zone where water is not available in sufficient quantity in the soil to evaporate at the potential rate.

Krishnamurthi et al. (1977) assumed no evapotranspiration losses from layers below the root zone in their model. Penman's (1948) work implies, however, that plant root systems can draw on moisture throughout a considerable depth of soil below the root zone. In the former study this phenomenon is not considered, since a water molecule passing through the lower boundary of the root zone has no opportunity to move upward, and it eventually becomes recharge to ground-water reservoirs. Soil moistures, measured at an earlier time at the bottom of the root zone,

were used as a boundary condition in this numerical model to study recharge rates in the Colorado High Plains.

Updegraff and Gelhar (1977) utilized the linear reservoir model of Gelhar (1974) to predict aquifer parameters and recharge in the Mesilla Valley, New Mexico.

Rabinowitz et al. (1977) used

$$R = 0.1\ P/\overline{P}$$

for recharge in their study of tritium as a hydrometeorologic tool in the Roswell Basin, New Mexico.

The studies on recharge are summarized in Table (2.4).

TABLE 2.4 A Summary of Ground-Water Recharge Studies

Type of Study	Reference	Description of the Method	Remarks
Direct Estimation of Recharge	(Outlined by) Meinzer (1949)	Use of Lysimeters General Inventory Soil Moisture Inventory Water Table Inventory Influent-seepage Inventory	These methods do not explain the physics of the process.
Indirect Estimation of Recharge	Hantush (1957)	$R = C_r \overline{P}_N$	System should be in dynamic equilibrium.
	Luckey (in Konikow and Bredehoeft, 1974)	$R_f = 1 - \frac{E_t}{B} \cdot \frac{\zeta}{\zeta+1}$ $E_t/B \geq 1$ $R_f = (\frac{B}{E_t})^{\zeta} \cdot \frac{1}{\zeta+1}$ $E_t/B \leq 1$	Does not take into account the plant characteristics. Insensitive to large ζ's. Applicability in a wide range of climates is not known.
	Krishnamurthi et al. (1977)	Solution of unsaturated flow equations.	No evapotranspiration losses below the root zone. Climatic variables are not incorporated.
	Rabinowitz et al. (1977a)	$R = \beta_r P^2/\overline{P}$	Do not take into account the evapotranspiration losses. Applicability in a wide range of climates is not known.
	Updegraff and Gelhar (1977)	Inverse problem of Gelhar's (1974) linear reservoir model.	Does not relate recharge to climatic and plant characteristics of the basin.

TABLE 2.4 A Summary of Ground-Water Recharge Studies (continued).

Type of Work	Reference	Description of the Method	Remarks
Water Table response	Werner (1957)	Solution of the Bousinesq equation	These studies involve water table response to given recharge rates rather than estimation of recharge
	Maasland (1957)		
	Hantush (1967)		
	Dagan (1957)	Solution of Laplace equation with free-surface boundary condition	
	Gelhar (1974)	Stochastic solution of linear, linear Dupuit, Laplace equations	
	Freeze (1969)	Solution of saturated and unsaturated flow equations for bare soils	Plants are not included. Soil surface evaporative fluxes are prespecified (i.e., climatic factors are not considered). Reduction in soil evaporative fluxes due to reduction in the soil moisture (i.e., soil-moisture effect on evaporation also) is not considered.
	Pikul et al. (1974)	A linked solution of unsatured flow and Bousinesq equations	Not applicable in arid and semi-arid climates.
	Present study	Solution of saturated and unsaturated flow equations with water extraction of plants	More study is needed on the form of the root extraction term used.

CHAPTER 3: OBJECTIVE AND SCOPE OF THIS STUDY

The general objective of this study is the understanding of recharge in different types of soils, plant communities, and climatologic conditions in a physically continuous saturated and unsaturated flow domain. The ultimate goal is the development of methods to predict recharge rates in arid and semi-arid climates. From the summary of the previous work, in Table (2.4), it is evident that the existing methods are limited in their treatment of the transpiration process of the plant soil system under moisture-deficient conditions. The first steps towards the understanding of recharge (Freeze, 1967; Pikul et al. 1974) are not complete and cannot be generalized for the following reasons: no consideration is given to plant transpiration (Freeze, 1967) and the implicit assumption that there is always available moisture in the soil to evaporate at a maximum rate (Pikul et al. 1974). In order to investigate recharge in a natural environment, a model to simulate plant transpiration rates is needed. However, all existing root extraction models have one of the following deficiencies:

a) vertical movement of soil moisture is not considered,

b) actual transpiration rates should be known beforehand, or

c) plants are forced to transpire at the potential rate.

Thus, to achieve the general objective of this study, the following specific objectives are established:

a) development of a root extraction model such that plant transpiration will decrease with decreasing moisture in the soil and will also be a function of climatologic factors,

b) development of a computer program to solve mathematically continuous saturated and unsaturated flow equations with a root extraction term,

c) testing the developed model with actual field data, and

d) investigation of the recharge process with hypothetical data for different types of soils, plant communities, and climatologic conditions.

The main feature of this work is the study of recharge as influenced by water uptake of plant roots. The effect of plant water uptake on recharge, together with other soil and climatologic characteristics of the basin, is studied in a vertical, one-dimensional mathematically continuous saturated and unsaturated flow domain. The non-linear partial differential equation governing the flow is solved by using the backward implicit finite difference scheme with a variable time step.

The upper boundary of the flow domain is defined by the climatic conditions, which include precipitation, net radiation, air temperature, wind velocity and air vapor pressure (both actual and saturated). The climatic factors governing evaporative conditions are lumped together as one property: the potential evapotranspiration rate. The flow domain is underlain by an impermeable or semi-imperable layer. The soil properties include the hydraulic conductivity and soil-water potential as related to the water content. The plant properties consist of plant root distribution as a function of depth from the ground surface and leaf area index of vegetative cover.

CHAPTER 4: DEVELOPMENT OF MATHEMATICAL MODEL

Transpiration is the escape of water (vapor) into the atmosphere from the soil zone, primarily through plant leaves. Transpiration basically involves three types of water movement: a) the extraction of water from the soil by the plant roots, b) the transportation of water from the roots to the leaves, and c) the escape of water in vapor form from the leaves into the atmosphere. Evaporation is the escape of water vapor into the atmosphere through the ground surface. The combined effect of evaporation and transpiration is called evapotranspiration. Because of the difficulties in determining the rate of actual evapotranspiration, most studies have been directed toward the concept of potential evapotranspiration. Potential evapotranspiration was defined by Penman (1956) as "evapotranspiration from the extended surface of a short green crop, actively growing, completely shading the ground, of uniform height and not short of water."

Replacement of actual evapotranspiration with a potential rate has been found sufficiently correct (Denmead, 1961) for practical applications if the requirements in the definition of potential evapotranspiration are met. However, an important question is: What will happen when soil moisture becomes limited for plant use? This has been the subject of scientific investigation for the past two decades. Potential rate may be interpreted as the demand of atmospheric conditions for evapotranspiration. Plants and soils will respond to this atmospheric demand according to the available moisture in the soil. This may be the idea that has led many researchers (Singh and Dickinson, 1975; Cowan, 1965, Feddes et al., 1974; Minhas et al., 1964, etc.) to use one of the potential evapotranspiration formulae as an indicator of actual evapotranspiration.

Availability of soil water to plants under limited moisture conditions has been experimentally studied by Denmead and Shaw (1962). In their experiments, 136 twenty-gallon containers (18 inches in diameter and 24 inches in depth) were set in the field with tops level with the ground surface at a spacing of 40 inches from center to center. A four-plant hill of corn was raised in each container. Field-grown corn also was raised on all sides. The soil used in this experiment was Colo silty clay loam. After the plants emerged, the soil surface was covered with black plastic film to prevent soil evaporation. Losses in soil moisture could then be attributed to transpiration. The treatment of each container was arranged so that there were a number of containers with different amounts of moisture, ranging from saturation to wilting point. Climatologic variables, net radiation, temperature, humidity, and wind velocity were also measured to calculate the potential evapotranspiration as defined by Penman (1956). Experimental results of Denmead and Shaw (1962) are shown in Fig. (4.1) and Fig. (4.2). Figure (4.1) indicates that actual evapotranspiration rate approaches different limiting values for different climatologic conditions as soil moisture increases, while Fig. (4.2) shows that this limiting value is the potential transpiration rate.

Potential rates may be considered to be the driving mechanism of actual plant transpiration and/or soil evaporation rates. In the next section, by taking into account moisture conditions in the soil, a possible mathematical relationship between actual and potential rates is developed.

4.1 Development of Root Extraction Model

The experimental results of Denmead and Shaw (1962) reveal that the

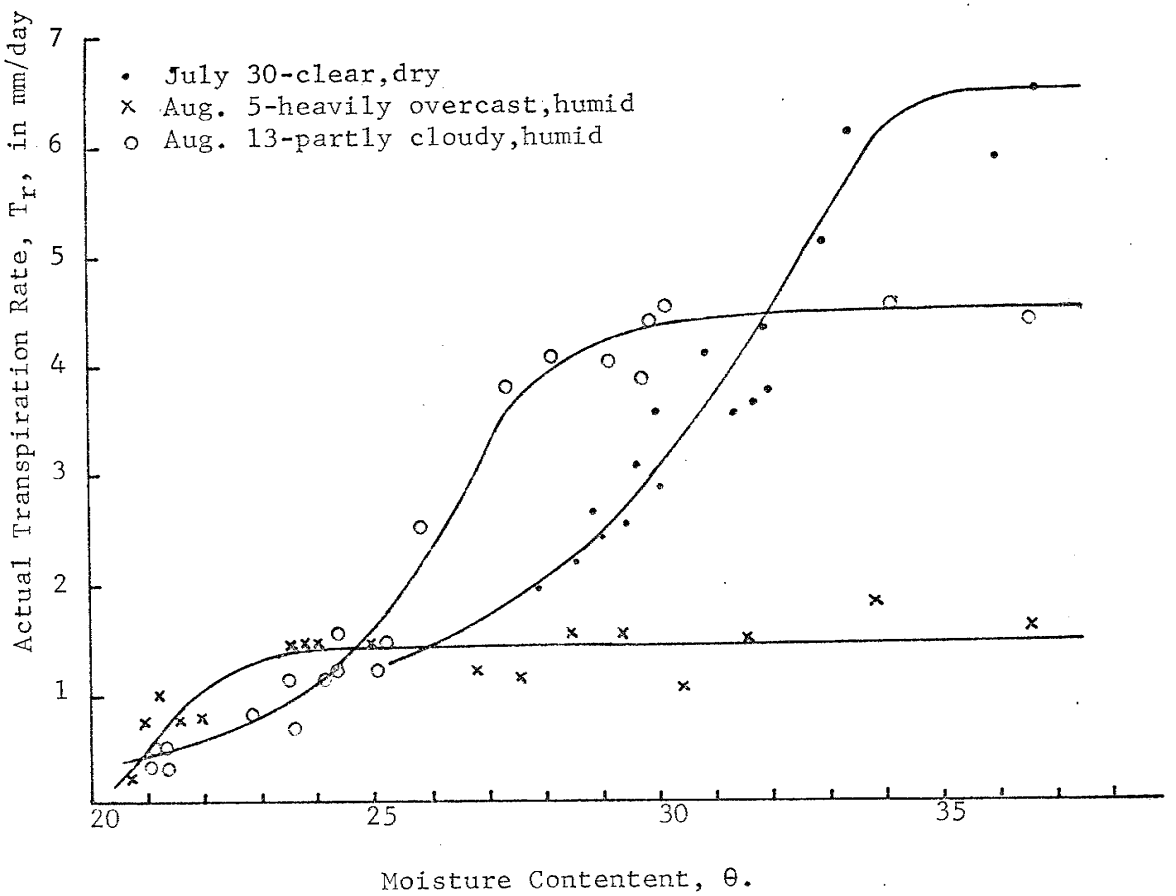

Figure 4.1 Actual transpiration rates as a function of moisture content for Colo silty clay loam (after Denmead and Shaw, 1962).

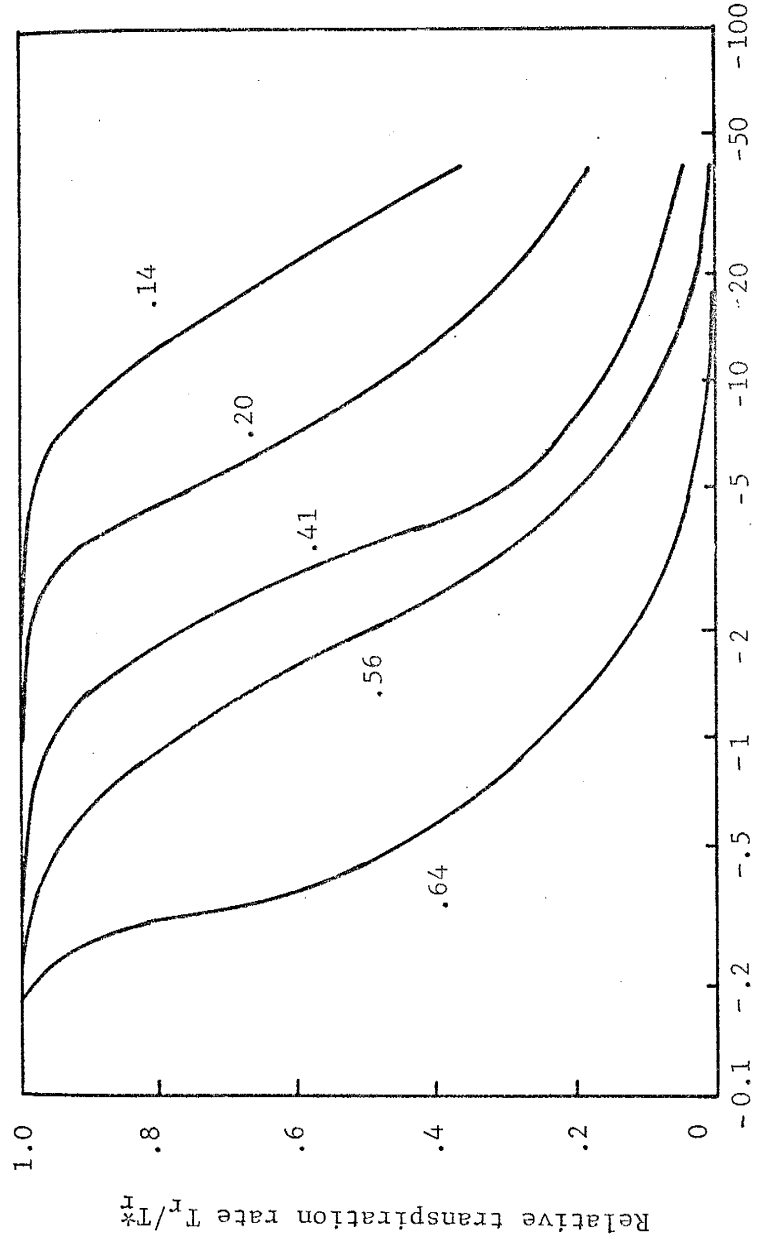

Figure 4.2: Relative transpiration rates as a function of soil water potential in Colo silty clay loam. (The numbers refer to values of potential transpiration rates in cm/day after Denmead and Shaw, 1962.)

actual transpiration rate approaches the potential rate as soil-water potential approaches zero, and goes to zero as soil-water potential goes to minus infinity (see Fig. 4.2). Mathematically, if the storage capacity of the plants is assumed to be negligible, the experimental results can be expressed as

$$\lim_{h \to o} \int_{o}^{d} A dz = T_r^* \tag{4.1a}$$

and

$$\lim_{h \to -\infty} A = 0. \tag{4.1b}$$

Since

$$\int_{o}^{d} A dz \leq T_r^*, \quad \text{one can also write}$$

$$\lim_{T_r^* \to o} A = 0. \tag{4.1c}$$

An examination of Fig. (4.2), when the ratio T_r/T_r^* equals 1 suggests that

$$\lim_{\substack{h \to o \\ T_r^* \to o}} \frac{dA}{dh} = 0 \tag{4.1d}$$

The change of water extraction with respect to water potential in the soil can be expressed mathematically with an infinite series,

$$\frac{dA}{dh} = \sum_{k=1}^{\infty} A^k \mu_k \tag{4.2}$$

where μ_k are coefficients.

Since root-water extraction is a joint function of both atmospheric energy and the available moisture in the soil, one can expect that the coefficient μ_k will be a function of both atmospheric demand for transpiration and moisture conditions in the soil. Thus, μ_k can be expressed as

$$\mu_k = \mu_k (T_r^*, h, K). \tag{4.3}$$

Equation (4.1d) implies that

$$\lim_{h \to o} \mu_k = 0. \tag{4.4}$$

In order to ensure convergence, the condition

$$\lim_{k \to \infty} \left| \frac{\mu_{k+1}}{\mu_k} \right| = 0 \tag{4.5}$$

should also be imposed on the coefficient of Eq. (4.2).

Since the form of the coefficients μ_k is unknown, except for the conditions expressed by Eq. (4.4) and Eq. (4.5), practical application of Eq. (4.2) is restricted. For simplification of the problem, one may assume that

$$\mu_k = 0 \quad \text{if } k \neq 1. \tag{4.6}$$

Equation (4.2) then takes the form

$$\frac{dA}{dh} = \mu A \tag{4.7a}$$

or

$$\frac{dA/A}{dh} = \mu. \tag{4.7b}$$

From Eq. (4.7b), it is clear that the coefficient μ physically represents fractional change of root extraction per unit change in soil water potential.

Solution of Eq. (4.7a) is given as

$$A = C_o(x,y,z,t)e^{\int \mu dh} \tag{4.8}$$

where $C_o(x,y,z,t)$ is an arbitrary function in time and space to be determined from boundary conditions. Time and space variables are treated as constants, since they appear in A, μ, and h. Utilization of Eq. (4.1a) and Eq. (4.8) yields

$$T_r^* = \int_o^d C_o(x,y,z,t)dz$$

or, by defining a function $f(x,y,z,t)$ such that

$$C_o(x,y,z,t) = T_r^* f(x,y,z,t),$$

one can deduce

$$\int_o^d f(x,y,z,t)dz = 1$$

and obtain

$$A = T_r^* f(x,y,z,t)e^{\int \mu dh}. \tag{4.9}$$

The function $f(x,y,z,t)$ can be interpreted as the root density function of plants varying in a horizontal plane, with depth from the soil surface. and in time. The allowance for variation in the horizontal plane

represents the areal changes in plant characteristics and the time factor allows for plant growth. For simplicity, variations of the plant-root density function in a horizontal plane and in time can be neglected. Equation (4.9) then reduces to

$$A = T_r^* f(z) e^{\int \mu dh} . \tag{4.10}$$

Using soil moisture versus water potential relations one can express the integral $\int \mu dh$ as $\int \mu \frac{dh}{d\theta} d\theta$ and assume that

a) $\mu \frac{dh}{d\theta} = 1/\phi$, and

b) the soil evaporation is also governed by the Eq. (4.7a).

Actual evapotranspiration can then be given as

$$E_t = C_v e^{\theta/\phi} \tag{4.11}$$

where C_v is the integration constant to be determined from boundary conditions. Equation (4.11) is identical to Eq. (12) of Singh and Dickinson (1975). Application of Eq. (4.7a) can be found in the literature in different forms (Feddes et al., 1975; Warrick, 1974, Minhas et al., 1974). However, the question of the proper form of μ still remains. Probably the simplest form of μ satisfying Eq. (4.4) is

$$\mu = - 2 T_r^* h/\alpha \tag{4.12}$$

where μ is a constant. Because of its simplicity this form of the function μ is used in this study. The numerical coefficient 2 is introduced only for integration purposes.

Substitution of Eq. (4.12) in Eq. (4.10) followed by integration of the resulting equation yields

$$\frac{T_r}{T_r^*} = \int_o^d f(z) e^{-T_r^* h^2/\alpha} \, dz.$$

The parameter α is estimated from the data of Denmead and Shaw (1962), Fig. (4.2). The values of h, in Fig. (4.2), represent average values over the root zone. Therefore, by assuming h is uniformly distributed over the root zone, the above equation is written in the form

$$\frac{T_r}{T_r^*} = e^{-T_r^* h^2/\alpha} . \qquad (4.12a)$$

The parameter α is then estimated with the aid of least square curve-fitting technique with the data obtained from Fig. (4.2). The result of curve fitting is shown in broken lines in Fig. (4.3). It is evident that the constant value of α is not representative of the plant root extraction term for a wide range of potential transpiration rates. Therefore, the parameter α is also estimated by using only the data points of $T_r^* = 0.64$ cm/day, and this particular value of α is used throughout the study by choosing relatively high potential transpiration rates. The comparison of actual data points and approximated curve for this particular value of T_r^* and corresponding α is also shown as solid lines in Fig. (4.3).

4.2 Soil Evaporation Rates

The model of Feddes et al. (1974) forces the soil moisture to evaporate at a maximum rate, while the thermodynamic relation, Eq. (2.26),

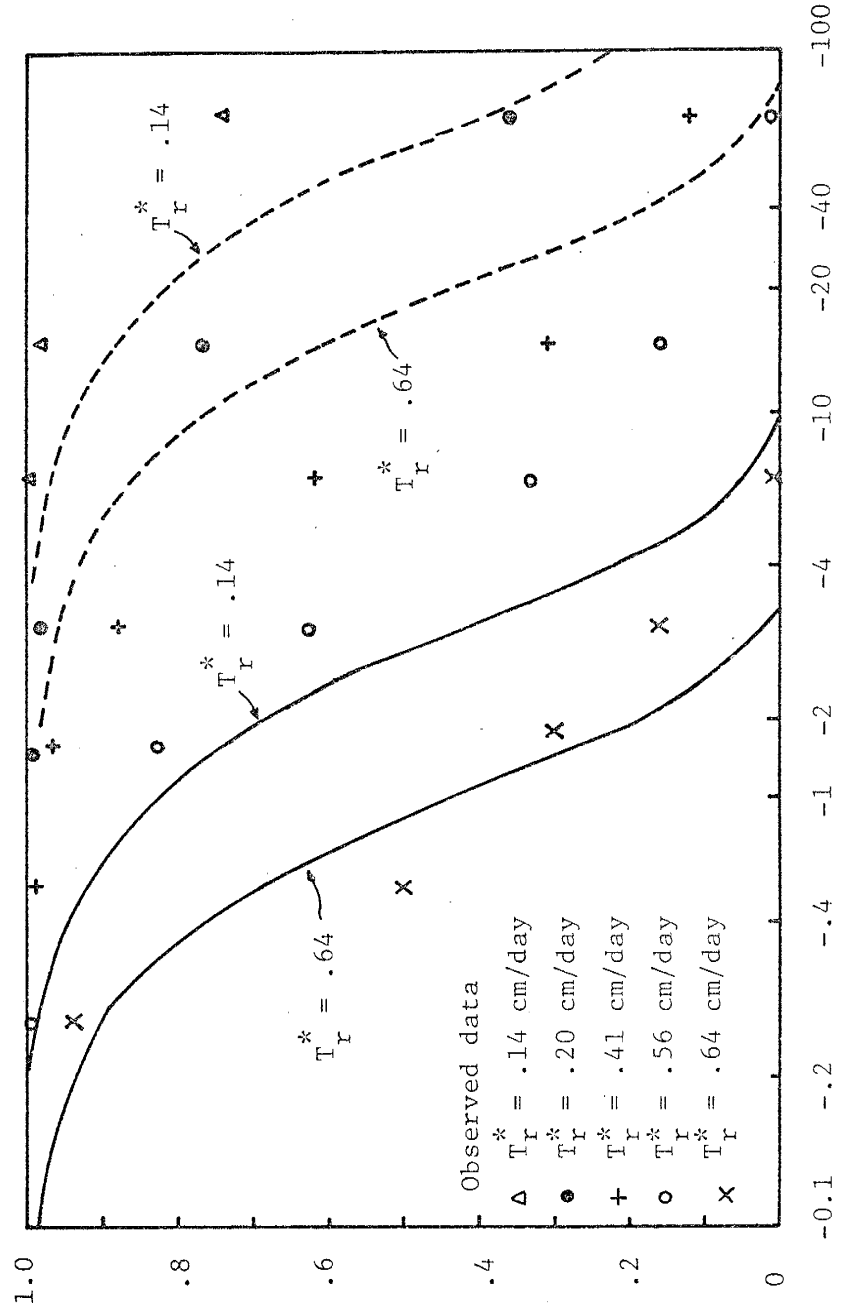

Figure 4.3 Comparison between curve fitted (using Eq. 4.12a) and observed relative transpiration rates. Dashed curves are for $\alpha = 37.06$ bar^2 cm/day which was obtained using all data points whereas the solid curves are for $\alpha = .371$ bar^2 cm/day which was obtained using the data points of $T_r^* = 0.64$ cm/day only.

used by Neuman et al. (1974) is very sensitive to soil surface temperature and relative humidity. These deficiencies stimulated a search for an equation that would be more useful for the objectives of this study. After some experimentation, it was decided that an equation similar to the transpiration equation could approximate the evaporation phenomenon, provided that the parameter α could be determined. Hence the equation

$$E_v = E_v^* \, e^{-E_v h_{so}^2/\alpha} \tag{4.13}$$

was adopted for this purpose, and the same value of α is used as in plant transpiration case. Since hypothetical data are used in this study, it was not necessary to calculate potential evapotranspiration; thus separation of the potential transpiration and soil evaporation rates were not needed. However, the potential evapotranspiration rates can be separated into its components, potential transpiration and soil evaporation, with the aid of Eq. (2.24) and Eq. (2.25). Alternatively, the equation proposed by Ritchie and Burnett (1971)

$$\frac{T_r^*}{E_t^*} = -0.21 + 0.7\sqrt{L_a} \tag{4.14}$$

can be used for this separation purpose.

4.3 Mathematical Description of Flow Problem

The substitution of Eq. (4.10) and Eq. (2.10) into the continuity equation, Eq. (2.6), yields the dynamic flow equation

$$\frac{\partial \theta}{\partial t} = \nabla \cdot [K\nabla(h - z)] - T_r^* \, f(z) e^{-T_r^* h^2/\alpha} = 0. \tag{4.15a}$$

By expressing

$$\frac{\partial \theta}{\partial t} = C \frac{\partial h}{\partial t} \tag{4.15b}$$

where $C = \frac{d\theta}{dh}$ is soil water capacity and writing Eq. (4.14) for one-dimensional vertical flow, one obtains

$$C \frac{\partial h}{\partial t} = \frac{\partial}{\partial z} \left[K\left(\frac{\partial h}{\partial z} - 1\right)\right] - T_r^* f(z) e^{-T_r^* h^2/\alpha} . \tag{4.16a}$$

The general behavior of soil water capacity C, defined by the ralation $d\theta/dh$, is fully described by Freeze (1971). Because $C = 0$ and $h \geq 0$ in the saturated zone, Eq. (4.16a) takes the form

$$K_o \frac{d^2 h}{dz^2} - T_r^* f(z) = 0. \tag{4.16b}$$

The saturated zone generally exists in arid and semi-arid climates far below the bottom of the root zone. In this region $f(z) = 0$ and Eq. (4.16b) reduces to a Laplacian equation

$$\frac{d^2 h}{dz^2} = 0. \tag{4.16c}$$

Initial and boundary conditions for Eq. (4.16a) are given as follows: The initial condition is

$$h = h(z) \qquad t = 0 \tag{4.17a}$$

and the surface boundary condition is either

$$\text{a)} \quad \left.\frac{\partial h}{\partial z}\right|_{z = 0} = - \frac{q_o - K}{K} \qquad \text{if } h_{so} < 0 \tag{4.17b1}$$

where q_o is the prespecified flux

$$q_o = \begin{cases} \text{rainfall intensity} & \text{if precipitation is taking place} \\ q_o(E_v^*, T_r^*) & \text{if evaporation is taking place} \end{cases}$$

or b) $h\Big|_{z=0} = 0 \qquad \text{if } t > t_o$ (4.17b2)

where t_o is the time when the soil surface potential becomes zero. After that time, the constant head boundary condition is applied, and the difference between rainfall intensity and infiltration is assumed to be lost to adjacent areas by surface runoff. Thus, no ponding is allowed at the soil surface.

Ruben and Steinhart (1963) demonstrated in their numerical study of rainfall infiltration that, in a semi-infinite medium, unsaturated hydraulic conductivity approaches (as a limiting process in time) the value of the rainfall intensity. As a consequence, soil water potential also approaches a limiting value determined by the relation $K^{-1}(h)$. Once this limiting value is attained, soil surface potential remains constant as long as there is no change in the rainfall intensity. As a result, Rubin and Steinhart concluded that the rain can continue indefinitely at this constant rate without giving rise to ponding, provided that the rainfall intensity is less than the saturated hydraulic conductivity of the soil. However, Freeze and Banner (1970) pointed out that the conclusion of Rubin and Steinhart (1963) is true only for a semi-infinite medium. Existence of a water table will cause a continuous increase in soil water potential, and ultimately a continuing rainfall will give rise to ponding.

The surface boundary condition defined by Eq. (4.17b1) and Eq. (4.17b2) takes into account the influence of a rising water table created by the presence of an impermeable or semi-impermeable boundary at the bottom of the soil column. The bottom boundary condition is

$$\left.\frac{\partial h}{\partial z}\right|_{z = \ell} = - \frac{q_b - K}{K} \tag{4.18}$$

where q_b is a prespecified bottom flux defined by the hydraulic properties of the layer below the bottom of the soil column, and ℓ is the thickness of the soil column.

Equation (4.16a) is a second order, nonlinear, parabolic, partial differential equation, for which an analytical solution is not yet known. Semi-analytical solutions given by Philip (1957, 1958, 1969, and 1973), Brutsaert (1968), Parlange (1971, 1972, and 1973), and Philip and Knight (1974) are not exact analytical solutions, and their use is severely restricted to certain types of problems (semi-infinite medium and no root extraction). Numerical techniques that have been developed using high-speed digital computers are the only approach suitable for the unsaturated-flow problem of interest here. The numerical model used in this study to solve Eq. (4.16a) is briefly explained in the next section, and documentation of the computer program is given in the appendix.

4.4 Finite-Difference Approximation of Flow Equation

Finite-difference approximation of a differential equation can be obtained by one of the following: a) Taylor's expansion, b) integration, and c) variational formulation methods. The following is the integration method used to obtain finite difference approximation to Eq. (4.16a).

For the integration of the left-hand side of Eq. (4.16a), the following approximation can be made (Varga, 1962):

$$\int_{z_{i-1/2}}^{z_{i+1/2}} C \frac{\partial h}{\partial t}\, dz \cong \frac{dh}{dt} \int_{z_{i-1/2}}^{z_{i+1/2}} C\, dz$$

$$\cong \frac{h_i^j - h_i^{j-1}}{\Delta t} \overline{C}_i \frac{\Delta z_i + \Delta z_{i+1}}{2} \qquad (4.19a)$$

The 3-point approximation on the right-hand side of Eq. (4.16a), by means of integration over the z axis and rearrangement, yields

$$\overline{C}_i^{j-1/2} \frac{h_i^j - h_i^{j-1}}{\Delta t} \cong \frac{2}{\Delta z_i + \Delta z_{i+1}} \left(K_{i+1/2}^{j-1/2} \frac{h_{i+1}^{j-1/2} - h_i^{j-1/2} - \Delta z_{i+1}}{\Delta z_{i+1}} \right.$$

$$\left. - K_{i-1/2}^{j-1/2} \frac{h_i^{j-1/2} - h_{i-1}^{j-1/2} - \Delta z_i}{\Delta z_i} \right) - \overline{A}_i \qquad (4.19b)$$

where i and j are running dummy variables in space and time, respectively, and

$$\Delta z_{i+1} = z_{i+1} - z_i;$$

$$z_{i+1/2} = z_i + \frac{\Delta z_{i+1}}{2};$$

$$z_{i-1/2} = z_i - \frac{\Delta z_i}{2};$$

$$K_{i+1/2}^{j-1/2} = \frac{(K_i^{j-1/2} + K_{i+1}^{j-1/2})}{2}, \quad K_{i-1/2}^{j-1/2} = \frac{(K_i^{j-1/2} + K_{i-1/2}^{j-1/2})}{2};$$

$$\overline{C}_i^{j-1/2} = \frac{2}{\Delta z_i + \Delta z_{i+1}} \int_{z_{i-1/2}}^{z_{i+1/2}} C^{j-1/2}\, dz$$

$$= \frac{\Delta z_i (C_i^{j-1/2} + C_{i-1/2}^{j-1/2}) + \Delta z_{i+1} (C_i^{j-1/2} + C_{i+1/2}^{j-1/2})}{2(\Delta z_i + \Delta z_{i+1})} ;$$

$$C_{i+1/2}^{j-1/2} = \frac{(C_i^{j-1/2} + C_{i+1}^{j-1/2})}{2}, \quad C_{i-1/2}^{j-1/2} = \frac{(C_i^{j-1/2} + C_{i-1}^{j-1/2})}{2} ;$$

$$\overline{A}_i = \frac{2}{\Delta z_i + \Delta z_{i+1}} \int_{z_{i-1/2}}^{z_{i+1/2}} A dz = \frac{T_r^*(F_i^* + F_{i+1}^*) e^{-T_r^*(h_i^{j-1/2})^2/\alpha}}{24(\Delta z_i + \Delta z_{i+1})} ; \text{ and}$$

$$F_i^* = \int_{z_{i-1}}^{z_i} f(z) dz$$

where i = 2, n - 1. Boundary conditions at the soil surface is

$$\left.\frac{\partial h}{\partial z}\right|_{z=0} \cong - \frac{h_2^{j-1/2} - h_1^{j-1/2}}{\Delta z_2} = - \frac{q_o - K_{1+1/2}^{j-1/2}}{K_{1+1/2}} . \qquad (4.19c)$$

If the conditions are evaporative, the soil surface flux q_o is given as

$$q_o = - \frac{E_v^* e^{-E_v^*(h_1^{j-1/2})^2/\alpha} + \frac{T_r^* F_2^* e^{-T_r^*(h_1^{j-1/2})^2/\alpha}}{2}}{24} .$$

T_r^* and E_v^* are potential transpiration and evaporation rates (cm/day), respectively. The second term in the numerator of the above equation represents the root extraction term in the first half of the first space

increment. Thus, the layer immediately below the soil surface is considered to be contributing only to soil evaporation but not to plant transpiration. If precipitation is taking place and $t \leq t_o$, then q_o is precipitation intensity. For time $t > t_o$, $h_1^{j-1/2} = 0$.

The bottom boundary condition is

$$\left.\frac{\partial h}{\partial z}\right|_{z=\ell} \cong \frac{h_n^{j-1/2} - h_{n-1}^{j-1/2}}{\Delta z_n} = -\frac{q_b - K_{n-1/2}^{j-1/2}}{K_{n-1/2}^{j-1/2}} \quad (4.19d)$$

The bottom flux q_b is flowing from the soil column if $q_b > 0$ and flowing into the soil column if $q_b < 0$. The time weighing scheme

$$h_i^{j-1/2} = \omega h_i^j + (1 - \omega) h_i^{j-1} \quad (4.20)$$

where $0 < \omega \leq 1$, is introduced. Note that this numerical method becomes the Crank Nicolson scheme if $\omega = 1/2$ and backward implicit scheme if $\omega = 1$. Equation (4.19b), together with Eq. (4.20) and the boundary conditions can be expressed as

$$-U_i h_{i+1}^j + W_i h_i^j - V_i h_{i-1}^j = D_i, \quad i = 2, n-1 \quad (4.21)$$

where n is the number of nodal points. The expression for U_i, W_i, V_i, and D_i can be obtained by carrying the unknowns, h_i^j, to left and leaving the knowns, h_i^{j-1}, on the right-hand side of Eq. (4.19b).

Equation (4.21) gives $(n-2)$ linear algebraic equations with $(n-2)$ unknowns, and the solution is given by Richtmyer and Morton (1967) as

$$E_i = \frac{U_i}{W_i - V_i E_{i-1}}, \quad i = 2, n-1 \quad (4.22a)$$

$$F_i = \frac{D_i + V_i F_{i-1}}{W_i - V_i E_{i-1}}, \quad i = 2, n-1. \tag{4.22b}$$

With this elimination process, the water potential at $(n-1)^{th}$ nodal point can be obtained as

$$h^j_{n-1} = F_{n-1} . \tag{4.22c}$$

The water potentials at the other nodal points can then be calculated from the recurrence relation

$$h^j_i = E_i h^j_{i+1} + F_i, \quad i = n-2, 2. \tag{4.22d}$$

Solution of Eq. (4.16a) by the aid of equations from (4.21) to (4.22d) may require an exorbitant amount of computer time. It is desirable, therefore, to use small time increments during periods of rapid change and larger increments as time goes on. Applicability of a varying time step in numerical solutions is discussed in detail by Douglas and Gallie (1955). For the backward implicit scheme, they suggest a relationship for selecting time increments of the form

$$\Delta t_j = (\alpha_d + \beta_d t_j)(\Delta z)^2 \tag{4.23}$$

where α_d and β_d are constants such that $\alpha_d > 0$, $\beta_d > 0$, t_j and Δt_j are the beginning and the length of j^{th} time step respectively, and Δz is space increment. Because of the applicability of a variable time step, the backward implicit scheme is used in this study. In other words, ω is set equal to one in Eq. (4.20). In order to be able to study the effects of diurnal variations in evapotranspiration, the time increments are not allowed to have a value greater than 12 hours. At the beginning

and at the end of each rainfall event, the time increment is set to the initial time increment Δt_o.

In the backward implicit scheme, hydraulic conductivities appearing on the right-hand side of Eq. (4.19b) represent hydraulic conductivities at the end of each time step. The term $\overline{C}_i^{j-1/2}$, in the left-hand side of Eq. (4.19b), is the dominating factor in producing errors and should be averaged in the time step (Price, 1977). Since they are not known beforehand, the iteration procedure outlined below is followed:

1. Calculate $\overline{C}_i^{j-1/2}$ and $K_{i+1/2}^{j-1/2}$ from the initial soil-water potential distribution by using soil-water retention curves.

2. Solve Eq. (4.19b) by using the equations from (4.21) to (4.22d).

3. Calculate soil-moisture content at each nodal point by using $h(\theta)$ and integrate over the soil solumn by the trapezoidal integration formula

$$S_t^j = \sum_{i=2}^{n} (\theta_i + \theta_{i-1}) \Delta z_i / 2$$

to obtain soil moisture storage S_t^j at the end of each time step.

4. Check the mass balance with the equation

$$e_{rs} = \frac{S_t^j - S_t^{j-1} - (q_o - E_t - q_b)\Delta t_{j-1}}{S_t^{j-1} + (q_o - E_t - q_b)\Delta t_{j-1}} 100$$

where e_{rs} is percent error in the mass balance.

5. If the absolute value of e_{rs} is greater than a prescribed tolerance, do the following:

a. Calculate $K_{i+1/2}^{j-1/2}$ from the soil-water potential distribution at the end of the time step.

b. Calculate soil-water capacities at each nodal point with the relation

$$C_i^{j-1/2} = \begin{cases} (\theta_i^j - \theta_i^{j-1})/(h_i^j - h_i^{j-1}) & \text{if } h_i \neq h_i^{j-1} \\ \text{use soil-moisture retention curve} & i = 1, n \\ \text{otherwise} \end{cases}$$

and average soil water capacities, defined as

$$\overline{C}_i^{j-1/2} = \frac{2}{\Delta z_i + \Delta z_{i+1}} \int_{z_{i-1/2}}^{z_{i+1/2}} C^{j-1/2}\, dz \qquad i = 2, n-1.$$

6. Repeat the same procedure starting from step number 2.

Since the absolute value of e_{rs} does not get any smaller than its value after a few iterations, the above procedure (step 2 through 6) is terminated after four iterations. The maximum value of e_{rs} after the fourth iteration ranged between $2*10^{-3}$ and $8*10^{-3}$. The variable time increment given by Eq. (4.23) can also be expressed as

$$\Delta t_j = \Delta t_{j-1} \, (1 + \beta_d (\Delta z)^2).$$

The values 0.05 hours and 0.01 were experimentally found to be optimum values of Δt_o and $\beta_d(\Delta z)^2$, respectively, in order to keep $|e_{rs}|$ less than 10^{-3}. Since the errors occurring in each time step are cumulative, 10^{-3} was also experimentally chosen as a tolerance limit of $|e_{rs}|$ in order to have an over-all error of less than 5% after 40 days of simulation.

The position of the water table is defined as the point where soil-water potential is zero. At the end of each time step, if the soil-water potential at the bottom of the soil column is greater than zero, starting from the $(n-1)^{th}$ nodal point the water potentials of each nodal point are checked successively, and the position of the water table is then located between the nodal points z_i and z_{i-1} by the water potential of the

first point where $h_{i-1} \leq 0$. Exact location of the water table is then determined by linear interpolation, and recharge is calculated from the relation

$$R = \phi_e \frac{W_t^j - W_t^{j-1}}{\Delta t_{j-1}}$$

where

$\phi_e = \phi - \theta_r$ is effective porosity,

θ_r is residual saturation, and

W_t^j and W_t^{j-1} are the distances between the water table and the bottom of the soil column at the beginning and at the end of the time step, respectively. Note that if $R < 0$, R then represents the discharge rate from the saturated zone.

Referring to Fig. (2.8), processes encountered in the formation of ground-water reservoirs, but not considered in this model, are:

a) interception,

b) plant stemflow,

c) natural or artificial hydraulic recharge into and discharge from the reservoir, and

d) horizontal components of moisture flow.

The major assumption involving the surface storage and surface runoff is that ponding of water at the soil surface is not allowed; thus unfiltrated water is assumed to be instantaneously lost to adjacent areas by surface runoff.

CHAPTER 5: VERIFICATION OF COMPUTER PROGRAM AND ROOT EXTRACTION MODEL

The model was tested with actual field data. Nimah (1972) published results of a field study which was carried out in 1970 and 1971. Actual evapotranspiration was measured with a weighing lysimeter. Soil moisture measurements were made regularly at predetermined time intervals. Measurement of solar radiation, wind velocity, and wet and dry bulb temperatures were also taken during the experiment. In 1970 the field was planted with oats and seeded with alfalfa, and in 1971 alfalfa was grown. The field was irrigated by an automated sprinkler system. Rain (or irrigation), actual evapotranspiration and potential evapotranspiration data, as measured between the dates May 15, and June 22, 1971, are graphically shown in Fig. (5.1). The root-distribution function and initial condition are given in Table (5.1). These data are used to test the present model. The ratio T_r^*/E_t^* was assumed to be 0.9 by Nimah (1972), and the same assumption is also made in the present comparison. Measured cumulative potential and actual evapotranspiration, and prediction of cumulative actual evapotranspiration by the present model for different values of α are shown in Fig. (5.2). The predicted and measured soil-moisture distributions, on May 31, 1971, are also shown in Fig. (5.3). Comparison of these two figures, Fig. (5.2) and Fig. (5.3), shows that with the larger value of α, the cumulative actual evapotranspiration can be predicted reasonably well by the model. However, with the larger value of α, the soil-moisture distribution deviates considerably from the actual data. This discrepancy may be the result of neglecting interception losses in the model. As shown in Fig. (5.1), actual evapotranspiration rates exceeded the potential rate (as calculated from the Penman

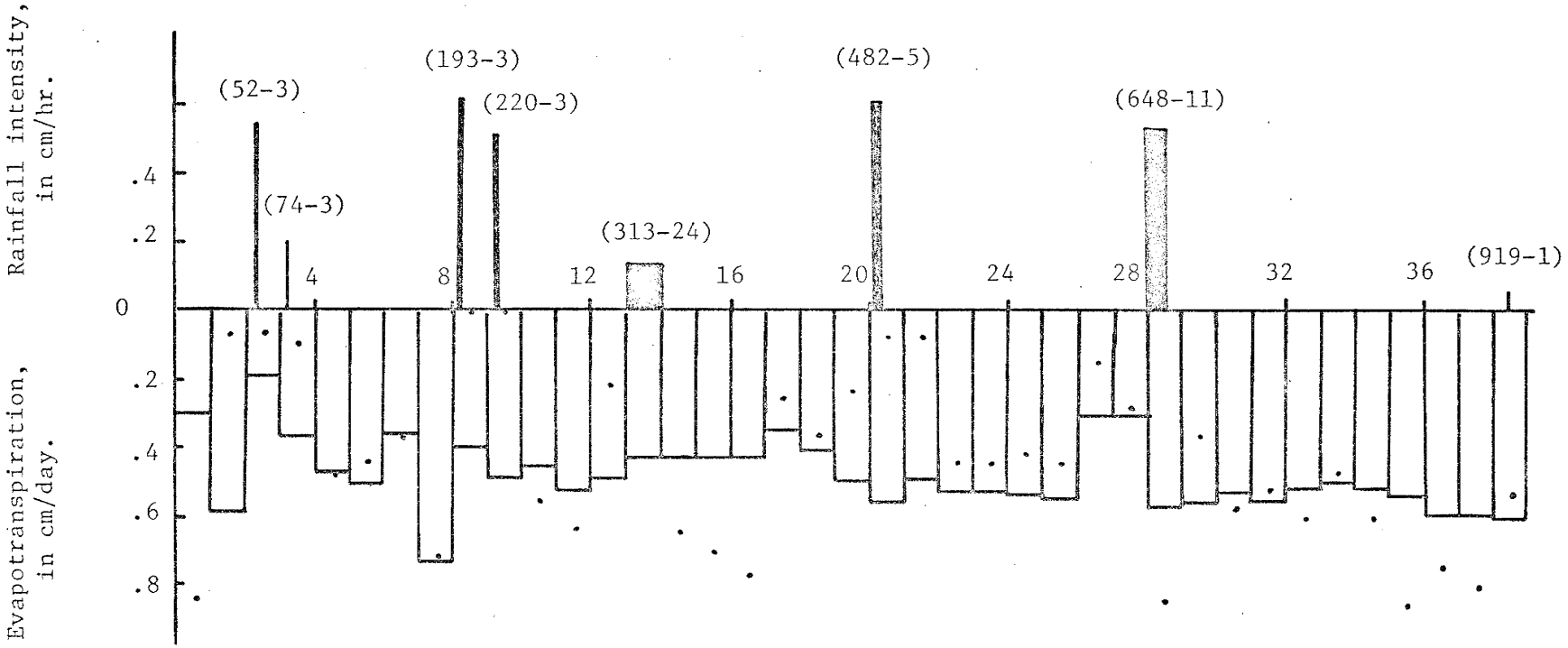

• Actual daily evapotranspiration measured using a weighing type lysimeter.

▬ Rainfall intensity in cm/hr.

▭ Potential evapotranspiration (Penman, 1956).

(313-24) are the length of the time, in hours, between the beginning of the rainfall and the simulation and the duration of the rainfall, respectively.

Horizontal axis is the time in days.

Figure 5.1 Field data used in testing the model developed herein (from Nimah, 1972).

TABLE 5.1

Root distribution function and (RDF) initial water content for alfalfa in 1971 (after Nimah, 1971).

Node No.	Depth (cm)	RDF(z) = $\int_{Z_{i-1}}^{Z_i} f(z)dz$	Initial condition θ %
1	0	----	.080
2	1	.028	.085
3	3	.056	.090
4	5	.056	.095
5	8	.084	.100
6	12	.1118	.110
7	16	.1042	.120
8	20	.0766	.130
9	25	.0967	.144
10	30	.0967	.155
11	35	.0637	.195
12	40	.0633	.225
13	45	.0633	.265
14	55	.0666	.267
15	70	.0344	.268
16	85	.00	.273
17	100	.00	.275
18	115	.00	.285
19	135	.00	.305
20	155	.00	.365
21	165	.00	.400

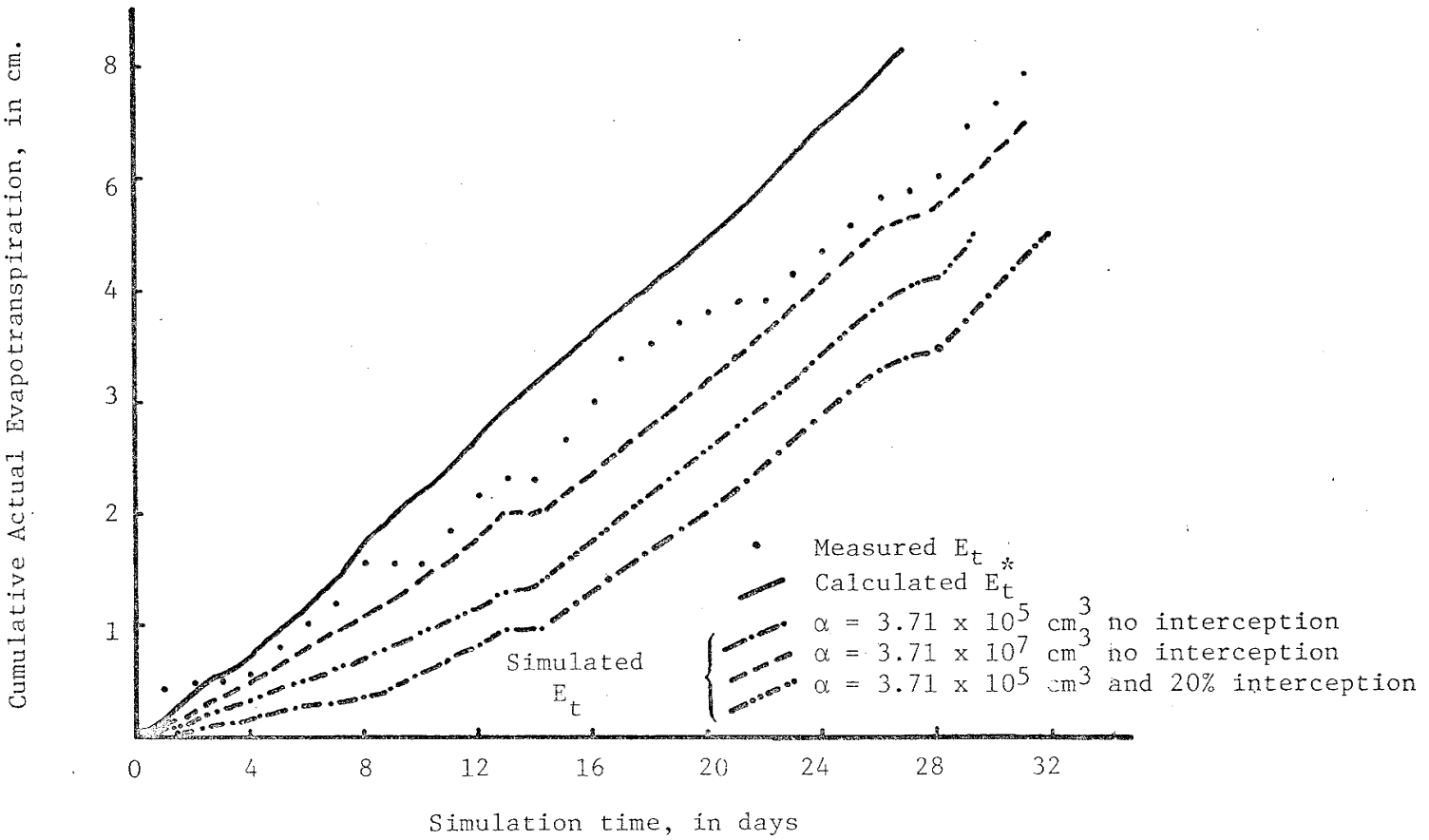

Figure 5.2 Comparison of cumulative actual evapotranspiration and the results of numerical simulation.

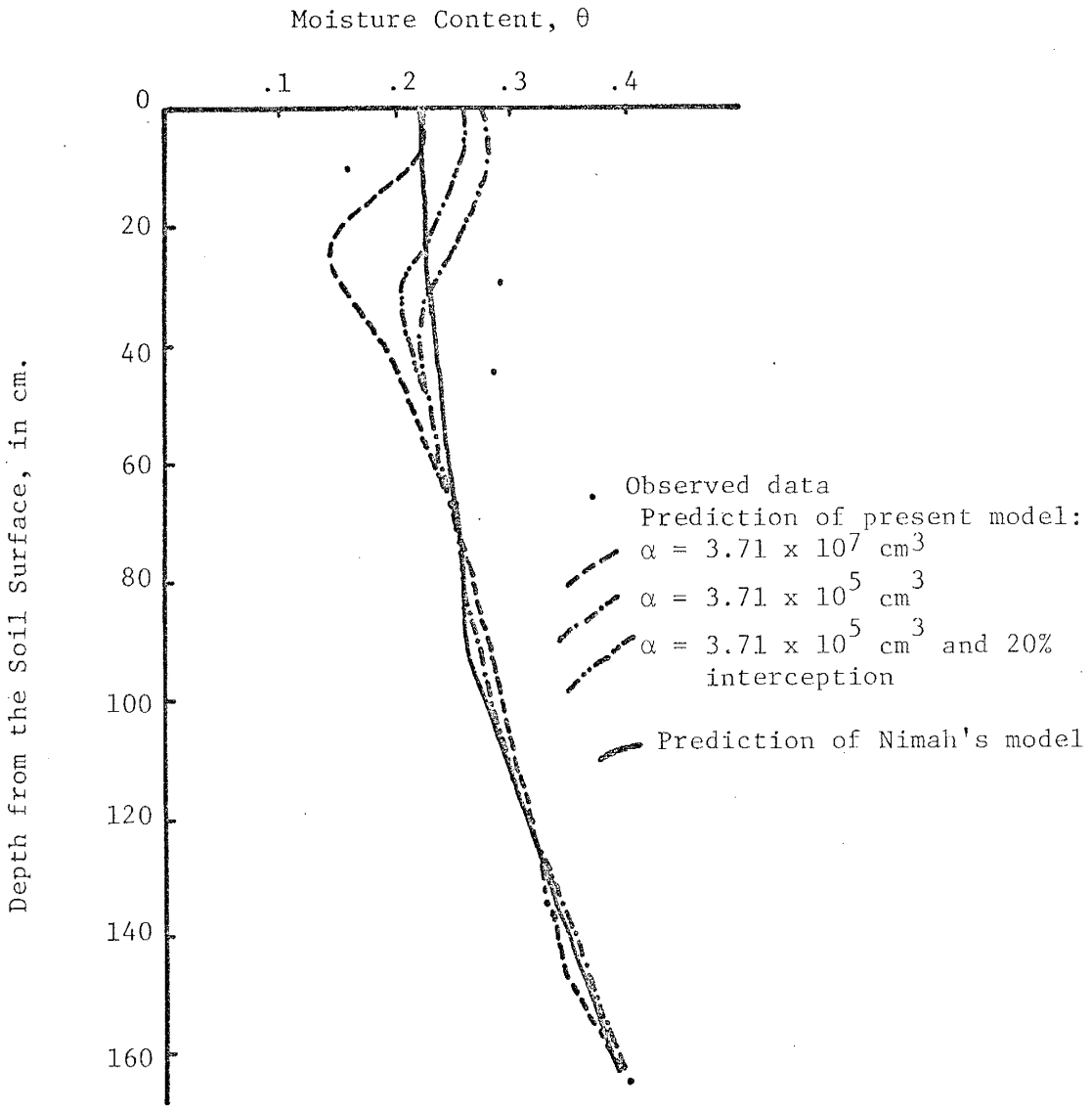

Figure 5.3 Comparison of moisture distribution for alfalfa on May 31, 1971.

equation) many times during the course of the experiment. The interception for alfalfa might be as much as 35% of the rainfall (Lull in Chow, 1964). If a certain percentage of the rainfall is intercepted by the plant body, then following rainfall the plant probably does not transpire as much. However, the measured evapotranspiration reflects both evaporation of intercepted water and depletion of stored soil moisture. Since intercepted water exposes more surface area to evaporation, it may be expected that following the rainfall the actual evapotranspiration will exceed the potential rate. This may be the phenomenon that is observed in the data of Nimah (1972). The model developed in this study, like the other root extraction models existing in literature, does not consider the interception process. Hence, in the existing models following the rainfall the plant is forced to use soil moisture to satisfy its transpiration requirements, and excessive extraction of the moisture from the soil may be simulated.

The present model is also tested very roughly for interception. The plant is still allowed to use the soil moisture to satisfy its transpiration requirements, but interception is assumed to be 20% of the applied water. At the end of 30 days simulation, this 20% intercepted water is uniformly distributed over the simulation time and added to the cumulative evapotranspiration obtained from the model. Cumulative evapotranspiration, considering interception losses, is shown in Fig. (5.2). The infiltration wetting front profile for this simulation is also shown in Fig. (5.3). As can be seen, both soil moisture profile and cumulative evapotranspiration are in good agreement with the actual data. Thus, considering its inherent assumptions, the model agrees reasonably well with actual data.

Other sources of errors may be:

a) The root extraction model was based on the data of Denmead and Shaw (1962). In the present comparison, it is applied to a different type of plant community and a different soil.

b) Constant value of α is not representative of actual transpiration for a wide range of potential evapotranspiration rates (see Fig. 4.3). In this comparison, however, α is kept constant for potential transpiration ranging from 0.2 to 0.74 cm/day.

CHAPTER 6: SIMULATION RESULTS AND DISCUSSION

Ground-water recharge is one of the fundamental concepts of hydrology; however, despite its basic character, recharge remains one of the least understood processes. Factors affecting the recharge are a) soil type, b) rainfall, c) initial depth to ground water, d) initial moisture distribution, e) rooting depth, f) vegetation density, and g) evapotranspiration. In order to understand the importance of these factors in affecting the recharge process, ground-water recharge is investigated in this section, by varying these factors one at a time, with the numerical model developed in this study. Shown in Table 6.1 are the factors affecting recharge which are considered in this study, characterization of each factor in the model, how each factor is varied to investigate the effect of that particular factor on ground-water recharge, and associated figures in which results are displayed. Characteristics of each factor affecting the ground-water recharge are selected to be representative of arid or semi-arid regions as much as possible.

In order to model a water table rise in a relatively short period of time, selection of simulation parameters for soil types is made by considering their saturated hydraulic conductivities only. The soil types used in this study are 50-500μ sand of Jackson et al. (1965) and Sarpy loam of Hanks and Bowers (1962). Saturated hydraulic conductivities of 50-500μ sand and Sarpy loam are 18.6 and 6.64 cm/hr, respectively. The soil model of Verma and Brutsaert (1970) is adopted in this study, and the soil properties are represented by the following functions:

$$S_n = \frac{\theta - \theta_r}{\phi - \theta_r} \tag{6.1}$$

TABLE 6.1 A summary of the problems considered in this study

Factor	Characterization	Comparison	Associated figures
Soil type	$K(h)$, $\theta(h)$, $C(h)$	50-500μ sand vs. Sarpy loam	6.5, 6.6 and 6.7
Rainfall	intensity and duration	Low-intensity (0.04 cm/hr), long duration (120 hrs) vs. high-intensity (0.48 cm/hr), short duration (10 hrs) rainfall. (Total amount of applied water in both cases is constant: 4.8 cm. of water)	6.7, 6.9 and 6.10
Initial depth to ground-water	L	Deep (4.m) vs. shallow (2.m) water table	6.7, 6.11 and 6.12
Initial moisture distribution	$\theta_i(z)$	Static vs. parabolic (at the surface layers) moisture distribution	6.12, 6.13 and 6.14
Rooting depth	d	Deep (.8m) vs. shallow (.2m) rooting depth	6.7, 6.15 and 6.16
Vegetation density	L_a	Dense vs. light vegetation	6.16, 6.17 and 6.18
Potential Evapotranspiration	E_t^*	Constant vs. diurnal potential evapotranspiration	6.16, 6.21 and 6.22

$$S_n = \frac{1}{1 + (\frac{h}{h_b})^{\lambda}}, \qquad \lambda > 1 \tag{6.2}$$

$$K = K_o S_n^{\varepsilon} \tag{6.3}$$

$$C = \frac{d\theta}{dh} = - \frac{\lambda(\phi - \theta_r)}{h_b} (\frac{h}{h_b})^{\lambda-1} S_n^2, \qquad \lambda > 1 \tag{6.4}$$

where

θ_r is residual moisture content,

S_n is normalized saturation, and

h_b, λ and ε are the soil parameters,

The soil parameters appearing in the above equations are calculated with the aid of the least square curve-fitting technique, using the data for Sarpy loam and the 50-500μ sand; the estimated values of these soil parameters are listed in Table (6.2). Actual data and least square fitted soil-retention curves are shown in Fig. (6.1), Fig. (6.2), Fig. (6.3), and Fig. (6.4). Although in Fig. (6.1), the actual data of 50-500μ sand exhibit a large hysteresis the model developed in this study does not take into account the hysteresis effect. However, the reason for selecting these soils from the literature is to avoid the use of unrealistic soil types in the simulations. Average soil parameters obtained from both sorption and desorption data do not contradict the purpose of this study.

Two rainfall events were chosen for simulation, having intensities of 0.48 and 0.04 cm/hr. The total applied water in both events is fixed at 4.8 cm. Rainfall intensity of 0.48 cm/hr with a duration of 10 hours may be observed occasionally in arid regions. Precipitation with 0.04 cm/hr intensity and 120 hours duration represents a light rainfall over

TABLE 6.2 Soil Parameters

Parameter	ϕ	θ_r	K_o	h_b	λ	ε
Soil type	%	%	cm/hr	cm		
Sarpy loam	41	5	6.64	-93.57	1.07	8.1
50-500μ sand	40	3	18.6	-79.54	3.37	3.97

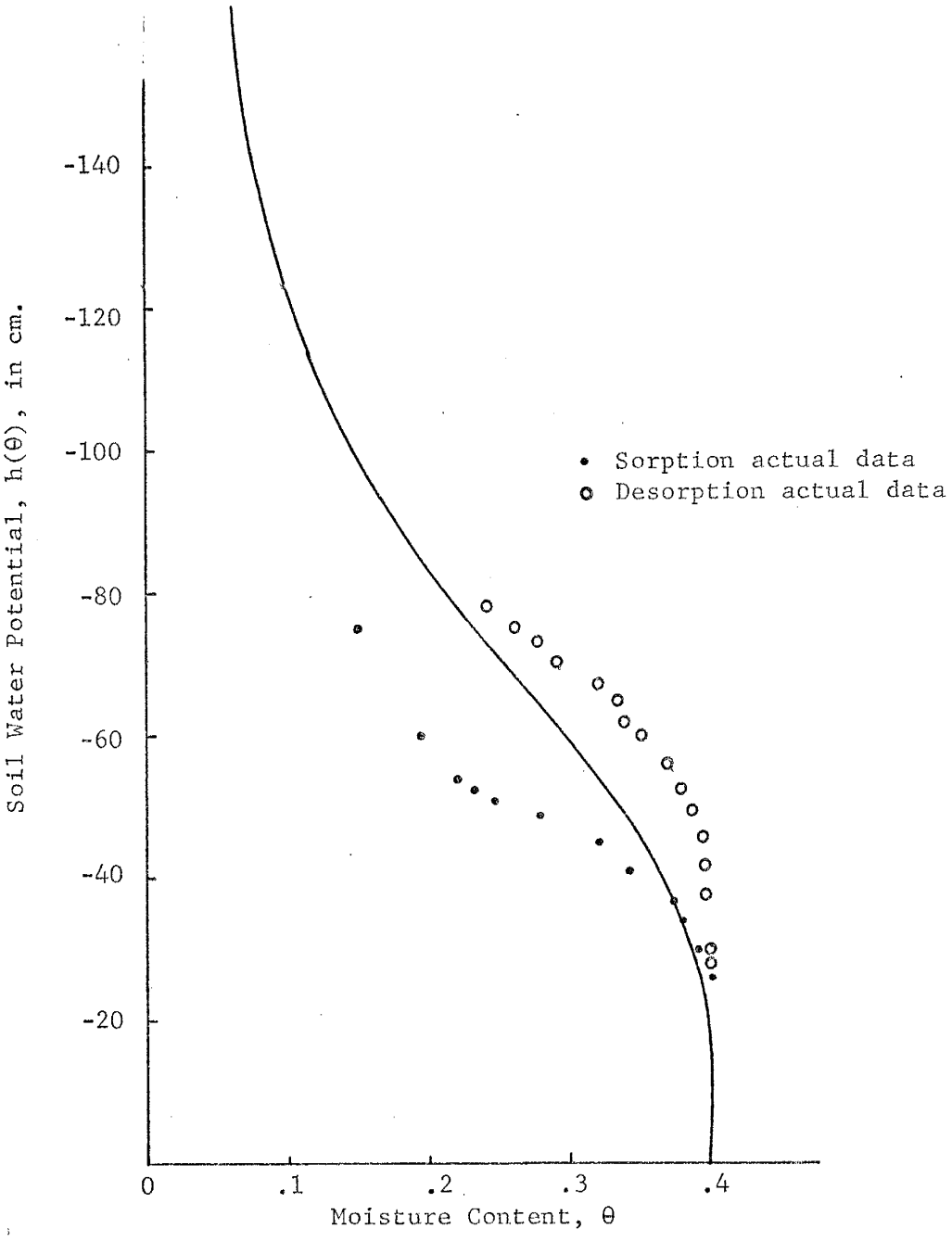

Figure 6.1: Water potential vs. moisture content curve for 50-500μ sand (data from Jackson et al., 1965)

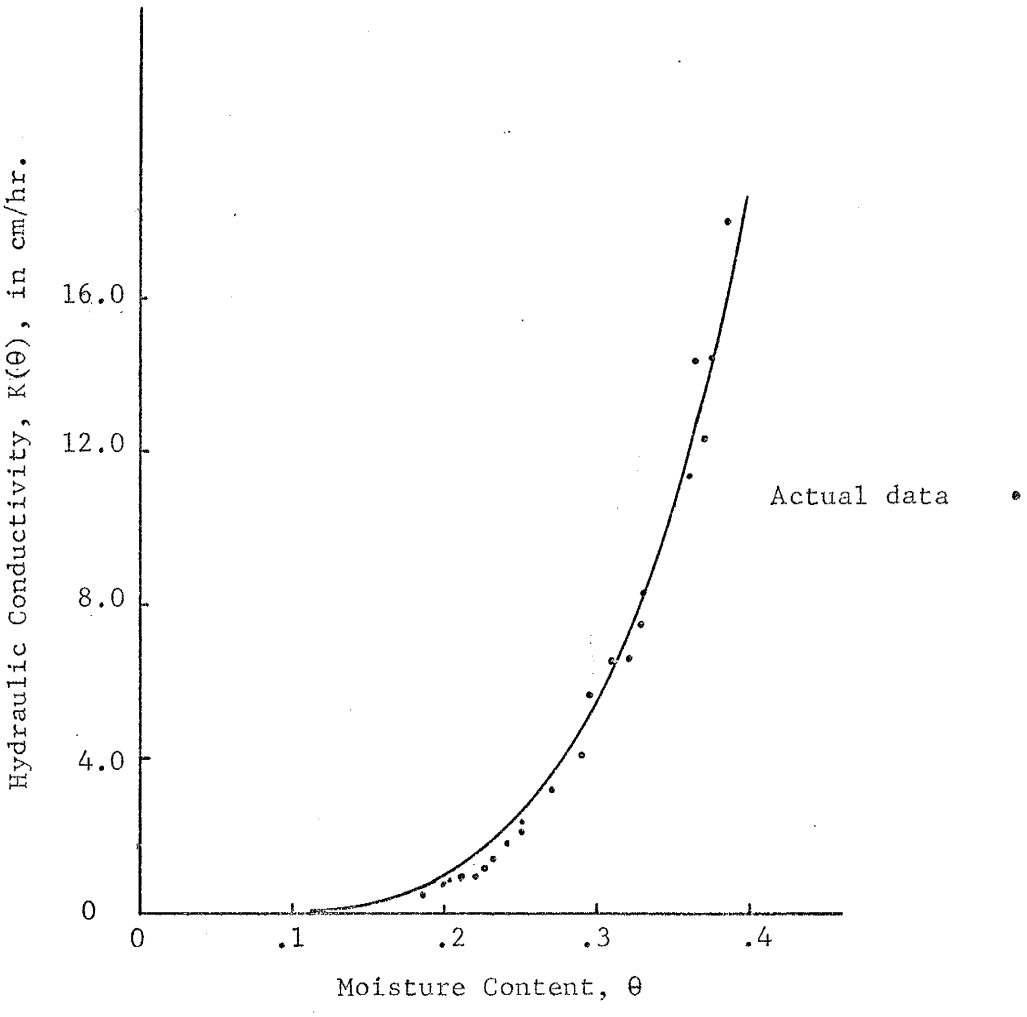

Figure 6.2 Unsaturated hydraulic conductivity vs. moisture-content curve for 50-500 μ sand (data from Jackson et al., 1965)

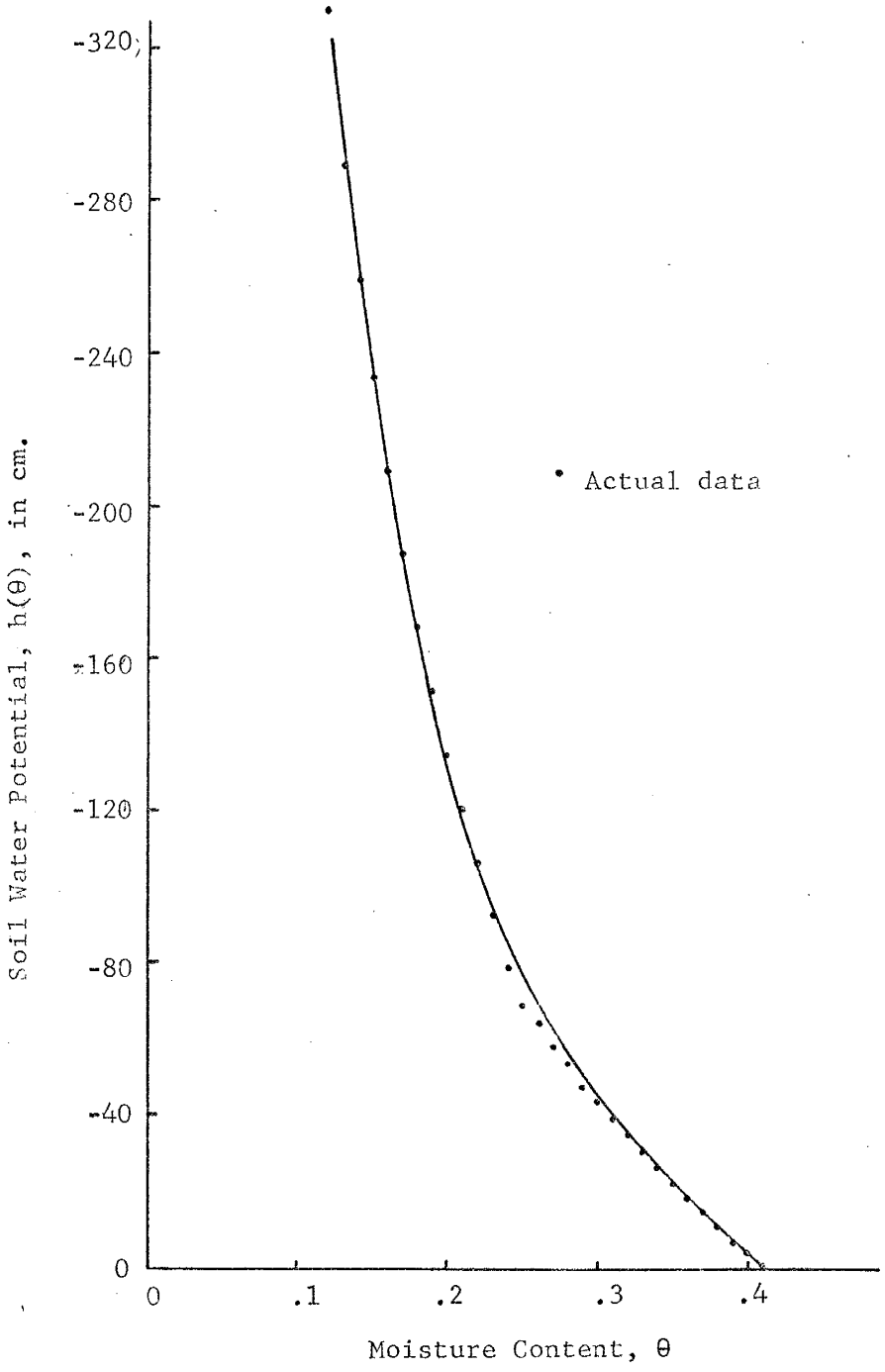

Figure 6.3: Water potential vs. moisture-content curve for Sarpy loam (data from Hanks and Bowers, 1962)

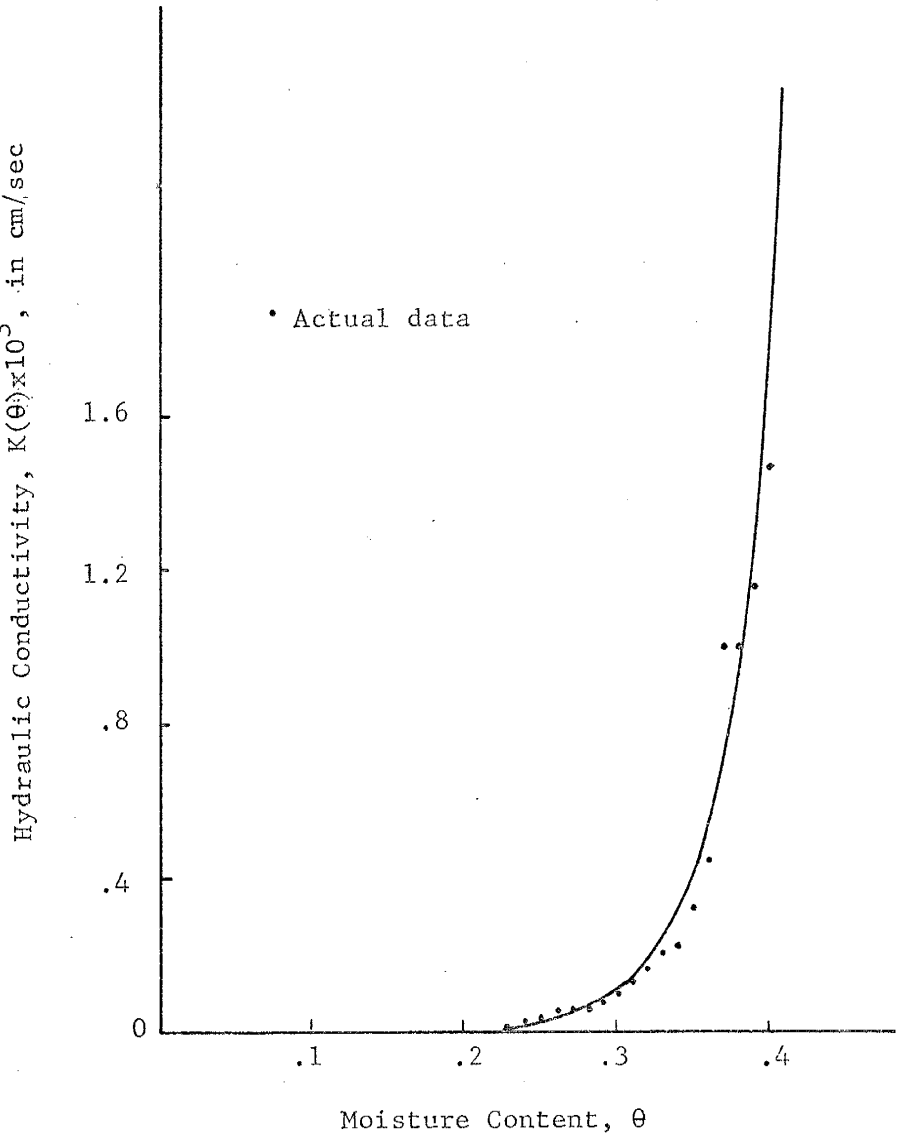

Figure 6.4: Unsaturated hydraulic conductivity vs. moisture-content curve for Sarpy loam (data from Hanks and Bowers, 1962).

an unusually long period, and also the conditions at the soil surface during a snowmelt period.

Because of limitations on computer time, the selection of initial depth to water table was restricted by the space increments (or by the number of nodal points) used in the simulations. In initial testing it was found that if the initial time increment is 0.05 hours, then space increments larger than 1 cm. through surface layers and 2 cm. for deeper layers generate a mass balance error greater than 10^{-3}% in each time step, which is cumulatively greater than 1% at the end of 40 days of simulation. Thus, by choosing 1 cm. space increment in the top 6 cm. soil layer and 2 cm. below, the over-all mass balance error is kept under 1%. A 40-day simulation under the above restrictions, with a depth to ground water of 2 m. (104 nodal points), uses about 40 minutes of computer time on the IBM 360/44 with the present model. Doubling the depth to ground water (204 nodal points) approximately doubles the computer time. Because of the cost of computation, an initial depth to ground-water greater than 4 m. was not attempted.

The bottom flux q_b in Eq. (4.18), which represents the leakage into or from the soil column, can be chosen arbitrarily. However, in order to observe the recharge as affected by only the factors listed in the first column of Table 6.1, the soil column is assumed to be underlain by an impermeable layer and, therefore, q_b is set equal to zero.

Steady state and parabolic type (within the upper layers) initial moisture distributions are selected for comparison of the effects of different initial conditions on the recharge process. In natural systems, evapotranspiration and rainfall take place sequentially by continuously changing their respective magnitudes through time. Therefore, the

requirement of constant climatologic conditions for a sufficiently long period of time for upward or downward steady-state flow is probably never met in nature. However, the initial moisture distribution generated by a steady-state flow is still preferred because it is the only moisture distribution that gives a stable water table. The selection of the parabolic distribution (in the surface layers) is completely arbitrary, but it may symbolize the climatologic history of the basin.

The effect of rooting depth on recharge is studied for two rooting depths of 20 and 80 cm. These depths are representative of rooting depths of summer annual desert plants and creosote bush, respectively. The roots are assumed to be uniformly distributed throughout the root zone, and the root distribution function is given as

$$f(z) = \begin{cases} 1/d & 0 \leq z < d \\ 0 & \text{otherwise} . \end{cases} \tag{6.5}$$

6.1 The Effect of the Soil Type

Two different soils were used to study the effect of soil type on recharge. Unfortunately, due to the complex effect of soils on recharge processes no concrete conclusions could be reached with regard to these soils.

Figure (6.5) compares cumulative recharge and evapotranspiration for Sarpy loam and 50-500μ sand. The response of the water table to changing surface conditions was characterized by a) the response time for precipitation defined as the time between the start of precipitation and at least a 0.01 cm. increase in water-table elevation, and b) the response time for evapotranspiration defined as the time between the end of precipitation and at least a 0.01 cm. drop in water table. The water-table

Figure 6.5

Comparison of recharge and actual evapotranspiration for two different types of soil.

Case 1: Sarpy loam

Case 2: 50-500μ Sand

Problem specifications:

Intensity of the rainfall: 0.04 cm/hr.

Duration of the rainfall: 120 hrs.

Thickness of the root zone: 20 cm.

Initial depth to water table: 200 cm.

Potential evapotranspiration: 0.5 cm/day

T^*_r/E^*_t : 0.9

Initial condition: static

Figure 6.6 and Fig. 6.7 are soil moisture content profiles for Case 1 and Case 2, respectively.

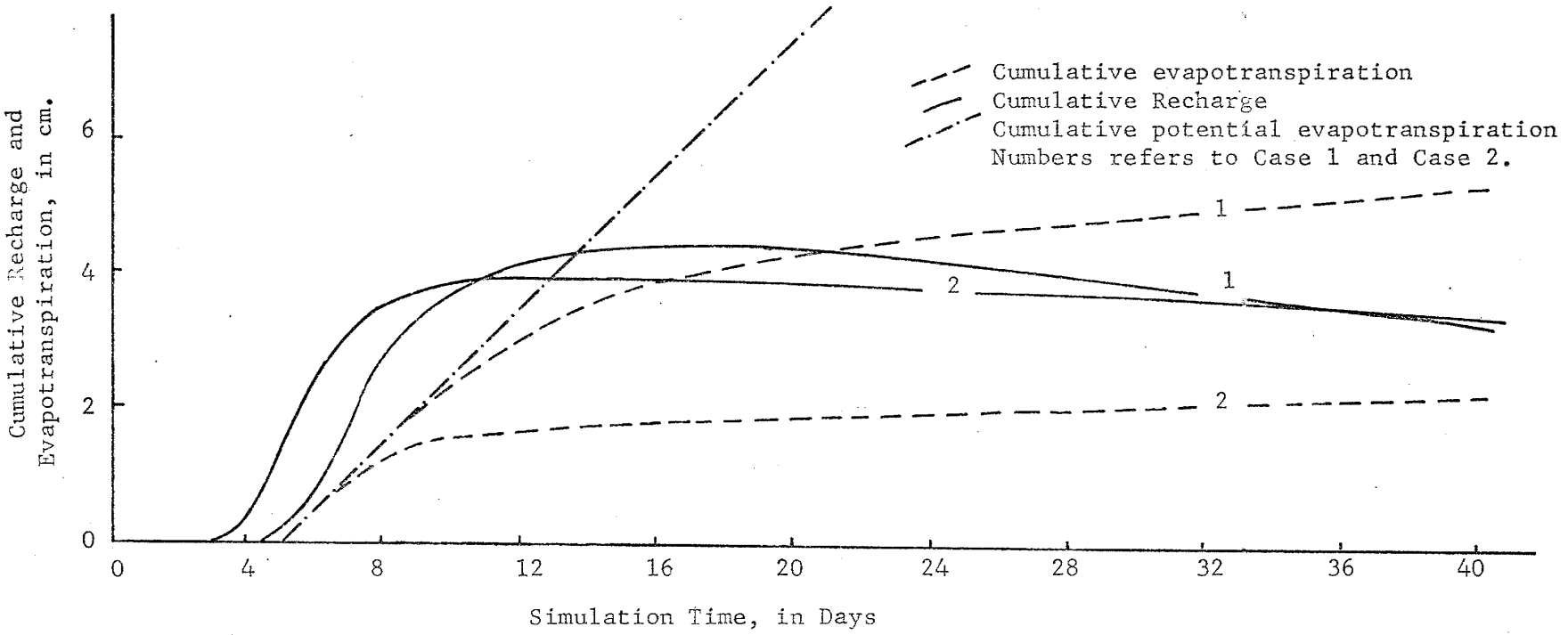
Cumulative Recharge and Evapotranspiration, in cm.
0
2
4
6
0
4
8
12
16
20
24
28
32
36
40
Simulation Time, in Days
Cumulative evapotranspiration
Cumulative Recharge
Cumulative potential evapotranspiration
Numbers refers to Case 1 and Case 2.
1
1
2
2

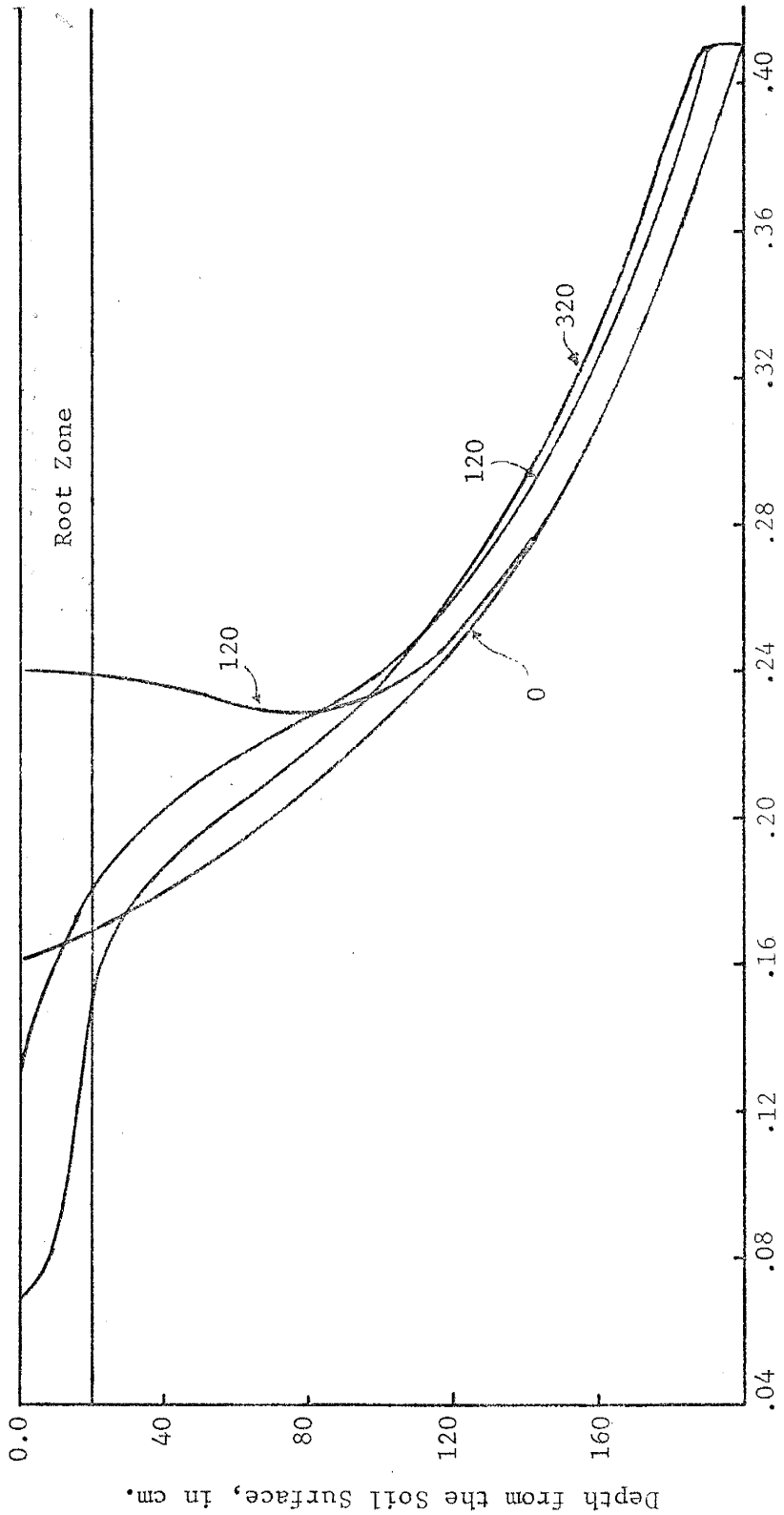

Figure 6.6 Soil moisture content profiles of Sarpy loam.
The numbers labeling the curves indicate the time in hours.

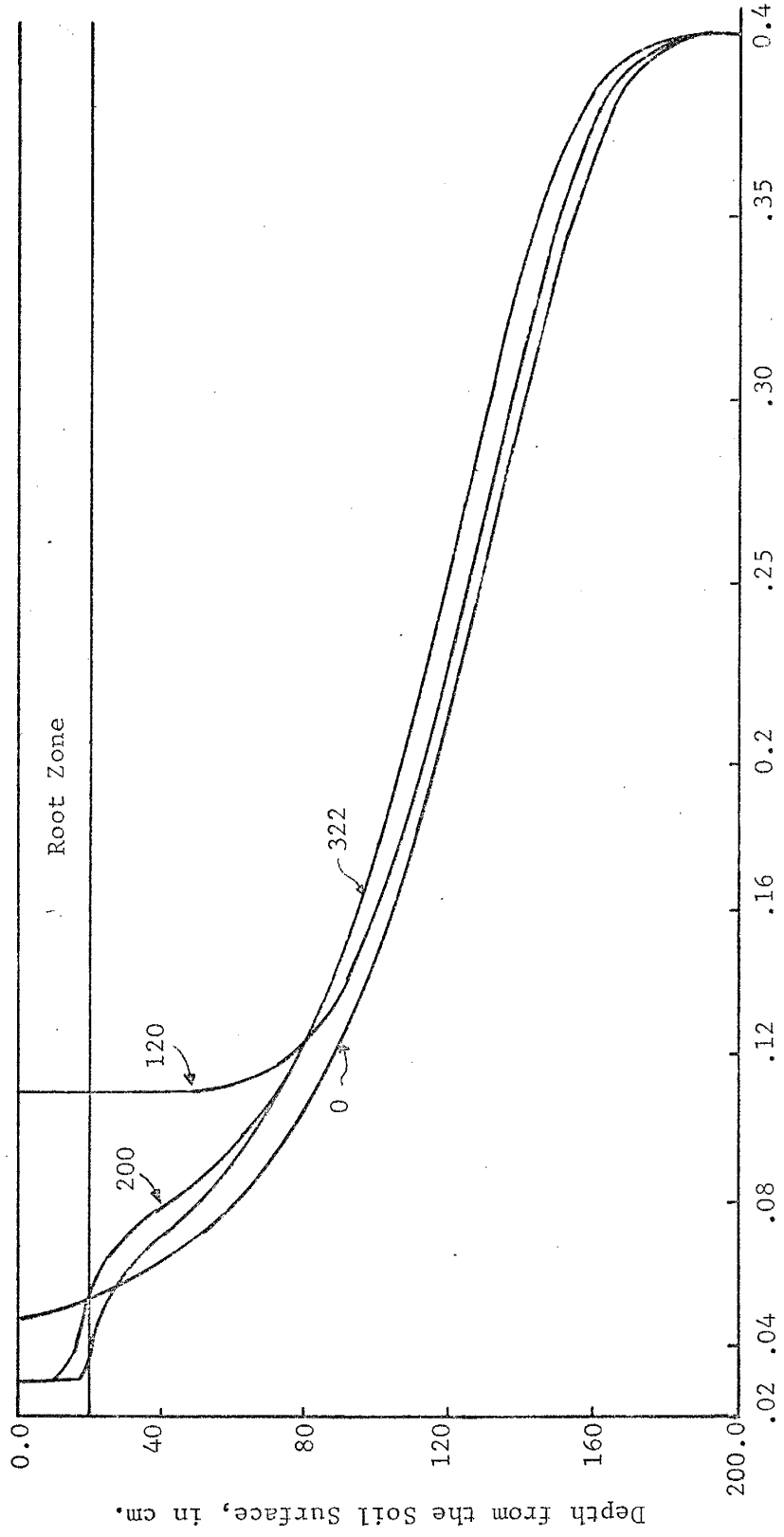

Figure 6.7 Soil moisture content profiles of 50-500μ sand.
The numbers labeling the curves indicate the time in hours.

response times of Sarpy loam and sand, for the low intensity and long duration precipitation selected in this section, are 115 and 83 hours, respectively. The water-table rise reached its maximum value of 12.2 cm. in 398 hours for loam and 10.5 cm. in 324 hours for sand. Cumulative evapotranspiration is constantly higher for Sarpy loam. Soil-moisture distributions at different times for both soils are shown in Fig. (6.6) and Fig. (6.7). The precipitation rate of 0.04 cm/hr is 0.6% and 0.22% of the saturated hydraulic conductivities of Sarpy loam and sand, respectively. For this rate of rainfall, the limiting value of surface-moisture content is 0.242 for loam and 0.109 for sand. Corresponding soil surface-water potentials are -83 and -117 cm. of water, respectively. Surface-moisture content reached its limiting value in approximately 90 hours in the sand case. Soil surface-moisture content and corresponding soil-water potential of loam, at the end of the rainfall period (120 hours), are 0.24 and -84 cm., respectively. Thus, in the loam case larger amounts of moisture accumulated at the soil surface during the course of the rainfall, and this behavior in turn increased evapotranspiration losses following the rainfall. Sarpy loam showed consistently longer response times to any input to the system. In the case of Sarpy loam, (see Fig. 6.6 and Fig. 6.7) evapotranspiration requirements are fulfilled mostly from the initial moisture storage of the upper zones. Initial moisture content at the soil surface of loam and sand are 0.161 and 0.046, while initial moisture storage of both soils are 45.8 and 38.8 cm. of water, respectively. Fulfillment of evapotranspiration requirements by the moisture of the upper zones and from the initial storage might result in a higher maximum water-table rise in Sarpy loam case

(see Fig. 6.5). Figure (6.8) compares the unsaturated hydraulic conductivities of the two soils. It is surprising to note that the loam is more permeable than the sand at low water potentials. This behavior indicates the complex effect of the soil parameters on the recharge process. However, if the case where several rainfall events take place within some time interval is considered, since evapotranspiration losses will be higher in Sarpy loam than the sand, it can be deduced that, in the long run, 50-500μ sand will be more effective in generating groundwater recharge than the Sarpy loam. Intuitively, it is expected that decreasing the time intervals between successive rainfall events will favor the generation of more ground water recharge in sandy soils.

6.2 The Effect of Rainfall Intensity and Duration

To examine the effect of various factors on recharge while keeping computer runs at a minimum, only 50-500μ sand soil type is used in the following sections. The results are compared with those obtained for the sand in Section 6.1 unless otherwise stated.

Precipitation intensity and duration chosen in this section are 0.48 cm/hr and 10 hours, respectively. This intensity of rainfall is classified as a moderate intensity (Linsley et al., 1975). However, a rainfall at this intensity and duration may be observed in arid and semi-arid regions only on rare occasions.

The average rate of snowmelt Q_m (in inches per day) can be expressed as (Gartska in Chow, 1964)

$$Q_m = K_m (T^* - 32) \tag{6.6}$$

where T^* is the air temperature in °F, and K_m is the melting constant.

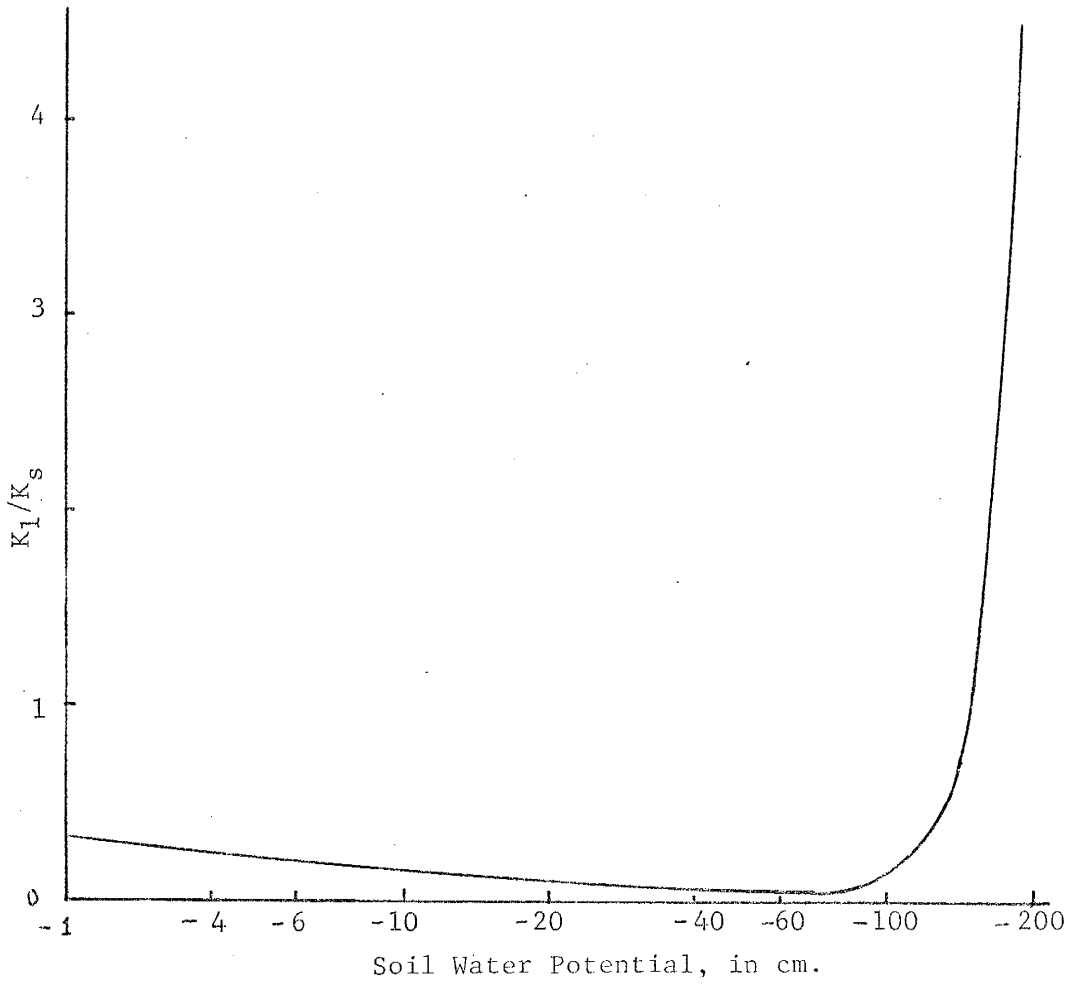

Figure 6.8: Comparison of unsaturated hydraulic conductivities of Sarpy loam (K_l) and 50-500μ sand (K_s).

The melting constant commonly ranges between 0.02 and 0.11 but has a maximum value of 0.30. Equation (6.6) yields a snowmelt rate which is equivalent to a rainfall event with an intensity of between 0.01 and 0.08 cm/hr when the air temperature is around 60°F, the specific gravity of snow is 0.25, and the melting constant ranges between 0.02 and 0.11. Thus, the conditions generated at the soil surface by a precipitation with 0.04 cm/hr intensity and 120 hours duration is comparable with the conditions generated by the melt of a 16-20 cm. (or more) snow layer during a snowmelt period.

The results of modeling these two types of precipitation on cumulative recharge and evapotranspiration are shown in Fig. (6.9). The water-table response time for high intensity rainfall is 22 hours. Water-table rise reached its maximum value of 9.73 cm. in 232 hours for this rainfall event. By the eighth day of simulation, cumulative recharge is consistently lower for the high-intensity rainfall, while cumulative evapotranspiration is consistently higher. Soil-moisture profiles of 50-500μ sand for high-intensity rainfall are shown in Fig. (6.10). The limiting value of the soil surface-moisture content for the rainfall having 0.48 cm/hr intensity is 0.177, which is about 1.62 times higher than the value for the case of the lower intensity rainfall. Corresponding soil water potential is approximately -90 cm. At the end of ten hours of precipitation, the soil surface-moisture content is 0.17. At the end of low-intensity rainfall this value is 0.109. Hence, a larger amount of moisture accumulates in the near-surface layers during high-intensity rainfall. The resulting near-surface moisture condition increases evapotranspiration losses subsequent to the rainfall.

Figure 6.9

Comparison of recharge and actual evapotranspiration for two different types of precipitation events.

Case 1: Precipitation intensity = 0.04 cm/hr.

Precipitation duration = 120 hours

Case 2: Precipitation intensity = 0.48 cm/hr.

Precipitation duration = 10 hours

Problem specifications:

Soil type: 50-500μ sand

Thickness of the root zone: 20 cm.

Initial depth to water table: 200 cm.

Potential evapotranspiration: 0.5 cm/day

T^*_r/E^*_t : 0.9

Initial condition: static

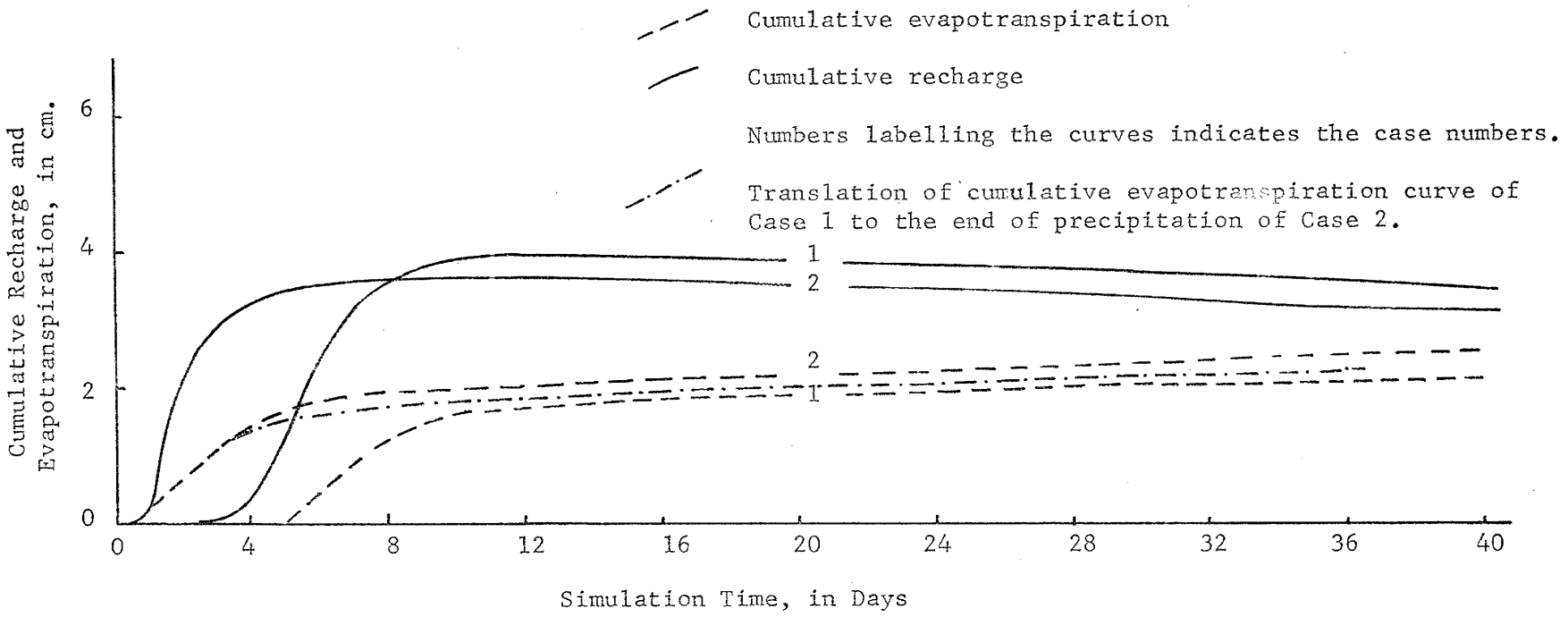
Cumulative evapotranspiration
Cumulative recharge
Numbers labelling the curves indicates the case numbers.
Translation of cumulative evapotranspiration curve of Case 1 to the end of precipitation of Case 2.
Cumulative Recharge and Evapotranspiration, in cm.
0
2
4
6
1
2
2
1
0
4
8
12
16
20
24
28
32
36
40
Simulation Time, in Days

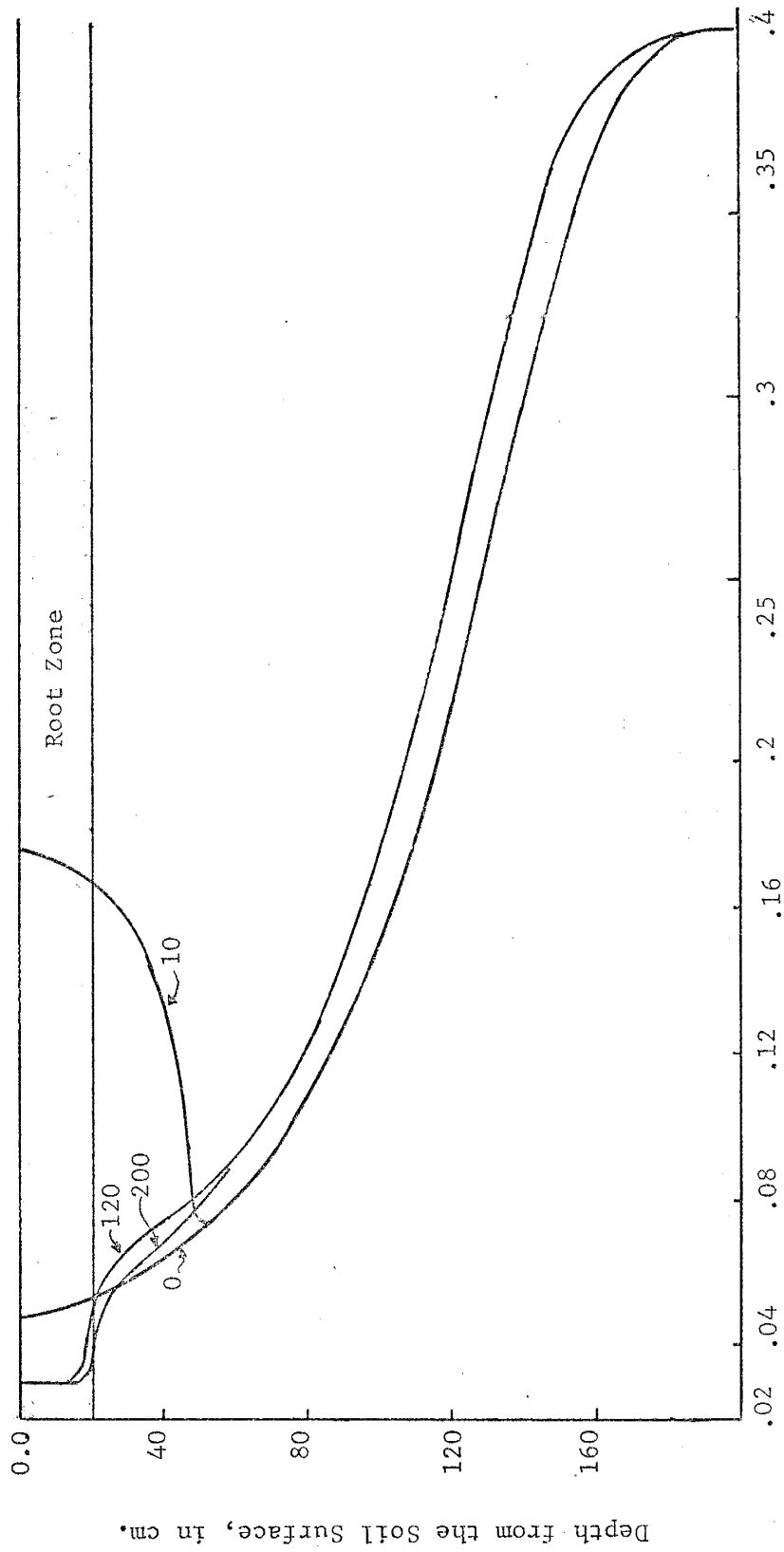

Figure 6.10 Soil moisture content profiles of 50-500μ sand for 0.48 cm/hr precipitation intensity and 10 hours duration. The numbers labeling the curves indicate the time in hours.

In both cases the presence of an impermeable layer at the bottom of the soil column did not show any effect at the soil surface during the period of rainfall. The saturated hydraulic conductivity of the sand is 18.6 cm/hr, and intensities of both rainfalls are significantly less (0.2% and 2.6%) than this value. For the rainfalls whose intensity is less than saturated hydraulic conductivity of the soil, the generation of surface runoff is not expected unless the duration allows the water table to rise to soil surface. The choice of a precipitation whose total amount is 4.8 cm. and duration and intensity are such that surface runoff will occur for 50-500μ sand would be unrealistic. Therefore, simulation of such an event was not attempted in this study. However, in natural terrains where some water is lost to adjacent areas by surface runoff, the effectiveness of high-intensity rainfalls in generating ground-water recharge will be further reduced.

6.3 Initial Depth to Ground-Water

The effect of the initial position of the water table on recharge is studied for two different depths: 200 cm. and 400 cm. A comparison of cumulative recharge and actual evapotranspiration for these initial depths is shown in Fig. (6.11). Since static moisture distribution, which is a special case of steady state flow where bottom flux $q_b = 0$, is used as an initial condition in both cases, the case with a 400 cm. initial depth to water table gives rise to dryer surface layers.

Doubling the initial depth to the water table increased the water-table response time from 83 hours to 2905. Almost no water-table rise was observed, even though the computer program was run for over 3000 hours of simulation time. In both cases the introduction of 4.8 cm.

Figure 6.11

Comparison of cumulative recharge and actual evapotranspiration for two different initial depth to ground-water.

Case 1: Initial depth to ground-water = 400 cm.

Case 2: Initial depth to ground-water = 200 cm.

Problem specifications:

Soil types: 50-500μ sand

Thickness of the root zone: 20 cm.

Precipitation intensity: 0.04 cm/hr.

Precipitation duration: 120 hours

Potential evapotranspiration: 0.5 cm/day

T^*_r/E^*_t : 0.9

Initial condition: static

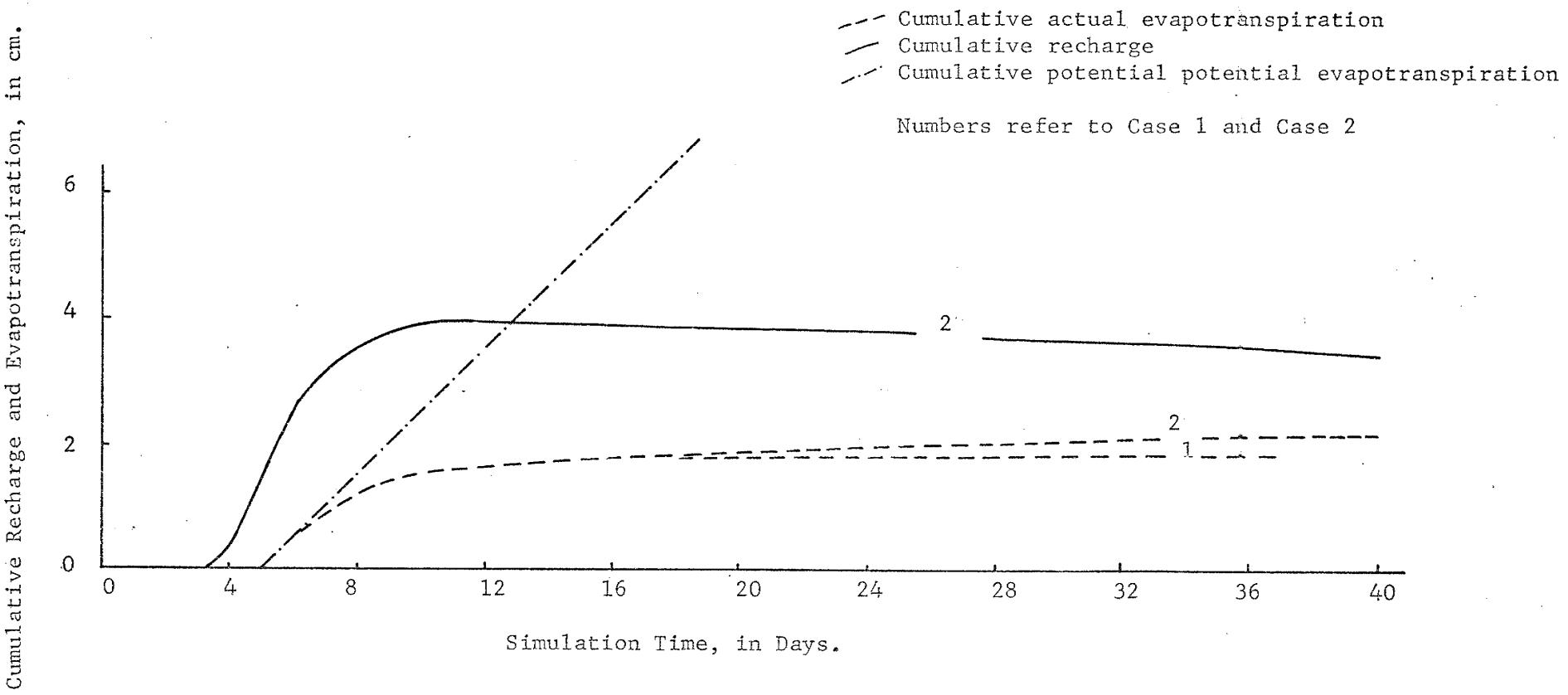
Cumulative actual evapotranspiration
Cumulative recharge
Cumulative potential potential evapotranspiration
Numbers refer to Case 1 and Case 2
Cumulative Recharge and Evapotranspiration, in cm.
0
2
4
6
0
4
8
12
16
20
24
28
32
36
40
2
2
1
Simulation Time, in Days.

of water into the soil column was simulated. Under evaporative conditions ensuing rainfall, 45.8% and 39.4% of the total amount of applied water is lost to the atmosphere by evapotranspiration by the 36^{th} day of simulation in shallow and deep water-table cases, respectively. On this day, the ratios of actual to potential evapotranspiration were 3.46% and 0.72%, respectively for the two cases, indicating an evapotranspiration rate about 4.8 times higher in the shallow water table case than in the deep water table case.

The soil-moisture profiles of the deeper water-table case are shown in Fig. (6.12). The rate of change of the shape of the soil-moisture profile significantly slowed down following the 885th hour. The soil zone below 250 cm. did not significantly respond to the rainfall even in longer simulation times. For the deep water table case, 52% of the total applied water was still remaining in the soil column at the end of 3000 hours of simulation, indicating that the initial moisture profile may have a significant effect on recharge, especially when the water table is at a considerable distance below the land surface.

6.4 Initial Condition

To investigate the effect of the initial condition on the recharge process, an alternative initial condition to the static one, defined by the parabolic equation

$$\theta_i(z,0) = \begin{cases} -1.95*10^{-6}z^2 + 6.25*10^{-4}z + 0.05 & 0 \leq z \leq 262 \\ \text{static} \end{cases} \tag{6.7}$$

was used in the simulation discussed in this section.

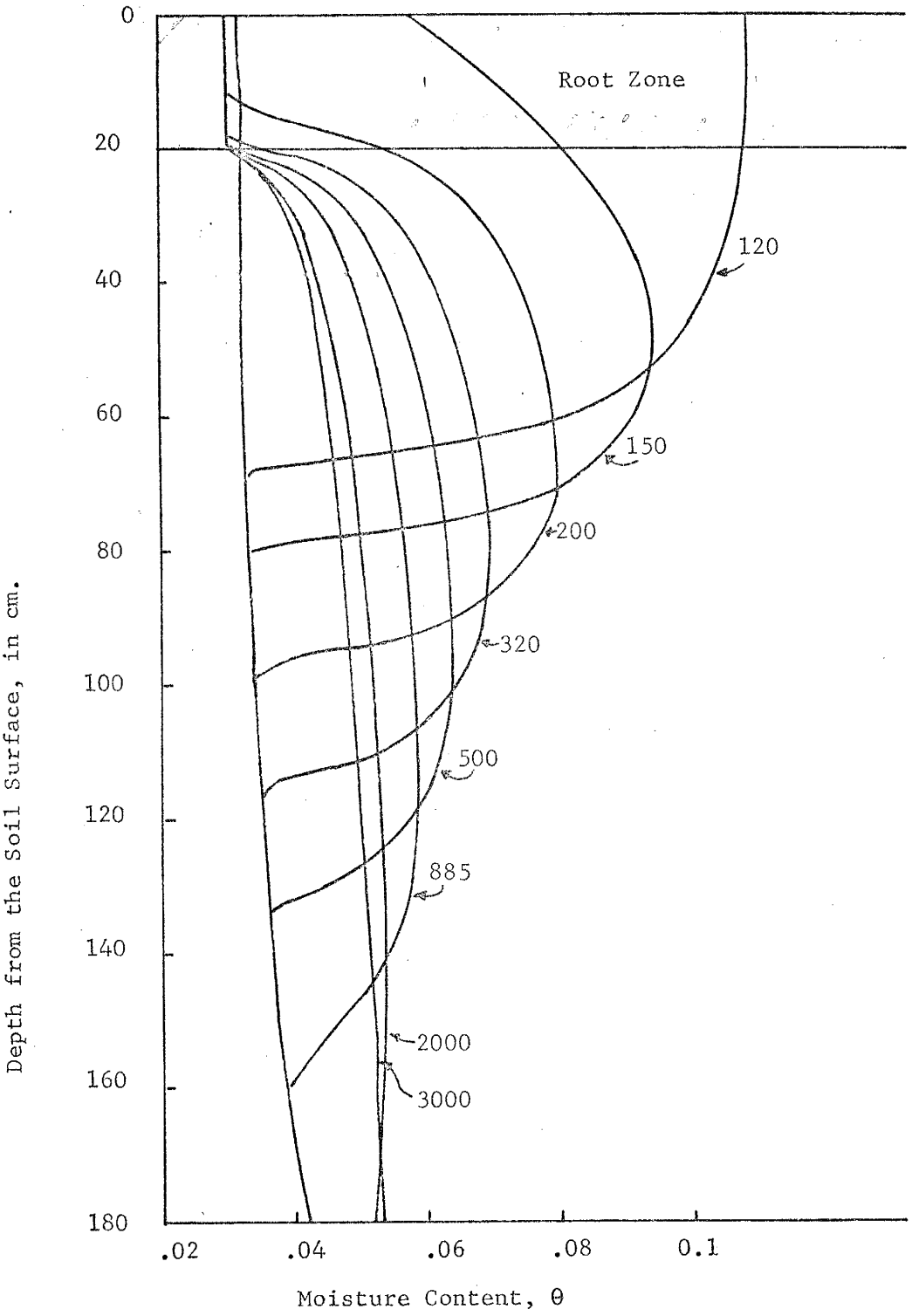

Figure 6.12 Soil moisture content profil of 50-500μ sand for 400 cm initial depth to ground-water. The numbers labeling the curves indicate the time in hours.

Figure (6.13) compares cumulative evapotranspiration and recharge as simulated with two distinctive initial conditions: static and parabolic. Soil-moisture profiles for the parabolic initial condition defined by Eq. (6.7) are shown in Fig. (6.14). The precipitation intensity and the soil-type are the same as in Section 6.3. The limiting value of soil surface-moisture content of sand for rainfall with 0.04 cm/hr intensity is 0.109. In both cases, soil surface-moisture content reached this limiting value within the duration (120 hours) of the rainfall (see Fig. 6.12 and 6.14). Since water potentials developed at the surface are the same in both cases, cumulative evapotranspiration for static and parabolic initial conditions did not show any significant differences in 336 hours of simulation time, while cumulative ground-water recharge is significantly higher for the wetter initial condition. For the wetter initial condition, the 4 m. deep water table responded in 7 hours and continued to rise without reaching a maximum during the 336 hours simulation time. The water-table rise at the end of 336 hours was 18.68 cm. This rise and rapid response of the water table is clearly due to the assumed initial condition, the determination of which would be based on climatological history of the basin. It can be concluded, at this point, that ground-water recharge taking place at any given time is not due to recent or current rainfall, but rather is the result of antecedent moisture stored in the soil column from previous rainfalls which have been displaced downward by successive bouts of infiltration.

The above result agrees with the findings of Horton and Hawkins (1965) in their laboratory experiment on infiltration, with Wilson and Gelhar (1974) in their analysis of dispersive mixing of unsaturated

Figure 6.13

Cumulative recharge and actual evapotranspiration for parabolic initial condition.

Case 1: Static

Case 2: Parabolic

Problem specifications:

Soil type: 50-500μ sand

Rainfall intensity: 0.04 cm/hr.

Rainfall duration: 120 hours

Initial depth to water table: 400 cm.

Rooting depth: 20 cm.

Potential evapotranspiration: 0.5 cm/day

T_r^*/E_t^* : 0.9

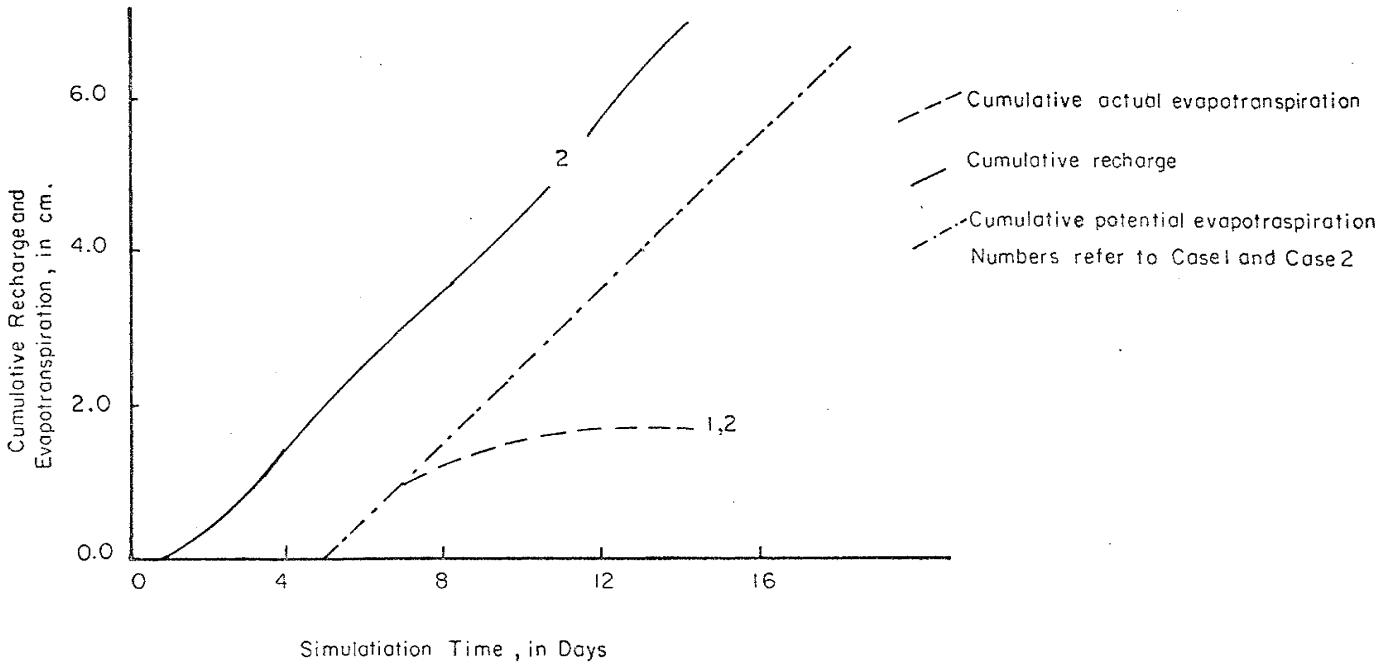
6.0
4.0
2.0
0.0
0
4
8
12
16
2
1,2
Cumulative Recharge and Evapotranspiration, in cm.
Simulatiation Time, in Days
Cumulative actual evapotranspiration
Cumulative recharge
Cumulative potential evapotraspiration
Numbers refer to Case1 and Case2

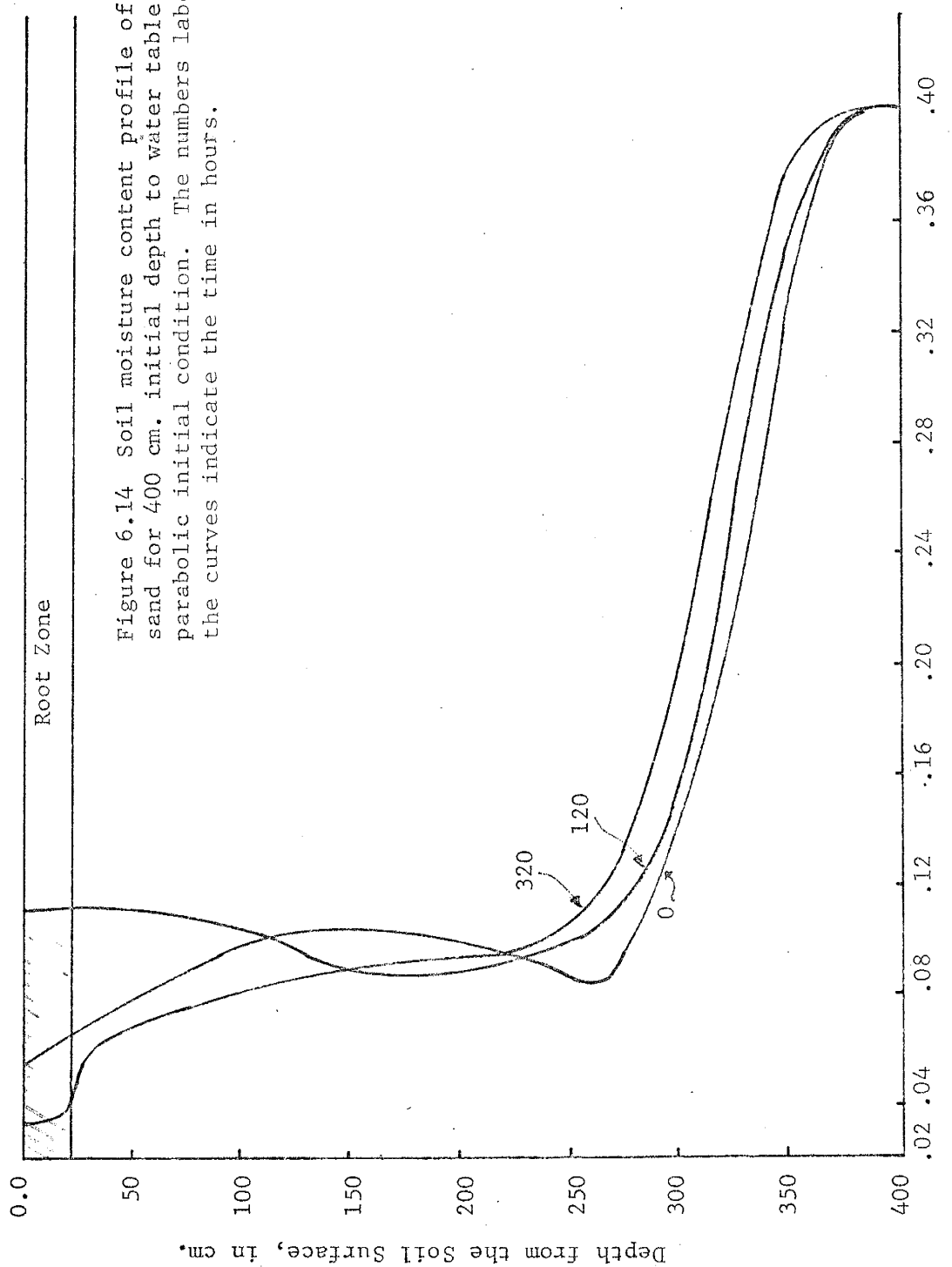

Figure 6.14 Soil moisture content profile of 50-500 μ sand for 400 cm. initial depth to water table and parabolic initial condition. The numbers labeling the curves indicate the time in hours.

porous medium, and with Oakes (1977) in his field observation of the movement of water and solutes through the unsaturated zone of the chalk formation in England. For example, Horton and Hawkins (1965) used a 4-foot-long by 2 inch plexiglass tube filled with a sandy clay soil. The column was saturated with water and was allowed to drain. Soil moisture after drainage was 30% by volume. A volume equivalent to 1 inch of rain, and containing 50μc of tritium per liter, was then added to the top of the column. Thereafter, the equivalent of 1 inch of rain, containing no tritium, was added daily (Monday through Friday of each week), and the column effluent was analyzed daily for tritium. Since tritium was not detected in the column effluent immediately after its addition, they concluded that flow through the sandy clay soil occurred primarily by downward displacement of water remaining in the soil after drainage. Sixty-seven percent of the water present in the soil at the time of the tritium addition was displaced before the effluent tritium concentration reached 2% of the feed concentration. Furthermore, 87% was displaced before the peak tritium concentration appeared in the effluent.

Freeze (1967) has also emphasized that the initial condition, which is determined from the climatological history of a basin, has a significant effect on ground-water recharge.

6.5 Rooting Depth

A detailed study of the root habits of desert plants is given by Cannon (1911). It is reported in this study that the roots of most annual desert plants reach no deeper than 20 cm. and the period of their activity is comparatively brief. The annual plants having deeper penetrating root systems survive longer after the wet season has passed. For example,

the summer annual, Kallstroemia grandiflora, which has a root system capable of penetrating the ground to a depth of more than 22 cm., outlives many other forms. The root penetration of the cactus, type Opuntia arbuscula, is between 2 to 5 cm. Among the perennials, the roots of Prosopis have been observed to reach 5 to 8 meters below the ground surface. Thames (in Sammis et al., 1977) indicated that the roots of creosote rarely penetrate below one meter.

The rooting depth of 20 cm. used in the simulations, then, is representative of annual desert plants. In order to investigate the effect of rooting depth on the recharge process, an additional root depth of 80 cm. was chosen, which may represent the root habits of creosote bush. The comparison of simulation results for cumulative recharge and actual evapotranspiration for two rooting depths is shown in Fig. (6.15). For the 80 cm. rooting depth, the water table reached its maximum value of 8.27 cm. in 197 hours, while for the 20 cm. rooting depth these values were 10.54 cm. and 324 hours, respectively. As seen in Fig. (6.15), cumulative evapotranspiration is significantly higher for the deeper rooting depth, and the saturated zone that developed during 120 hours of rainfall, completely disappeared in 589 hours of simulation time. Depletion of the saturated zone indicate the capability of plants having deep penetrating roots in extracting water from ground-water reservoirs. Soil moisture profiles for the deeper rooting depths is shown in Fig. (6.16).

6.6 Vegetation Density

Ritchie (1971) showed that the ratio of potential transpiration to potential evapotranspiration can be expressed as

Figure 6.15

Comparison of recharge and actual evapotranspiration for two different thickness of root depth.

Case 1: Rooting depth 80 cm.

Case 2: Rooting depth 20 cm.

Problem specifications:

Soil type: 50-500μ sand

Precipitation intensity: 0.04 cm/hr.

Precipitation duration: 120 hours

Initial depth to water table: 200 cm.

Potential evapotranspiration: 0.5 cm/day

T_r^*/E_t^* : 0.9

Initial condition: static

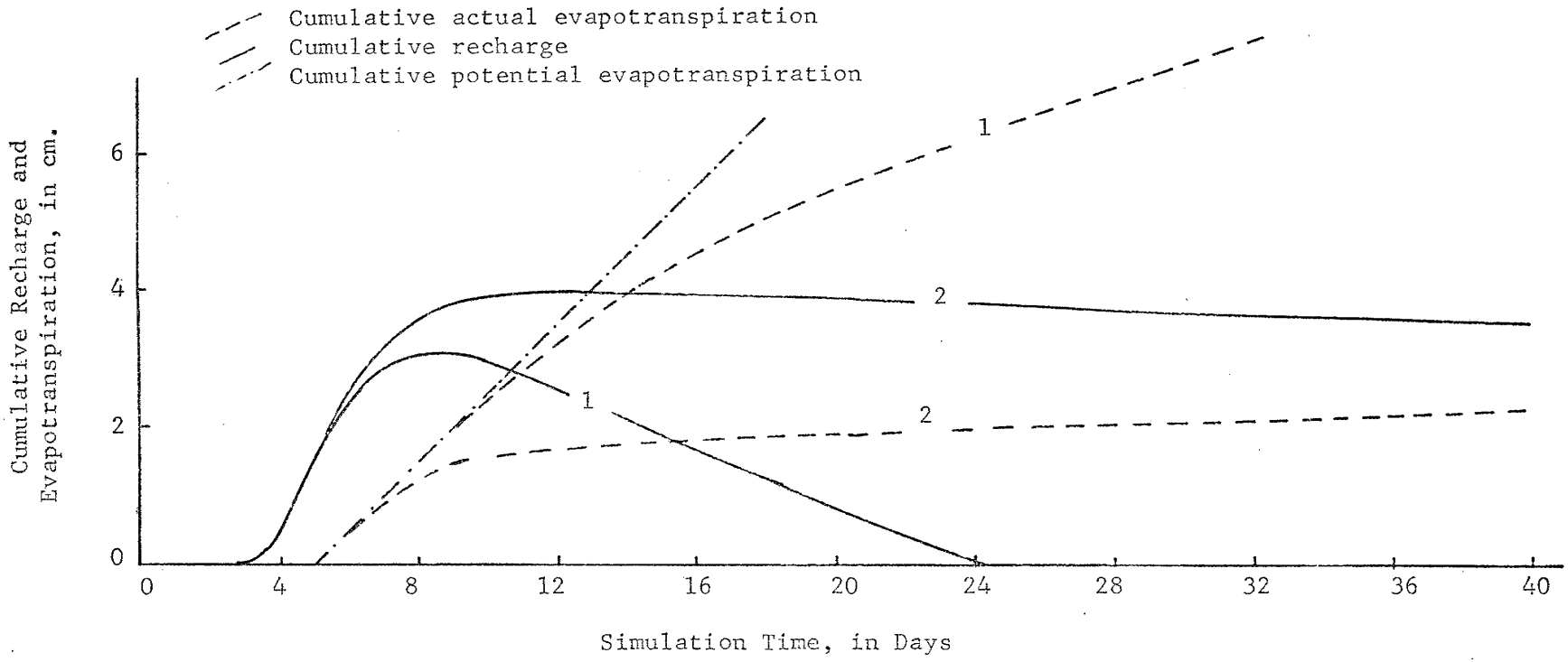
Cumulative actual evapotranspiration
Cumulative recharge
Cumulative potential evapotranspiration
Cumulative Recharge and Evapotranspiration, in cm.
0
2
4
6
0
4
8
12
16
20
24
28
32
36
40
Simulation Time, in Days
1
2
1
2

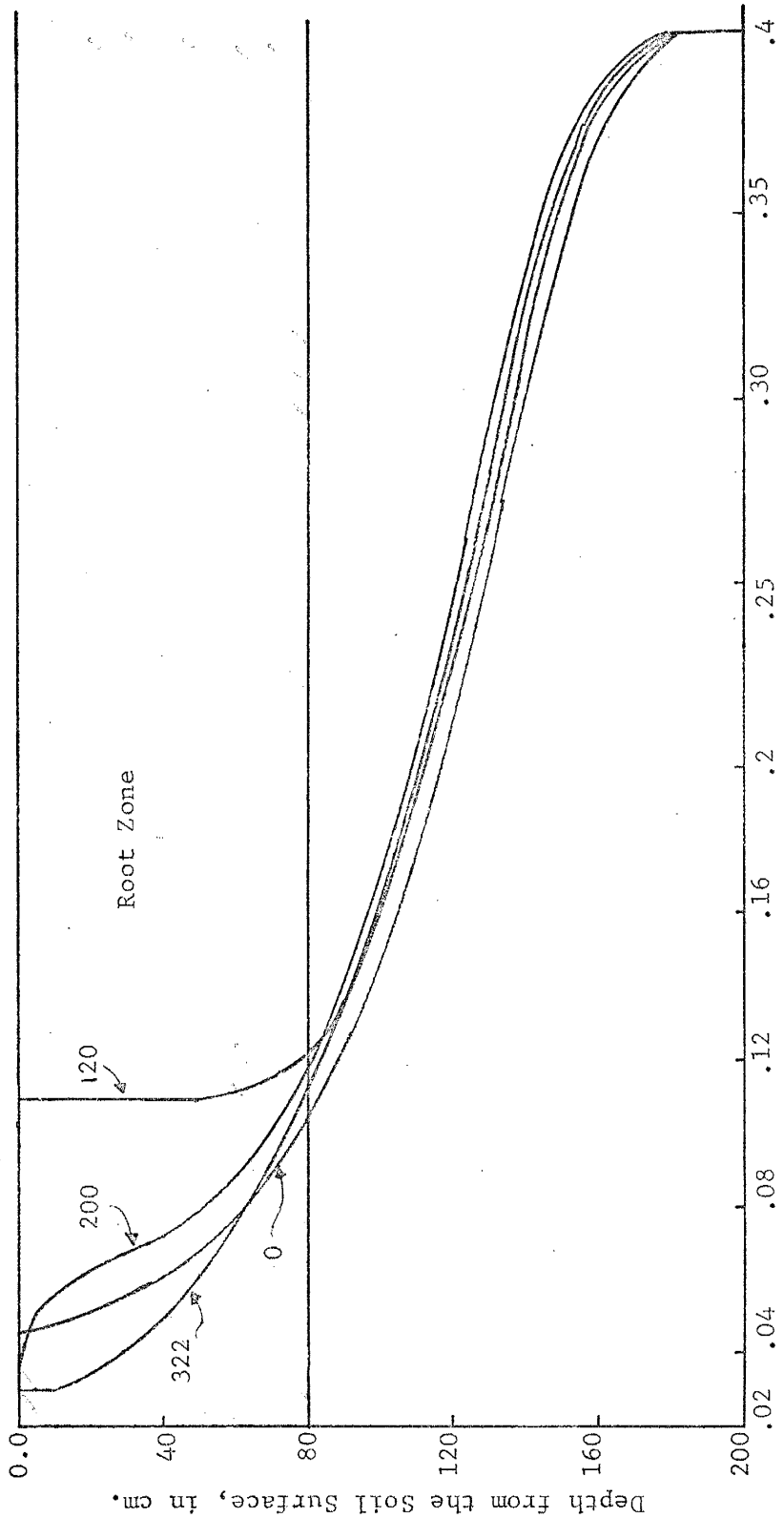

Figure 6.16 Soil moisture content profile of 50-500μ sand for 80 cm. rooting depth. The numbers labeling the curves indicate the time in hours.

$$T_r^*/E_t^* = -0.21 + 0.7\sqrt{L_a} \qquad (6.9)$$

within the limits $0.1 \leq L_a \leq 2.7$. Since this equation is empirical its applicability to all climates and crops is seemingly doubtful (Ritchie, 1972). However, after examining the data of Monteith et al. (1965, reported in Ritchie, 1972) for barley in England and Brun et al. (1972, reported in Ritchie, 1972) for soybeans and sorghum in Kansas, Ritchie concluded that Eq. (6.9) is approximately correct. Because of its simplicity, Eq. (6.9) is adopted in this study, so that an idea of the vegetation densities corresponding to given T_r^*/E_t^* ratios can be obtained.

In this section T_r^*/E_t^* is assumed to be 0.4, whereas 0.9 was used for simulations in the previous sections. The ratios 0.4 and 0.9 correspond to leaf-area indices of 0.76 and 2.51 or, in other words, they represent a light and a dense vegetation, respectively.

The comparison of cumulative recharge and evapotranspiration for simulation results is shown in Fig. (6.17). Light-density vegetation reduced the evapotranspiration losses and increased the ground-water recharge, as expected. Soil-moisture profiles for light-density vegetation are shown in Fig. (6.18).

6.7 Diurnal Variations in Potential Evapotranspiration

Two typical E_t^* curves are given in Fig. (6.19). Ward (1967) has indicated that the shape of the diurnal curve of E_t^* is more important than the daily totals on the amount of actual evapotranspiration. The effect of diurnal fluctuations of E_t^* on evaporative discharge from the saturated zone is also discussed by Ward (1967). He suggests that losses of ground-water by evapotranspiration during the day when

Figure 6.17

Comparison of cumulative recharge and cumulative evapotranspiration for two different vegetation densities.

Case 1: Leaf area index 2.51%

Case 2: Leaf area index .76%

Problem specifications:

Soil type: 50-500μ sand

Rainfall intensity: 0.04 cm/hr

Rainfall duration: 120 hours

Initial depth to water table: 200 cm.

Rooting depth: 80 cm.

Potential evapotranspiration: .5 cm/day

Initial condition: static

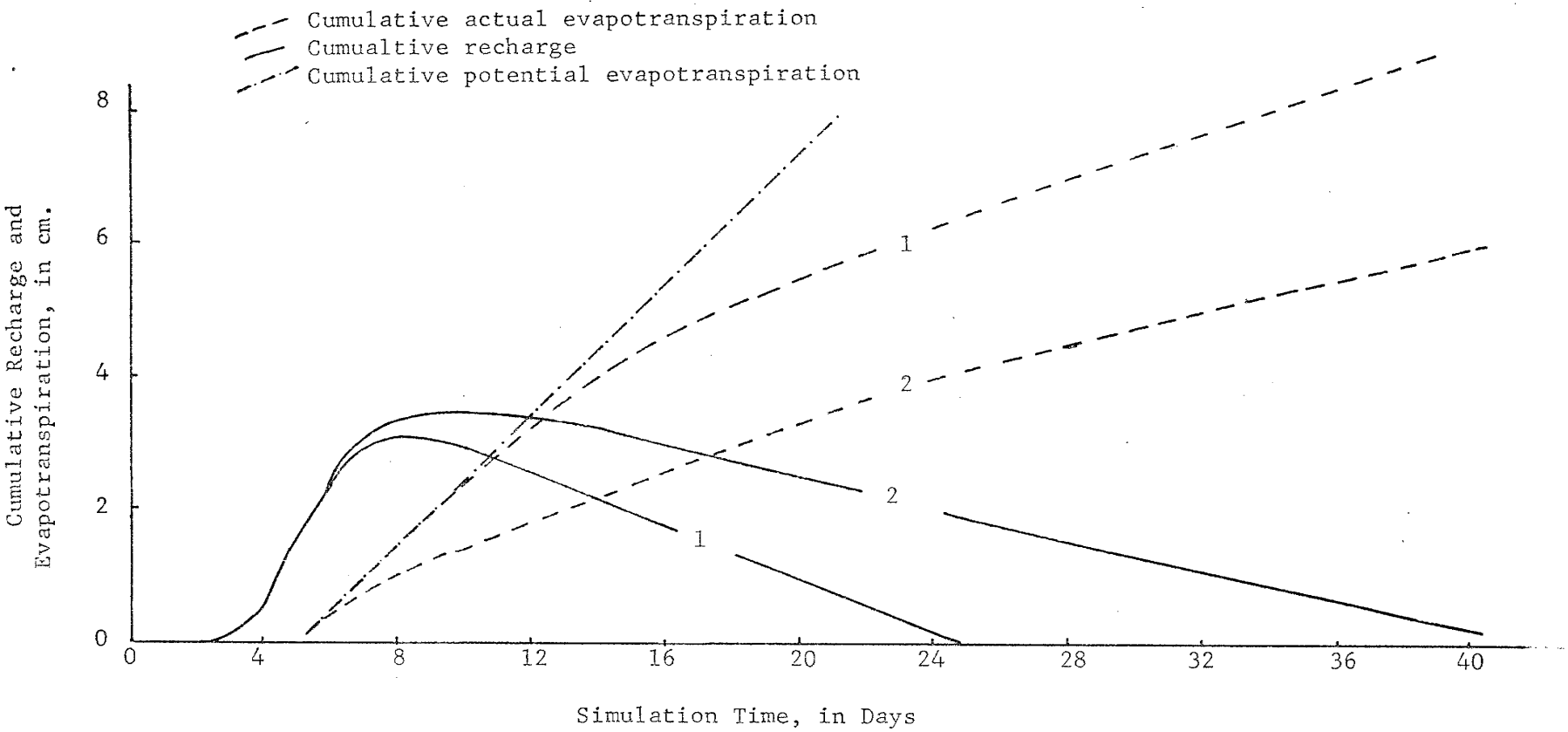
Cumulative actual evapotranspiration
Cumualtive recharge
Cumulative potential evapotranspiration
Cumulative Recharge and Evapotranspiration, in cm.
0
2
4
6
8
0
4
8
12
16
20
24
28
32
36
40
Simulation Time, in Days
1
2
2
1

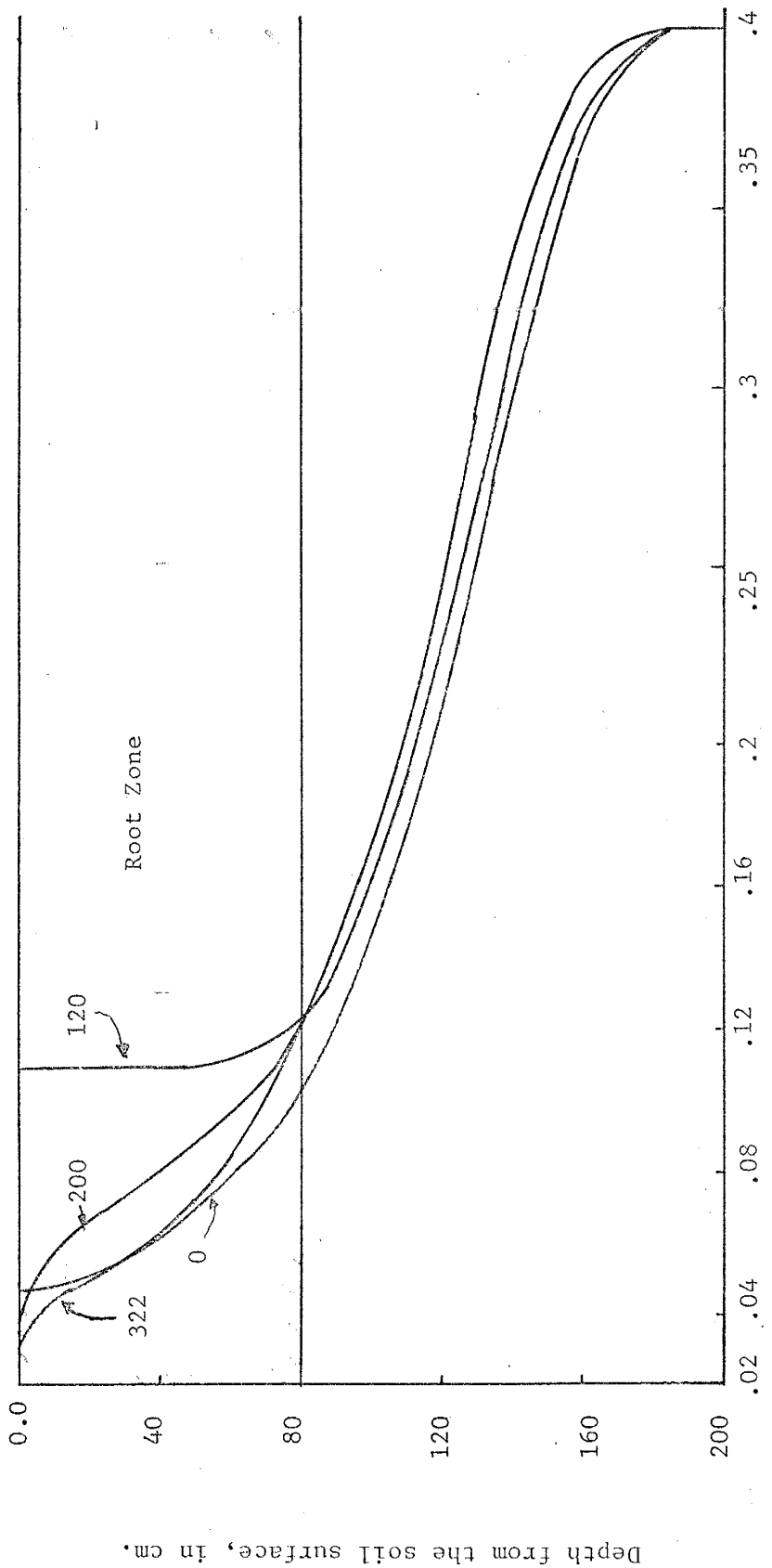

Figure 6.18: Soil moisture content profiles of 50-500μ sand for 0.76 leaf area index. The numbers labeling the curves indicate the time in hours.

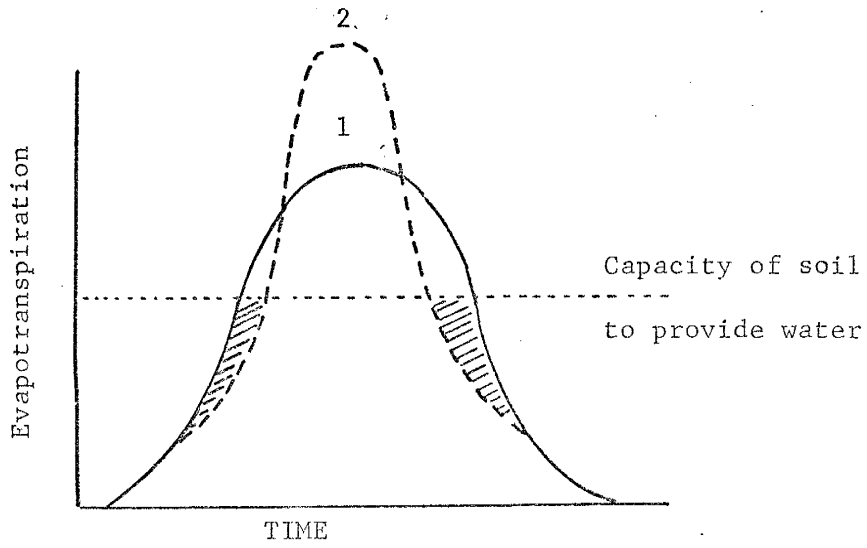

Figure 6.19: Diurnal variations of potential evapotranspiration throughout a 24-hour period. Total T_r^* represented by each curve is identical but more evapotranspiration in fact occurs at the potential rate in the case of curve (1) than in the case of curve (2), the difference being represented by the shaded area of the graph. (After Visser, in Ward 1967).

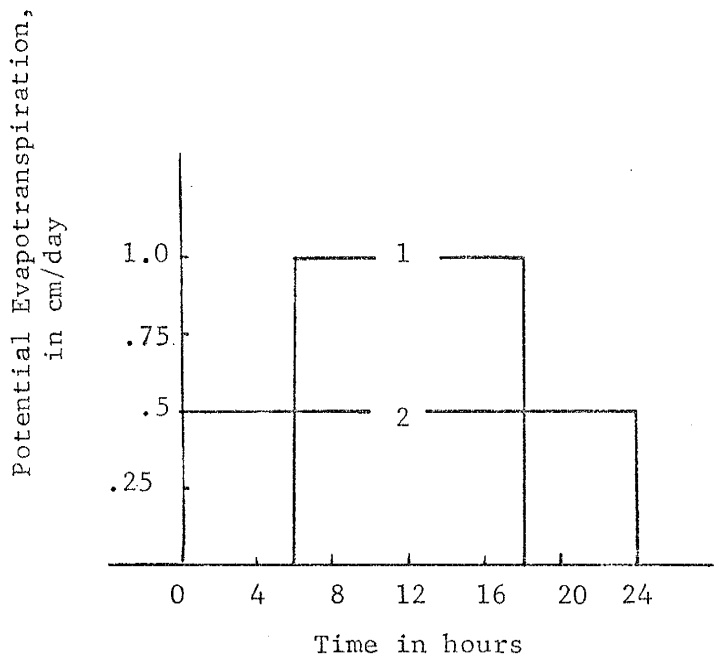

Figure 6.20: Definition of diurnal potential evapotranspiration in the present model. Numbers (1 and 2) labelling the curves are diurnally varying and uniform T_f^* curves respectively. Notice that the areas under the two curves are identical.

atmospheric evapotranspiration demand is high may exceed the groundwater inflow rate from the surrounding areas and thus cause the water table to drop. During the evening when evapotranspiration is reduced the water table may recover.

In the present model, diurnal variation of E_t^* curve is modeled with the expression

$$E_{td}^* = \begin{cases} 2E_t^* & \text{if } N_{DR} \text{ is even} \\ 0 & \text{if } N_{DR} \text{ is odd} \end{cases} \tag{6.10}$$

and

$$N_{DR} = \text{Integer } ((t + t_{lag})/12)$$

where

E_{td}^* is diurnally varying potential evapotranspiration,

t is the time in hours,

t_{lag} is the time difference between the beginning of the simulation and the previous 6 AM, and

N_{DR} is an integer number indicating the time of day (even) or night (odd).

The diurnally varying E_t^* curve as defined by Eq. (6.10) is schematically shown in Fig. (6.20). A comparison of simulated cumulative recharge and actual evapotranspiration for diurnally varying and uniform evapotranspiration is shown in Fig. (6.21). The diurnal variations in potential evapotranspiration reduced the rate of water-table drop and evapotranspiration losses significantly, reflecting the effect pointed out by Visser (in Ward, 1967). Another implication of this result is that a rainfall that takes place during the day will be more effective

Figure 6.21

The effect of diurnal variations of potential evapotranspirations on cumulative recharge and actual evapotranspirations.

Case 1: Potential evapotranspiration is zero at night and maximum during the day (1 cm/day).

Case 2: Potential evapotranspiration constant all time (.5 cm/day).

Note: Daily totals are the same in both cases.

Problem specifications:

Soil type: 50-500μ sand

Rainfall intensity: 0.04 cm/hr.

Rainfall duration: 120 hours

Initial depth to water table: 200 cm.

Rooting depth: 80 cm.

T_r^*/E_t^* : 0.09

Initial condition: static

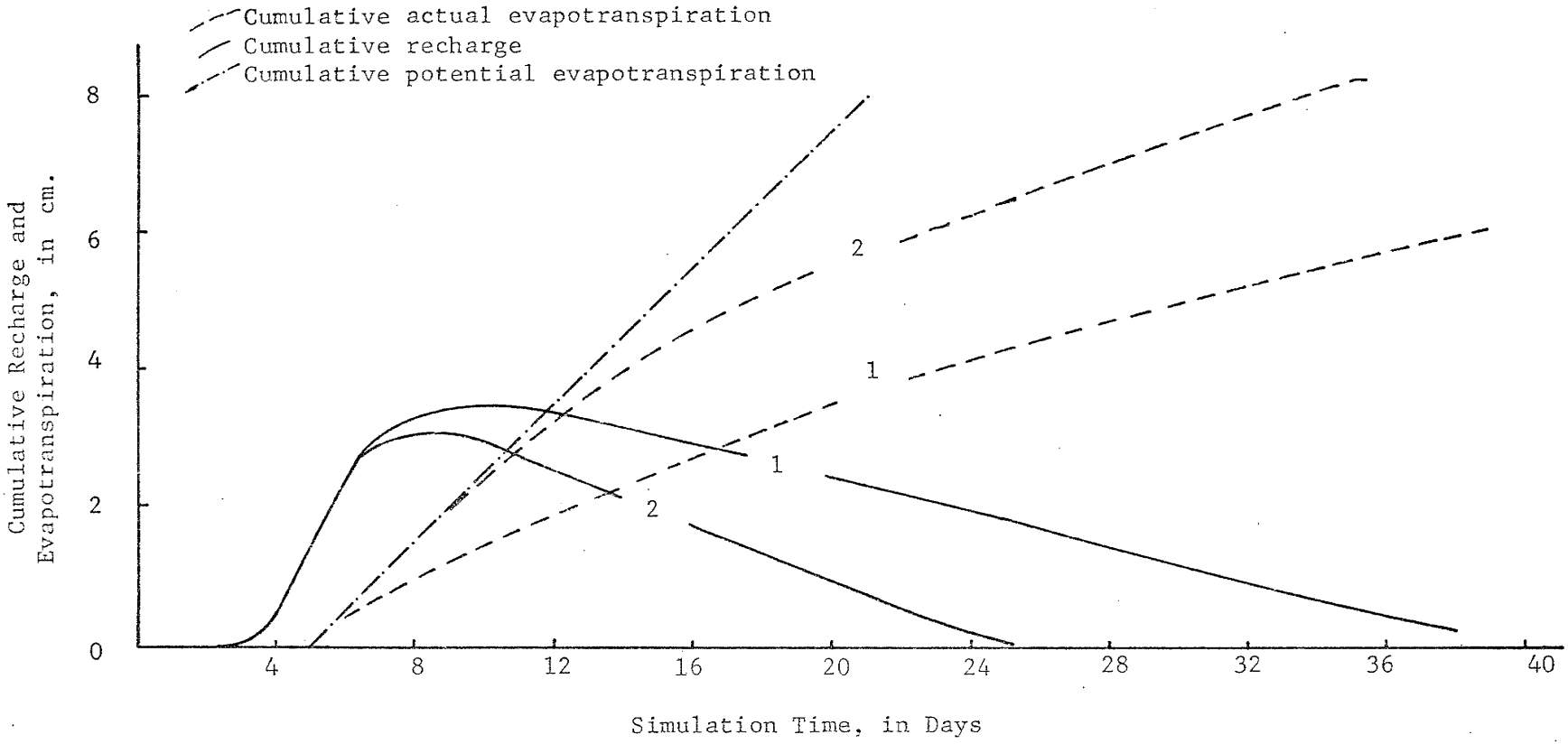
Cumulative actual evapotranspiration
Cumulative recharge
Cumulative potential evapotranspiration
Cumulative Recharge and Evapotranspiration, in cm.
0
2
4
6
8
4
8
12
16
20
24
28
32
36
40
1
2
1
2
Simulation Time, in Days

in generating ground-water recharge than one that takes place at night.

The soil moisture profiles of diurnally varying E_t^* are shown in Fig. (6.22). A comparison of Fig. (6.17) and (6.23) indicates that the soil moisture is moving vertically upward and accumulating in the surface zone at night when E_{td}^* is minimum, and that this stored moisture in the surface layers of the soil is used by plants during the day when atmospheric demand for evapotranspiration is maximum.

A summary of all simulations is given in Table (6.3).

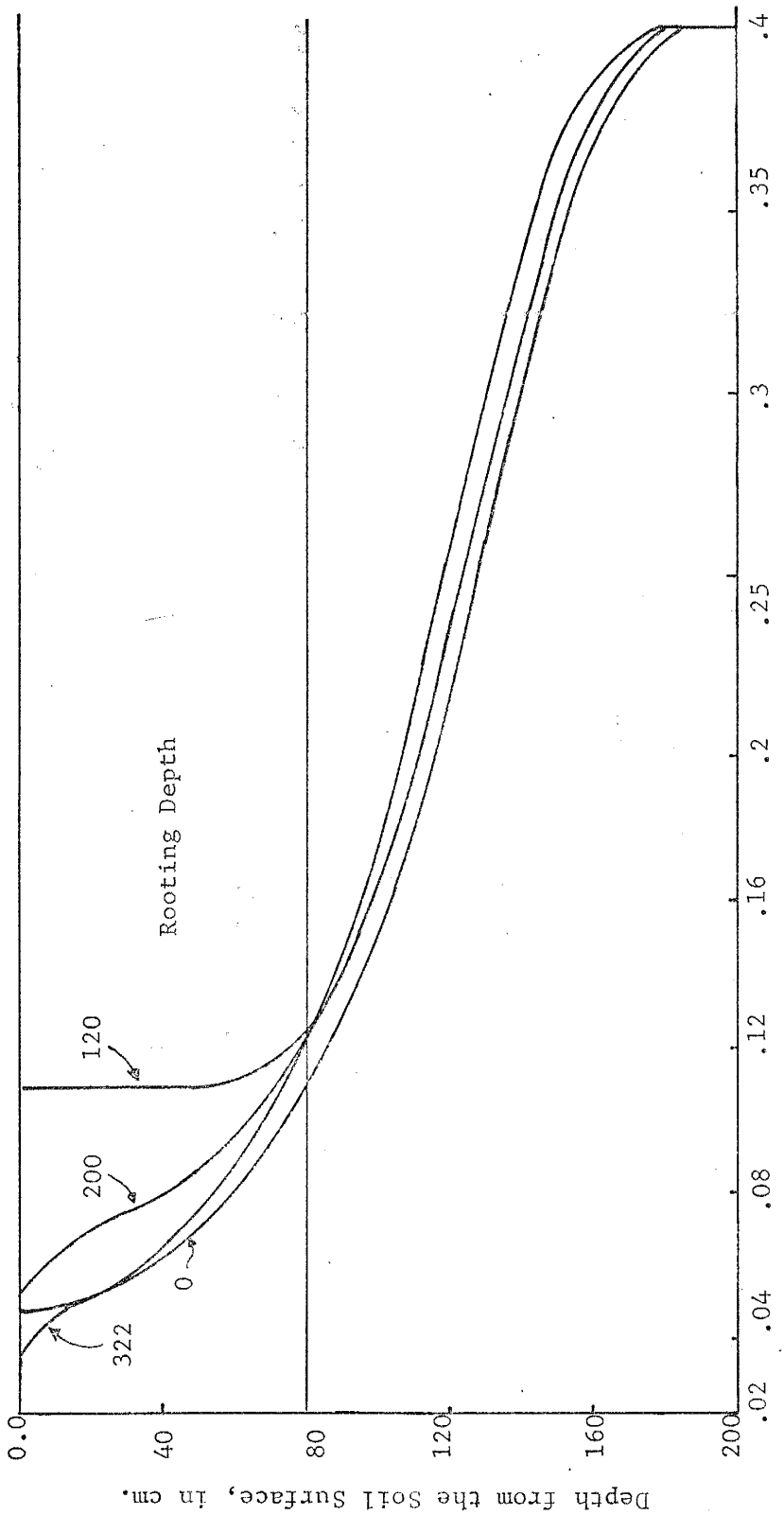

Figure 6.22: Soil moisture content profiles of 50-500 sand by considering diuarnal variations in potential evapotranspiration. The numbers labeling the curves indicate the time in hours.

TABLE 6.3: A summary of some results of computer simulations. St. and Pr. refer to static and parabolic, defined by Eq. (6.8), type initials conditions, respectively.

Soil Type	Loam	Sand	Sand	Sand	Sand	Sand	Sand	Sand
Rainfall Intensity (cm/hr)	0.04	0.04	0.04	0.48	0.04	0.04	0.04	0.04
Rainfall Duration (hrs)	120	120	120	10	120	120	120	120
Initial Depth to Water Table (cm)	200	200	400	200	200	200	200	400
Initial Condition	St.	St.	St.	St.	St.	St.	St.	Pr.
Rooting Depth	20	80	20	20	80	80	20	20
Max. Pos. Soil E_v^*/T_r^*	0.1	0.1	0.1	0.1	0.6	0.1	0.1	0.1
Diurnally varying Potential Evapotranspiration	No	No	No	No	No	Yes	No	No
Water Table Response Time (hr)	115	83	2905	22	83	83	83	7
Max. WTBL Rise (cm)	12.17	8.27	None	9.73	9.41	9.35 9.73	10.54	
Time to Max. WTBL rise (hr)	398	197	None	232	231	226 234	324	

SUMMARY AND CONCLUSIONS

It is generally recognized that existing methods of estimating recharge fail to explain the effects of different environmental factors on the recharge process. Therefore, the primary objective of this study was the investigation of various environmental factors on ground-water recharge. A better understanding of the effects of various factors would, hopefully, help investigators to develop better methods of estimating ground-water accretion rates in arid and semi-arid regions.

In order to include the effect of plant transpiration, a model representing the water extraction by plant roots was developed. This root extraction model basically assumes that the fractional change of the root extraction per unit change of water potential can be represented by a function $\mu = \mu(T_r^*, h, K)$. The field experiments of Denmead and Shaw (1962) confirms the validity of the above assumption. However, since the proper form of the function μ is unknown, it was necessary to assume that $\mu = -2h\, T_r^*/\alpha$. The results of curve fitting to the data of Denmead and Shaw (1962) revealed that a constant value of α is not representative of plant root extraction for a wide range of potential transpiration rates. At this stage of the study, however, a constant value of α is considered to be satisfactory. By substituting the root extraction term into the continuity equation, the nonlinear partial differential equation was obtained for moisture flow in a physically continuous saturated-unsaturated domain with a root-extraction term governed by atmospheric conditions and moisture conditions in the soil.

Because of the restrictions on the applicability of analytical methods in the solution of nonlinear partial differential equations, the

above flow equation was solved using a backward implicit finite difference scheme with a variable time step. The developed model was tested with actual field data collected by Nimah (1972). Model predictions compared well with actual observed data if a submodel representing the evaporation of intercepted water from a dense vegetative cover is added. With the developed model, the effects of a) soil type, b) rainfall, c) initial depth to ground-water, d) initial moisture conditions, e) rooting depth, f) vegetation density, and g) diurnally varying potential evapotranspiration on recharge and actual evapotranspiration were studied by using hypothetical data.

The following conclusions relating to the recharge process are drawn from this study:

1. Ground-water recharge is strongly dependent on initial moisture conditions. This strong dependence on initial conditions leads to the observation that recharge taking place into ground-water reservoirs at any given time is not dependent solely on current rainfall and evapotranspiration; rather, recharge occurs through downward displacement of previously stored rain water by successive bouts of infiltration.

2. Diurnally varying potential evapotranspiration tends to reduce evapotranspiration losses and increase ground-water recharge.

3. Low-intensity, long-duration rainfalls generate more recharge and less evapotranspiration than high-intensity, short-duration rainfalls.

4. The soil moisture profile in the soils covered by a dense vegetation with large leaf areas is greatly influenced by interception losses.

5. Evapotranspiration losses increase and ground-water recharge decreases with increasing thickness of the root zone and vegetation density.

6. Deep water tables tend to reduce evapotranspiration.

7. This study did not yield conclusive results regarding the effect of soil type on the recharge process. However, in case of loam soils, large amounts of moisture may accumulate in the surface zone during a rainfall, and this behavior in turn increases evapotranspiration losses.

With regard to recharge prediction the following observations are recommendations for future study:

1. The root extraction term given by Eq. (4.10) proved useful in describing the plant transpiration rates under limited moisture conditions. However, more research on the function μ for different types of plant communities and soils is needed.

2. In this study, the initial soil-moisture condition was found to be the decisive factor in the determination of recharge for a certain period of time. Initial conditions are, however, the result of climatological history of any given basin. The necessity of starting the calculations at a particular time in the past gives rise to the concept of memory in the system. The memory of a system may be defined as the length of climatological history that is effective in generating ground-water recharge at the present. For instance, Hantush (1957) found it necessary to use three years of precipitation data to calculate the recharge rates in the Roswell Basin, New Mexico. Hence, the memory of the Roswell Basin may be assumed to be approximately three years. However, the effect of the various basin parameters on the memory of the system should be the subject of a detailed future investigation.

3. The utility of numerical methods to the study of ground-water recharge in arid and semi-arid regions which are characterized by deep water tables is limited by computational costs. However, since moisture

gradients in deeper parts of the soil column are significantly smoothed (see Fig. 6.12), by increasing the space increments in this particular portion of the soil, the prediction of ground-water recharge in arid and semi-arid regions still may be feasible. Large space increments in the certain portion of the soil should be addressed in future research.

4. For a better understanding of recharge, the effects of a) air flow in the soil column, b) temperature gradients in the soil, and c) hysteresis of unsaturated soil characteristics need to be included in the model.

5. For a better estimation of both soil-moisture distribution and evapotranspiration, specifically for a dense vegetative cover with large leaf areas, a submodel taking into account the evapotranspiration during the evaporation of intercepted water should be introduced into the present model.

REFERENCES

Baver, L.D., Gardner, W.H., and Gardner, W.R., 1972, "Soil Physics", John Wiley and Sons Inc., New York, p. 488.

Bear, J., 1972, "Dynamics of Fluids in Porous Media", Amer. Elsevier Publishing Co., New York, p. 764.

Bolt, G.H., and Groenevelt, P.H., 1969, "Coupling Phenomena as a Possible Cause of Non-Darcian Behavior of Water in Soil", Bull. Inter. Assoc. Sci. Hydrol., XIV, 2, pp. 17-26.

Brutsaert, W., 1968, "A Solution for Vertical Infiltration into a Dry Porous Medium", Water Resour. Res., Vol. 4, pp. 1031-1038.

Cannon, W.A., 1911, "The Root Habits of Desert Plants", Carnegie Institution of Washington Publ., No. 131, p. 96.

Cisler, J., 1972, "Unsaturated Flow of Water in Anisotropic Porous Media", Proc. of the Second Symposium on Fundamentals of Transport Phenomena in Porous Media V.1, University of Geulph, Ontario, Canada, pp. 403-412.

Corey, A.T., 1969, "Flow in Porous Media", Colorado State University Agricultural Engineering Department Publ., p. 259.

Corey, A.T., and Rathjens, C.H., 1956, "Effect of Stratification on Relative Permeability", Petroleum Trans., AIME, Vol. 207, pp. 358-360.

Cowan, I.R., 1965, "Transport of Water in the Soil-Plant-Atmosphere System", J. of Applied Ecology, Vol. 2, pp. 221-229.

Dagan, G., 1967, "Linearized Solutions of Free-Surface Ground-Water Flow with Uniform Recharge", J. Geophys. Res., Vol. 72, pp. 1183-1193.

Danielson, R.E., 1967, "Root Systems in Relation to Irrigation", Irrigation of Agricultural Lands, No. 11, edited by Hogan, R.M., Haise, H.R., and Edminister, T.W., Amer. Soc. of Agron, Madison, Wisconsin.

Denmead, O.T., 1961, "Availability of Soil Water to Plants", Ph.D. Dissertation, Iowa State University of Science and Technology, p. 125.

Denmead, O.T., and Shaw, R.H., 1962, "Availability of Soil Water to Plants as Affected by Soil Moisture Content and Meterological Conditions", Agron. J., Vol. 45, pp. 385-390.

Douglas, J. and Gallie, T.M., 1955, "Variable Time Steps in the Solution of the Heat Equation by a Difference Equation", Proc. Amer. Math. Soc., Vol. 6, pp. 787-793.

Elric, D.E., and Bowman, D.H., 1964, "Note on an Improved Apparatur for Soil Moisture Flow Measurements", Soil Sci. Soc. Amer. Proc., Vol. 28, pp. 450-453.

Feddes, R.A., Bresler, E., and Neuman, S.P., 1974, "Field Test of a Modified Numerical Model for Water Uptake by Root Systems", Water Resour. Res., Vol. 10, pp. 119-1206.

Feddes, R.A., Kowalik, P., Malinka, K.K., and Zaradny, H., 1975, Personal Communication.

Freeze, R.A., 1967, "The Continuity Between Ground-Water Flow Systems and Flow in the Unsaturated Zone", Proc. of Hydrol. Symposium held at University of Saskatchewan, No. 6, pp. 205-232.

Freeze, R.A., 1971, "Three Dimensional, Transient, Saturated-Unsaturated Flow in a Ground-Water Basin", Water Resour. Res., Vol. 7, pp. 347-366.

Freeze, R.A., and Banner, J., 1970, "The Mechanism of Natural Ground-Water Recharge and Discharge: 2. Laboratory Column Experiments and Field Measurements", Water Resour. Res., Vol. 6, pp. 138-155.

Gardner, W.R., 1960, "Dynamic Aspects of Water Availability to Plants", Soil Sci., Vol. 89, pp. 63-73.

Gardner, W.R., and Ehling, C.F., 1962, "Some Observations on the Movement of Water to Plant Roots", Agron. J., Vol. 54, pp. 453-456.

Gartska,W.U., 1964, "Snow and Snow Survey", Handbook of Applied Hydrology, edited by Chow, V.T., McGraw-Hill Book Co., New York, pp. 10.1 - 10.57.

Gelhar, L.W., 1974, "Stochastic Analysis of Phreatic Aquifers", Water Resour. Res., Vol. 10, pp. 539-545.

Hanks, R.J., and Bowers, S.A., 1962, "Numerical Solution of the Moisture Flow Equation for Infiltration into Layered Soils", Soil Sci. Soc. Proc., Vol. 26, pp. 530-534.

Hantush, M.S., 1957, "Preliminary Quantitative Study of the Roswell Ground-Water Reservoir, New Mexico", New Mexico Inst. of Mining and Tech., Res. and Development Division, p. 118.

Hantush, M.S., 1967, "Growth and Decay of Ground-Water-Mounds in Response to Uniform Percolation", Water Resour. Res., Vol. 3, pp. 227-234.

Hendricks, D.W., and Hansen, V.E., 1962, "Mechanics of Evapotranspiration", J. Irrig. and Drainage Div. Proc. Amer. Soc. Civil Eng., Vol. 88, IR2, pp. 67-82.

Honert, T.H. Van Den, 1948, "Water Transport in Plants as a Catenary Process", Discussions Faraday Soc., Vol. 3, pp. 146-153.

Horton, J.H., and Hawkins, R.H., 1965, "Flow Path of Rain from the Soil Surface to the Water Table", Soil Sci., Vol. 100, pp. 377-383.

Jackson, R.D., Reginato, R.J., and Van Bavel, C.H.M., 1965, "Comparison of Measure and Calculated Hydraulic Conductivities of Unsaturated Soils", Water Resour. Res., Vol. 1, pp. 375-380.

Jacob, C.E., 1943, "Correlation of Ground-Water Levels and Precipitation on Long Island, New York", Trans. AGU, Vol. 24, pp. 564-573.

Kirkham, D., and Powers, W.L., 1972, "Applied Soil Physics", Wiley-Interscience, New York, p. 534.

Konikow, L.F., and Bredehoeft, J.D., 1974, "Modeling Flow and Chemical Quality Changes in an Irrigated Stream-Aquifer System", Water Resour. Res., Vol. 10, pp. 546-562.

Krishnamurthi, N., Sunada, D.K., and Longenbaugh, R.A., 1977, "Mathematical Modeling of Natural Ground-Water Recharge", Water Resour. Res., Vol. 13, pp. 720-724.

Lemon, E.R., Stewart, D.W., and Shawcroft, R.W., 1971, "The Sun's Work in a Cornfield", Science, Vol. 174, pp. 371-378.

Lemon, E.R., Stewart, D.W., Shawcroft, R.W., and Jensen, S.E., 1973, "Experiments in Predicting Evapotranspiration by Simulation with a Soil-Plant-Atmosphere Model (SPAM)", in Field Soil Water Regime, edited by Bruce, R.R., Flach, K.W., and Taylor, H.M., Soil Sci. Soc. Amer. Special Publication, No. 5, pp. 57-76.

Linsley, R.K., Kohler, M.A., and Paulhus, J.L.H., 1975, "Hydrology for Engineers", McGraw-Hill Book Company, New York, p. 482.

Lull, H.W., 1964, "Ecological and Silvicultural Aspects", Handbook of Applied Hydrology, edited by Chow, V.T., McGraw-Hill Book Co., New York, pp. 6.1-6.30.

Maasland, M., 1959, "Water Table Fluctuations Induced by Intermittent Recharge", J. Geophys. Res., Vol. 64, pp. 549-559.

Meinzer, O.E., 1949, "Ground-Water", in Hydrology, edited by Meinzer, O.E., Dover Publications Inc., New York, pp. 385-477.

Minhas, B.S., Parikh, K.S., and Srinivasan, T.N., 1974, "Toward the Structure of a Production Function for Wheat Yields with Dated Inputs of Irrigation Water", Water Resour. Res., Vol. 10, pp. 383-392.

Molz, F.J., and Remson, I., 1970, "Extraction Term Models of Soil Moisture Use by Transpiring Plants", Water Resour. Res., Vol. 6, pp. 1346-1356.

Neuman, S.P., Feddes, R.A., Bresler, E., 1974, "Finite Element Simulation of Flow in Saturated-Unsaturated Soils Considering Water Uptake by Plants", Third Annual Report, Project No. ALO-SWC-77, Hydraulic Engineering Laboratory, Technion, Haifa, Israel, p. 104.

Nielsen, D.R., and Biggar, J.W., 1961, "Measuring Capillary Conductivity", Soil Sci., Vol. 92, pp. 192-193.

Nimah, M.N., 1972, "Model for Estimating Soil Water Flow, Water Content", Ph.D. Dissertation, Utah State University, Logan, Utah, p. 118.

Nimah, M.N., and Hanks, R.J., 1973a, "Model for Estimating Soil Water, and Atmospheric Interrelations: I. Description and Sensitivity", Soil Sci. Soc. Amer. Proc., Vol. 37, pp. 522-527.

Nimah, M.N., and Hanks, R.J., 1973b, "Model for Estimating Soil Water Plant, and Atmospheric Interrelations: II. Field Test of Model", Soil Sci. Soc. Amer. Proc., Vol. 37, pp. 528-532.

Oakes, D.B., 1977, "The Movement of Water and Solutes Through the Unsaturated Zone of the Chalk in the United Kingdom", Third Fort Collins Hydrology Symposium, Fort Collins, Colorado, in Press.

Parlange, J.-Y., 1971, "Theory of Water Movement in Soild: 1. One-Dimensional Absorption", Soil Sci., Vol. III, pp. 134-137.

Parlange, J.-Y., 1971, "Theory of Water Movement in Soils: 3. Two- and Three-Dimensional Steady Infiltration", Soil Sci., Vol. 113, pp. 96-101.

Parlange, J.-Y., 1972, "Theory of Water Movement in Soils: 5. Multi-Dimensional Unsteady Infiltration", Soil Sci., Vol. 113, pp. 156-161.

Parlange, J.-Y., 1972, "Theory of Water Movement in Soils: 6. Effect of Water Depth Over Soil", Soil Sci., Vol. 113, pp. 308-312.

Parlange, J.-Y., 1972, "Theory of Water Movement in Soils: 7. Multi-Dimensional Cavities Under Pressure", Soil Sci., Vol. 113, pp. 379-382.

Parlange, J.-Y., 1972, "Theory of Water Movement in Soils: 8. One-Dimensional Infiltration with Constant Flux at the Surface", Soil Sci., Vol. 114, pp. 1-4.

Parlange, J.-Y., and Aylor, D., 1972, "Theory of Water Movement in Soils: 9. The Dynamics of Capillary Rise", Soil Sci., Vol. 114, pp. 79-81.

Parlange, J.-Y., 1973, "Theory of Water Movement in Soils: 10. Cavities With Constant Flux", Soil Sci., Vol. 116, pp. 1-7.

Penman, H.L., 1948, "Natural Evaporation from Open Water, Bare Soil and Grass", Proc. Roy Soc. Ser. A. 193, pp. 120-146.

Penman, H.L., 1956, "Evaporation: An Introductory Survey", Netherland J. Agr. Sci., Vol. 4, pp. 9-29.

Pikul, M.F., Street, R.L., and Remson, I., 1974, "A Numerical Model Based on Coupled One-Dimensional Richards and Boussinesq Equations", Water Resour. Res., Vol. 10, pp. 295-302.

Price, H.S., 1977, Oral Communication.

Philip, J.R., 1957, "The Theory of Infiltration: 1. The Infiltration Equations and Its Solution", Soil Sci., Vol. 83, pp. 345-357.

Philip, J.R., "The Theory of Infiltration: 2. The Profile of Infinity", Soil Sci., Vol. 83, pp. 435-448.

Philip, J.R., 1957, "The Theory of Infiltration: 3. Moisture Profiles and Relation to Experiment", Soil Sci., Vol. 84, pp. 163-178.

Philip, J.R., 1957, "The Theory of Infiltration: 4. Sorptivity and Algebraic Infiltration Equations", Soil Sci., Vol. 84, pp. 257-264.

Philip, J.R., 1957, "The Theory of Infiltration: 5. The Influence of Initial Moisture Content", Soil Sci., Vol. 84, pp. 329-339.

Philip, J.R., 1958, "The Theory of Infiltration: 6. Effect of Water Depth Over Soil", Soil Sci., Vol. 85, pp. 278-286.

Philip, J.R., 1958, "The Theory of Infiltration: 7.", Soil Sci., Vol. 85, pp. 333-337.

Philip, J.R., 1969, "Theory of Infiltration", in Advances in Hydroscience, edited by Chow, V.T., Academic Press, New York, Vol. 5, pp. 215-296.

Philip, J.R., 1973, "On Solving the Unsaturated Flow Equation: 1. The Flux Concentration Relation", Soil Sci., Vol. 116, pp. 328-335.

Philip, J.R., and Knight, J.H., 1974, "On Solving the Unsaturated Flow Equation: 3. New Quasi-Analytical Technique", Soil Sci., Vol. 117, pp. 1-13.

Rabinowitz, D.D., Gross, G.W., and Holmes, C.R., 1977, "Environmental Tritium as a Hydrometeorologic Tool in the Roswell Basin, New Mexico, I. Tritium Input Function and Precipitation-Recharge Relation", J. of Hydrol., Vol. 32, pp. 3-17.

Richtmeyer, R.D., and Morton, K.W., 1967, "Difference Methods for Initial Value Problems", Interscience Publisher, New York, p. 405.

Ritchie, J.T., 1972, "Model for Predicting Evaporation from a Row Crop with Incomplete Cover", Water Resour. Res., Vol. 8. pp. 1204-1213.

Ritchie, J.T., and Burnet, E., 1971, "Dryland Evaporative Flux in a Subhumid Climate: II. Plant Influences", Argon. J., Vol. 63, pp. 56-62.

Rubin, J., and Steinhardt, R., 1963, "Soil Water Relations During Rain Infiltration: I. Theory", Soil Sci. Soc. Amer. Proc., Vol. 27, pp. 246-251.

Sammis, W.T., Young, D.W., and Constant, C.L., 1977, "Construction Calibration and Operation of a Monolith Weighing Lysimeter", Proc. for Hydrol. Section Arizona Academy of Science, Vol. 6.

Shawcroft, R.W., 1971, "The Energy Budget at the Earth's Surface: Water Relations and Stomatal Response in a Corn Field", U.S. Army Ecom. Technical Report 2-69-1-7, p. 94.

Singh, V.P., and Dickinson, W.T., 1975, "An Analytical Method to Determine Dail Soil Moisture", Proc. of Second World Congress, International Water Resour. Assoc., New Delhi, India, Vol. 4, pp. 335-364.

Stewart, D.W., and Lemon, E.R., 1969, "The Energy Budget at the Earth's Surface: A Simulation of New Photosynthesis of Field Corn", U.S. Army Ecom. Technical Report 2-68-1-6, p. 132.

Swartzendruber, D., 1962a, "Modification of Darcy's Law for the Flow of Water in Soils", Soc. Sci., Vol. 93, pp. 22-28.

Swartzendruber, D., 1962b, "Non-Darcy Flow in Liquid-Saturated Porous Media", J. Geophys. Res., Vol. 67, pp. 5205-5213.

Swartzendruber, D., 1963, "Non-Darcy Behavior and the Flow of Water in Unsaturated Soils", Soil Sci. Soc. Amer. Proc., Vol. 27, pp. 491-494.

Swartzendruber, D., 1969, "The Flow of Water in Unsaturated Soils", in Flow Through Porous Media, edited by DeWiest, R.J.M., Academic Press, New York, pp. 215-292.

Thornthwaite, C.W., and Mather, J.R., 1957, "Instructions and Tables for Computing Potential Evapotranspiration and Water Balance", Publ. in Climatol, Lab. of Climatol, Centerton, J.J., pp. 185-311.

Updegraff, D., and Gelhar, L.W., 1977, "Parameter Estimation for a Lumped Parameter Ground-Water Model of the Mesilla Valley, New Mexico, in Press.

Van Bavel, C.H.M., Stirk, G.B., and Brust, K.J., 1968, "Hydraulic Properties of a Clay Loam Soil and the Field Measurement of Water Uptake by Roots, 1, Interpretation of Water Content and Pressure Profiles", Soil Sci. Soc. Amer. Proc., Vol. 32, pp. 167-174.

Varga, R.S., 1962, "Matrix Iterative Analyses", Prentice-Hall Inc., New York, p. 322.

Verma, R.D., and Brutsaert, W., 1970, "Unconfined Aquifer Seepage by Capillary Flow Theory", J. Hydraul. Div. Amer. Soc. Civil Engr., 96(HY6), pp. 1331-1334.

Walton, W.C., 1970, "Ground-Water Resource Evaluation", McGraw-Hill Book Company, New York, p. 664.

Ward, R.C., 1967, "Principles of Hydrology", McGraw-Hill Book Company, New York, p. 403.

Warrick, A.W., 1974, "Solution to the One-Dimensional Linear Moisture Flow Equation with Water Extraction", Soil Sci. Soc. Amer. Proc., Vol. 38, pp. 573-576.

Werner, P.W., 1957, "Some Problems in Non-Artesian Ground-Water Flow", Trans. AGU, Vol. 38, pp. 511-518.

Wilson, J.L., and Gelhar, L.W., 1974, "Dispersive Mixing in a Partially Saturated Porous Medium", Ralph M. Parson Laboratory, Report No. 191, Massachusetts Inst. of Technology, Cambridge, Mass., p. 353.

APPENDIX

DOCUMENTATION OF THE COMPUTER PROGRAM

A. General Description of the Program

The computer program developed in this study is written in standard Fortran. The size of the problem is limited by the computer core available. As a guide, a problem with 1000 total nodes, 100 nodes in the root zone and 100 days of simulation requires approximately 90K words of central memory on an IBM 360/44 computer.

The overall program consists of one main program and eight subroutines. The main program reads and prints the input data, calls subroutines whenever they are needed and checks the mass balance equation at the end of each time step. If convergence criterion (to be specified by the user) is met, the program proceeds to calculate the recharge rate and cumulative transpiration, evaporation, and recharge. If not, then the program starts to iterate the water potential values at the end of the time step as explained in Section 4.3. If the convergence criterion is still not met at the end of the fourth iteration it proceeds to perform the same calculations, whatever the size of the error may be. The main program prints out the results at the end of each time step, as well as the percent mass balance error of each time step. A percent mass balance error less than convergence criterion indicates the convergence of the solution for this particular time step. If the cumulative time is less than the total simulation time, which also has to be specified by the user, the main program proceeds to the next time step; otherwise it terminates the calculations by printing out the overall percent mass balance error.

The subroutines are TABLE, EVAPO, INTER, HYDC, SWCAP, MOIST, and POTH and are briefly described below.

1. Subroutine TABLE searches for the location of the water table.

This subroutine is called by the main program if the water potential at the bottom of the soil column is greater than zero

2. Subroutine EVAPO calculates the sink term of each nodal point inside the root zone and the soil evaporation. By integrating the sink terms over the root zone, EVAPO calculates actual transpiration rates. This subroutine uses the soil evaporation and root extraction models defined respectively by Eq. (4.13) and Eq. (4.10). If any other model or models are desired for the determination of plant transpiration and/or soil evaporation, they can be used in place of subroutine EVAPO, with appropriate adjustments in the call statement.

3. Subroutine SOLVE sets the n linear equations with n unknowns and solves by elimination and back substitution.

4. Subroutine INTER locates the position of any given number in an ordered nonuniformly distributed set of numbers. Generally, moisture contents are uniformly distributed, while water potentials and hydraulic conductivities are not, if the relation between these variables are given in tabulated form. In this case, if the determination of corresponding moisture content or hydraulic conductivity for a given potential is needed, the location of this water potential should be determined first in order to proceed with interpolation. Thus, this subroutine only locates the position of any given water potential or hydraulic conductivity in the tabulated data. Subroutine INTER is called by subroutines HYDC and MOIST.

5. Subroutine HYDC calculates the corresponding hydraulic conductivity of a given water potential. In HYDC, subroutine INTER is called first to locate the position of a specified water potential in the tabulated data. Then, using the next upper and lower members in the

tabulated data, a corresponding hydraulic conductivity is calculated by linear interpolation.

6. Subroutine SWCAP calculates the corresponding soil water capacity of a given water potential. This subroutine is called by the main program right after HYDC, to avoid calling INTER for the same water potential twice.

7. Subroutine MOIST calculates corresponding water content of a given water potential using the same procedure as in subroutine HYDC.

8. Subroutine POTH calculates corresponding water potential of a given moisture content. This subroutine locates the position of given moisture content with the expression.

$$i = \text{INTEGER}\left(\frac{\theta^* - \theta_1}{\Delta\theta} + 1.0\right)$$

where

θ^* is the given moisture content,

θ_1 is the smallest moisture content in the tabulated data,

i is the index of next lower moisture content to θ^*, and

$\theta_i < \theta^* < \theta_{i+1}$.

The subroutine then calculates the corresponding water potential by linear interpolation. Note that, to use this subroutine, moisture contents should be uniformly (constant $\Delta\theta$) distributed.

If the relations between moisture content, water potential, and hydraulic conductivity are given in functional form, the subroutine INTER becomes obsolete, and it can be omitted from the program. In this case, the subroutines HYDC, SWCAP, MOIST, POTH should also be replaced by the desired model.

B. Data Preparation

The data must be punched on cards according to the following instructions:

Group	Number of the Cards in the Group	Format	Variables (in sequencial order)	Description of the Variables
1	1	14I5	NODX (1-5)	Number of nodal points
			NDAT (6-10)	Length of simulation in days (whole number)
			NPRP (11-15)	Number of precipitation during the course of simulation
			NRDF (16-20)	Number of nodal points in the root zone
			IBC (21-25)	1 if bottom flux is zero 0 otherwise
			NTAB[1] (26-30)	Number of the points in the moisture content vs. water potential and unsaturated hydraulic conductivity table
			IDRF (31-35)	1 if diurnal variations in potential evapo-transpiration is con-sidered 0 otherwise

[1] if a functional relationship is used between the mentioned variables can be left blank.

The numbers in parenthesis indicate the columns where the variables are to be punched.

Group	Number of the Cards in the Group	Format	Variables (in sequencial order)	Description of the Variables
2	2	7D10.4	DELT (1-10)	Initial time increment
			DRUN (11-20)	Length of simulation in hours
			DPRN (21-30)	Minimum time interval (in hours), a moisture content profile desired to be printed
			BFLX (31-40)	Bottom flux in cm/hr
			CDT (41-50)	A desired coefficient such that $\Delta t_{i+1} = CDT*\Delta t_i$
			TOL (51-60)	Desired tolerance for the water balance at end of each time step
			OMGA (61-70)	1.0
			TMLG (1-10)	Time difference (in hours) between the beginning of the simulation and previous 6 AM.

Group	Number of the Cards in the Group	Format	Variables (in sequencial order)	Description of the Variables
3	NODX/7 + 1	7D10.4	XX(I)	Depth of i^{th} node
4	NDAT/7 + 1	7D10.4	PETP(I)	Potential evapotranspiration rate in cm/day of the i^{th} day
5	NDAT/7 + 1	7D10.4	PEVP(I)	Maximum soil evaporation rate in cm/day of the i^{th} day
6	NPRP/7 + 1	7D10.4	PRBE(I)	The time, the i^{th} precipitation started
7	NPRP/7 + 1	7D10.4	PRDU(I)	Duration of the i^{th} precipitation
8	NPRP/7 + 1	7D10.4	PRIN(I)	Intensity (in cm/hr) of i^{th} precipitation
9	NODX/7 + 1	7D10.4	WW(I)	Initial moisture content of the i^{th} node
10	NRDE/7 + 1	7D10.4	RDF(I)	Proportion of total active root in depth increment ΔZ at i^{th} node
11	NTAB/7 + 1	7D10.4	PRES(I)[1]	Water potential at the i^{th} point in tabulated data
12	NTAB/7 + 1	7D10.4	COND(I)[1]	Unsaturated hydraulic conductivity at the i^{th} point tabulated data
13	NTAB/7 + 1	7D10.4	TETA(I)[1]	Moisture content at the i^{th} point in tabulated data

[1] if the soil characteristic curves are given in functional form, these cards should be replaced.

Group	Number of the Cards in the Group	Format	Variables (in sequencial order)	Description of the Variables
14	1	7D10.4	DELW(1-10)	Water content increment corresponding to table increments
			SATK(11-20)	Saturated hydraulic conductivity of the soil
			PORE(21-30)	Porosity of the soil
			ALFA(31-40)	The parameter used in the sink function
			HWET(41-50)	0.0 (generally)

Note: Only seven variables to be read on each data card.

C. Flow Charts of the Main Program and Subroutines

Main Program

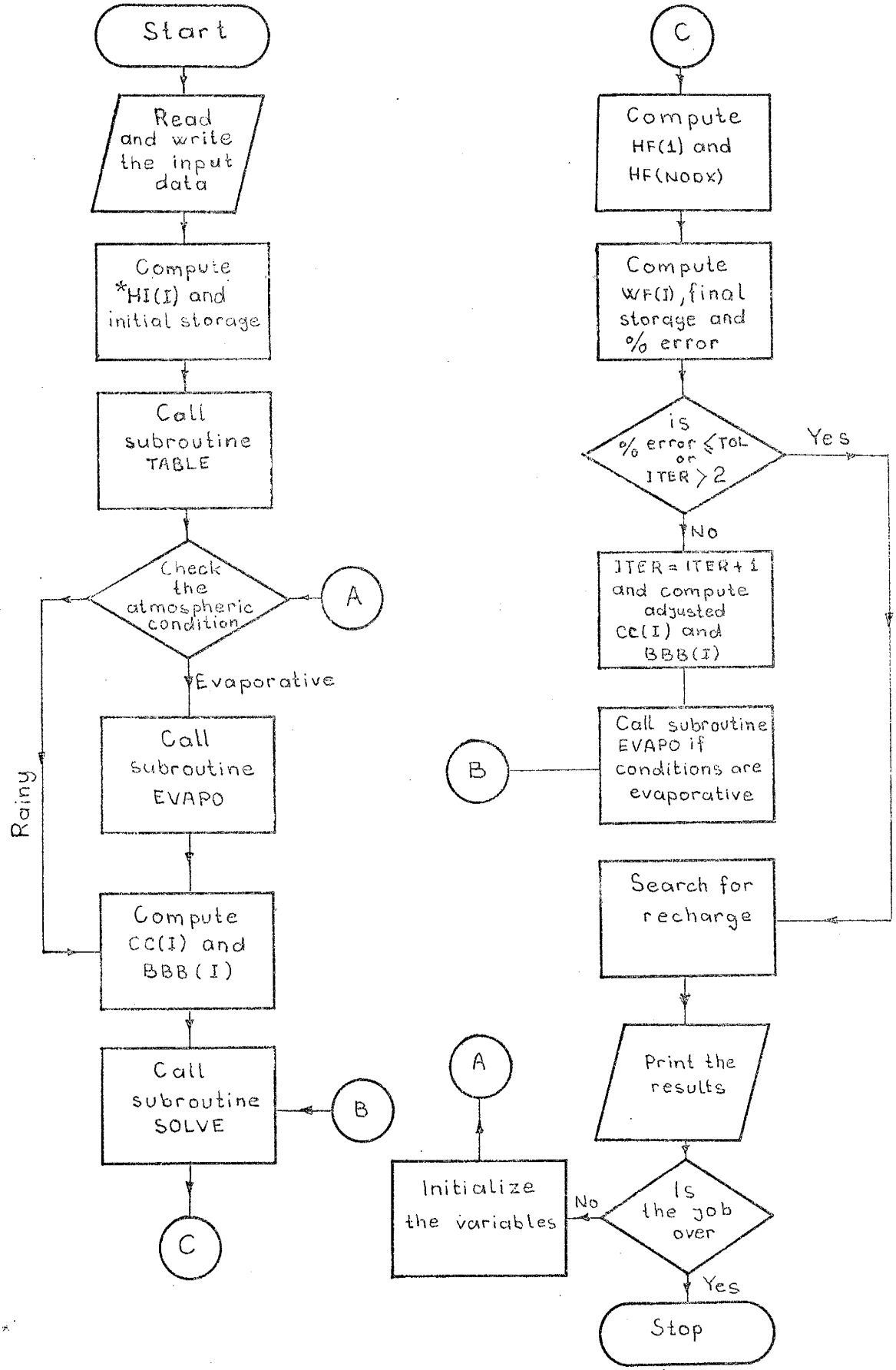

*Explanation of the symbols used in the flow charts if given at the end of this section

Subroutine Table

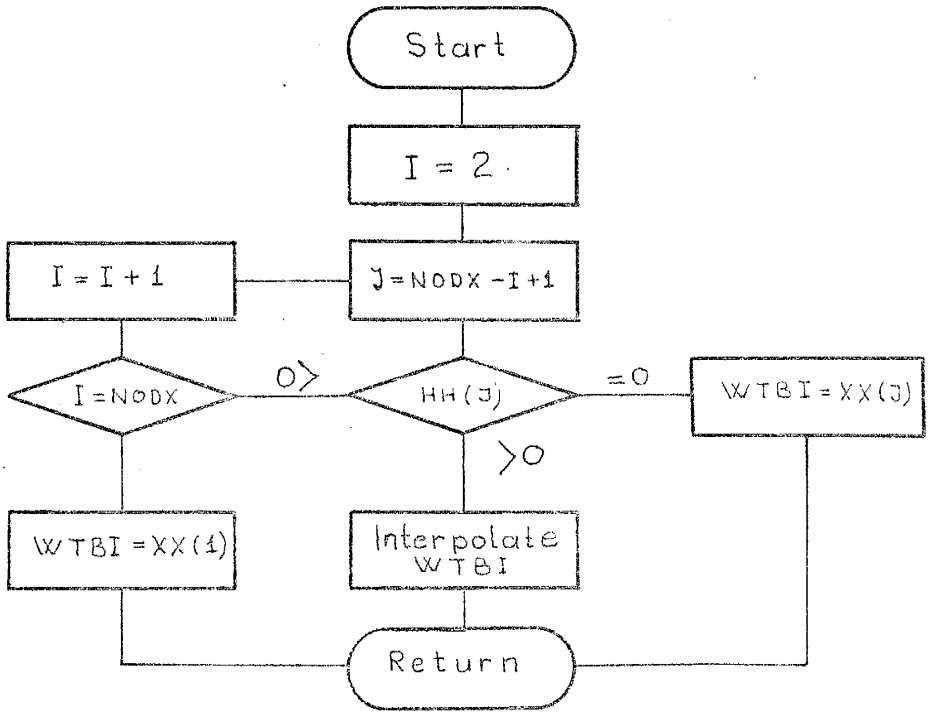

Soubroutine EVAPO

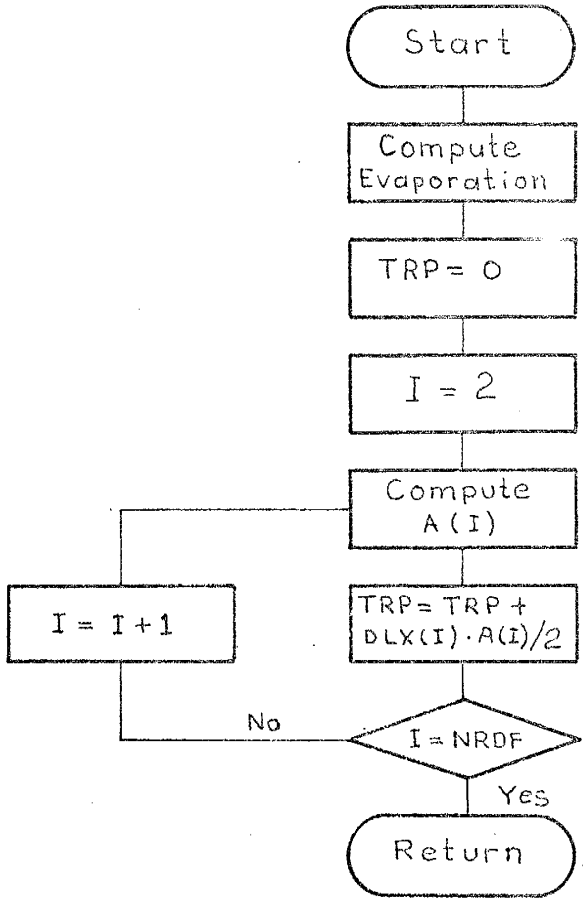

Subroutine Solve

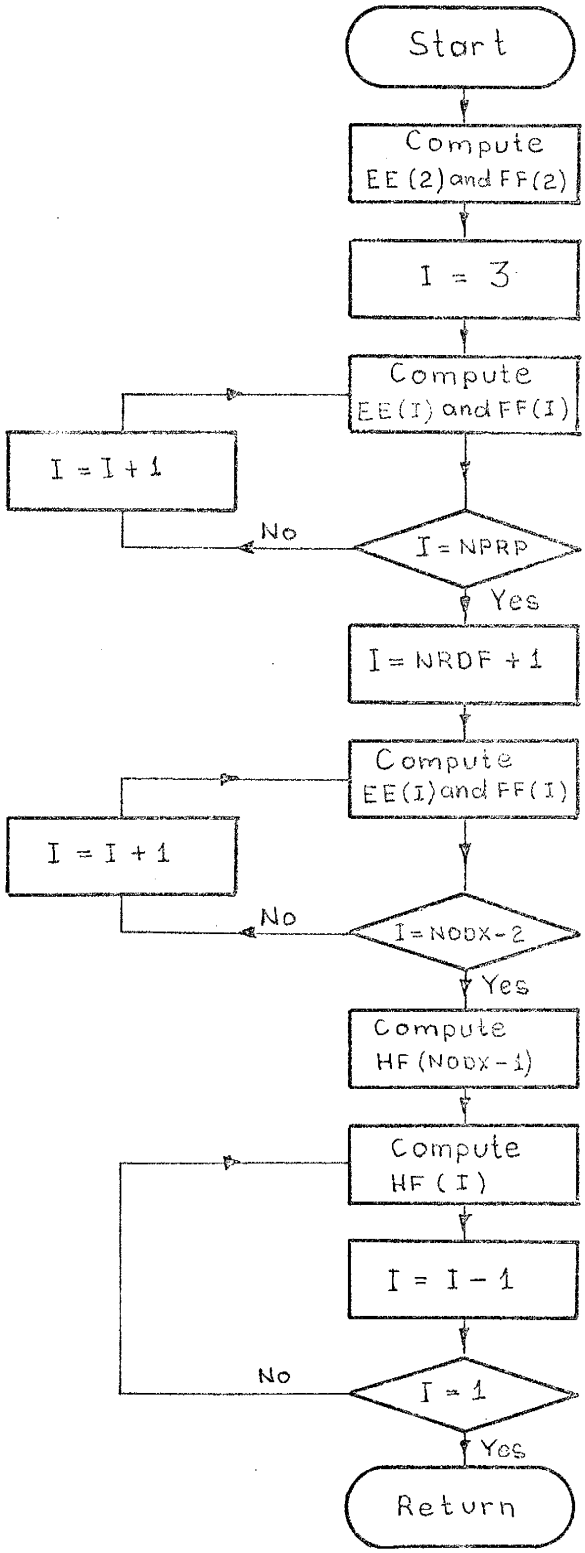

Subroutine INTER

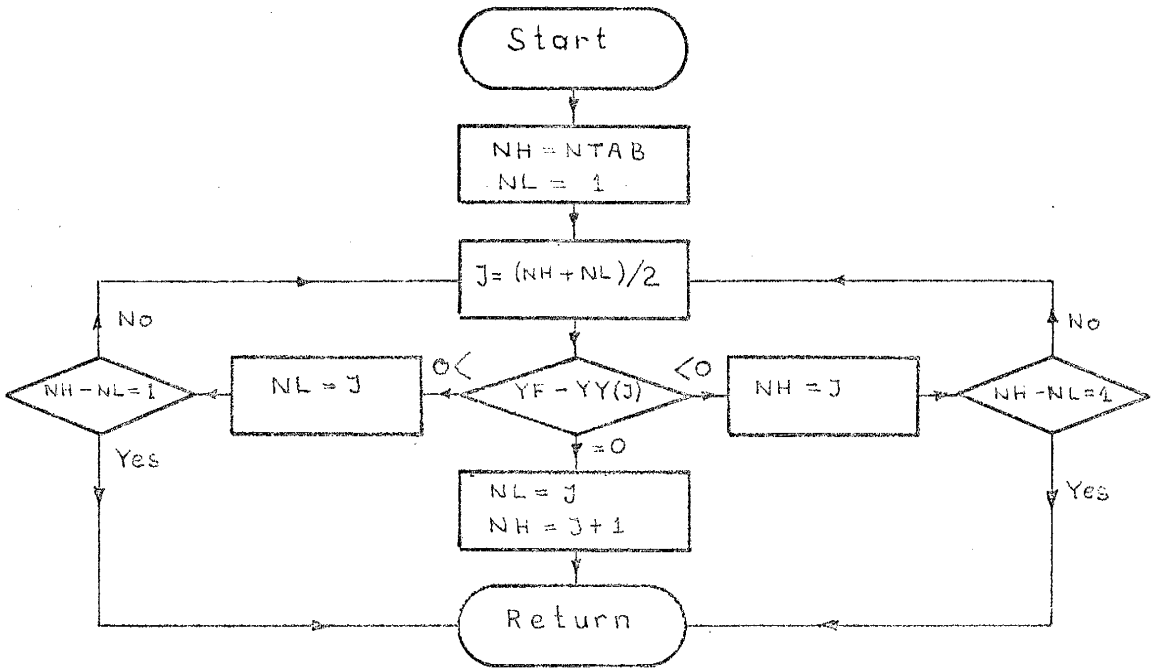

Subroutine HYDC

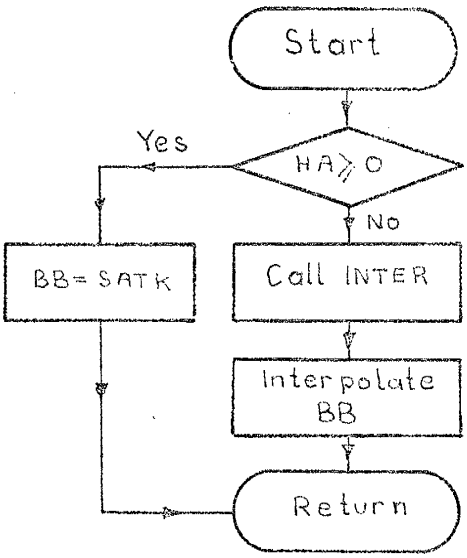

Subroutine POTH

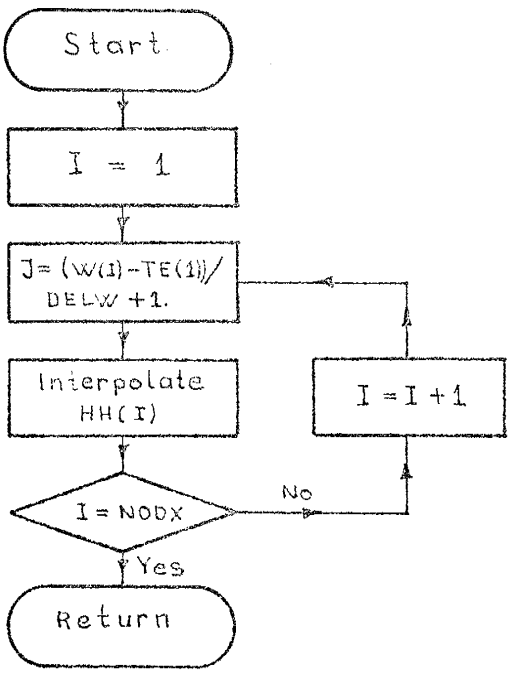

Subroutine MOIST

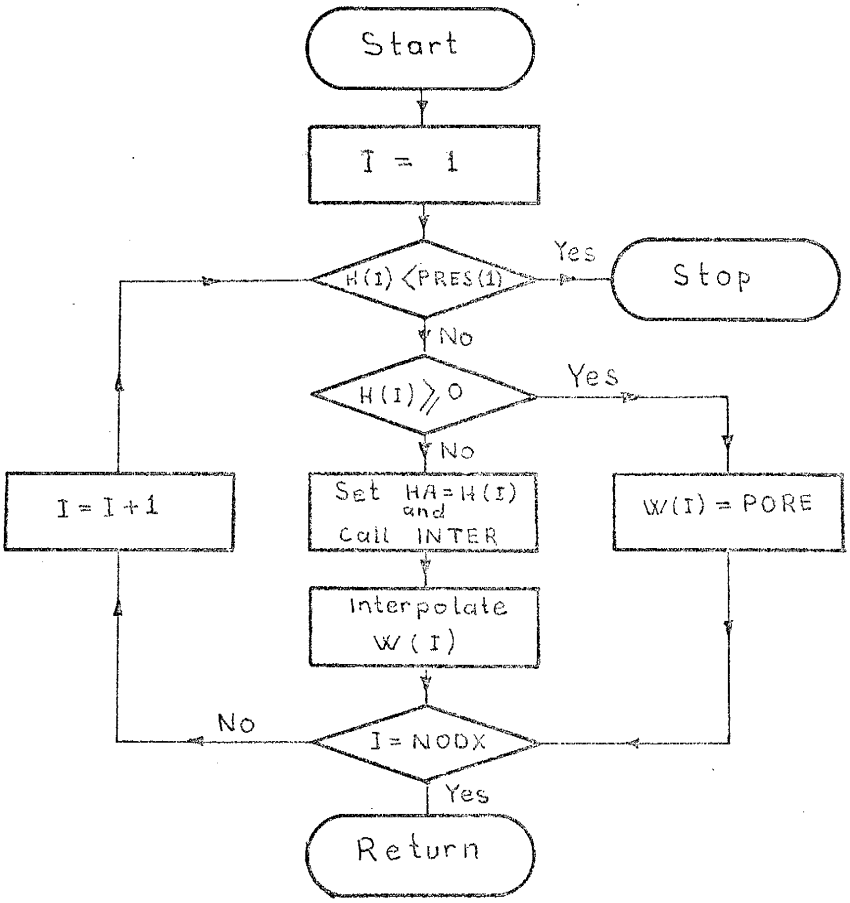

Subroutine SWCAP

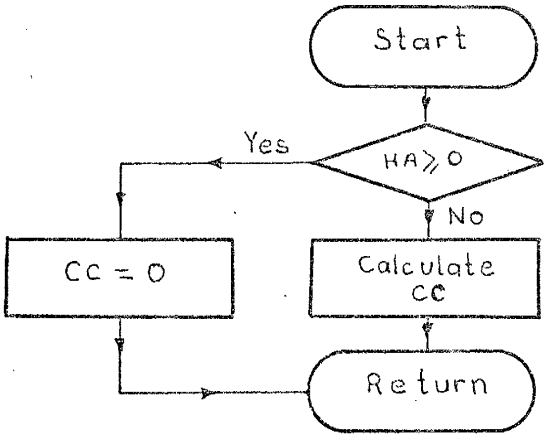

EXPLANATION OF THE VARIABLES USED IN THE FLOW CHARTS

Main program

HI(I) is soil water potential at the beginning of the time step at the i^{th} node

HF(I) is soil water potential at the end of the time step at at i^{th} node

CC(I) is soil water capacity at the i^{th} node

BBB(I) = $K^{j-1/2}_{j+1/2}$ or $K^{j-1/2}_{j-1/2}$

WF(I) is soil moisture content at the end of the time step

TOL is specified tolerance

ITER is number of iterations

Subroutine SOLVE

EE(I) and FF(I) are the variables defined by Eq. (4.22a) and and Eq. (4.22b), respectively

Subroutine TABLE

HH(J) is soil water potential at the i^{th} node carried to the subroutine table by the main program

WTBI is the distance between the water table and the bottom of the soil column

Subroutine EVAPO

TRP is actual transpiration rate

A(I) is the water extraction of the plant roots at the i^{th} node

DLX(I) = $z_{i+1} - z_{i-1}$

Subroutine INTER

YF is a particular soil water potential or hydraulic conductivity value to be located in tabulated data

YY(J) is the tabulated soil water potential or hydraulic conductivity

NH is the index of the next upper node to YF

NL = NH-1 if the index of the next lower node to YF

Subroutine HYDC

HA is soil water potential whose hydraulic conductivity to be calculated

BB is corresponding conductivity to HA

Subroutine POTH

W(I) is soil moisture content whose corresponding soil water potential value to be calculated

HH(I) is corresponding soil water potential

Subroutine MOIST

H(I) is the soil water potential whose moisture content to be determined

PRESS(I) is the lowest soil water potential in tabulated data

W(I) is corresponding moisture content

Subroutine SWCAP

HA is the soil water potential whose soil water capacity to determined

CC corresponding soil water capacity

D. Listing of the Program

```
      IMPLICIT REAL*8 (A-H,O-Z)
      DIMENSION XX(1000),DX(1000),DLX(1000),PETP(100),PEVP(100),
     1PTRT(100),PRBE(50),PRDU(50),PRIN(50),WW(1000),WF(1000),HI(100),
     2HE(1000),CC(1000),BBB(1000),EE(1000),FF(1000),SINK(100),ROF(100)
     3PRES(100),COND(100),TETA(100)
      INTEGER IPSW(2)
      CALL IFPCK(&141,IPSW)
C
CCC   READ THE DATA    ***
C
C     A. MISCELLANEOUS
      READ(5,10) NODX,NDAT,NPRP,NRDE,IBC,NTAB,IDRF
      READ(5,11) DELT,DRUN,DRFN,BELX,COT,TOL,OMGA,TMLG
      READ(5,11) (XX(I),I=1,NODX)
C     B. CLIMATOLOGICAL INFORMATION
      READ(5,11) (PETP(I),I=1,NDAT)
      READ(5,11) (PEVP(I),I=1,NDAT)
      READ(5,11) (PRBE(I),I=1,NPRP)
      READ(5,11) (PRDU(I),I=1,NPRP)
      READ(5,11) (PRIN(I),I=1,NPRP)
C     C. INITIAL CONDITION
      READ(5,11) (WW(I),I=1,NODX)
C     D. PLANT PROPERTIES
      READ(5,11) (RDF(I),I=1,NRDE)
C     E. SOIL PROPERTIES
      READ(5,11) (PRES(I),I=1,NTAB)
      READ(5,11) (COND(I),I=1,NTAB)
      READ(5,11) (TETA(I),I=1,NTAB)
      READ(5,11) DELW,SATK,PORE,ALFA,HWET
C
CCC   ***   PRINT THE DATA    ***
C
      NA=NODX-1
      WRITE(6,21)
      DO 22 I=1,NPRP
      PTRT(I)=PETP(I)-PEVP(I)
   22 WRITE(6,23) I,PETP(I),PEVP(I),I,PRBE(I),PRDU(I),PRIN(I)
      N=NPRP+1
      DO 25 I=N,NDAT
      PTRT(I)=PETP(I)-PEVP(I)
   25 WRITE(6,23) I,PETP(I),PEVP(I)
      WRITE(6,24) NODX,PORE,NDAT,NRES,NPRP,PLA,IBC,PNA,DELT,RPR,COT,
     1HWET,DRFN,SATK,DRUN,BELX,COIN,ALFA
      WRITE(6,31)
      JTO=NODX/5
      IF(NODX.NE.(NODX/5)*5) JTO=JTO+1
      JHI=4-JTO
      JRH=NRDE/JTO
      IF(NRDE.EQ.(NRDE/JTO)*JTO) JRH=JRH-1
      JRH=JRH*JTO
      DO 32 I=1,JTO
      IF(I.EQ.(I/52)*52) WRITE(6,31)
      JHI=JHI+1
      IF(JHI.GT.NODX) JHI=JHI-JTO
      JRH=JRH+1
      IF(JRH.GT.NRDE) JRH=JRH-JTO
      JRP=JRH+JTO
      IF(I.GT.NRDE) GO TO 133
      WRITE(6,33) (XX(JJJ),WW(JJJ),RDF(JJJ),JJJ=I,JRH,JTO),
     1(XX(JJJ),WW(JJJ),YY,JJJ=JRP,JHI,JTO)
      GO TO 32
  133 WRITE(6,33) (XX(JJJ),WW(JJJ),YY,JJJ=I,JHI,JTO)
   32 CONTINUE
      WRITE(6,41)
      DO 160 I=1,NTAB
  160 WRITE(6,43) TETA(I),PRES(I),COND(I)
      WRITE(6,95)
C
CCC   ***   DO INITIALIZATION AND CALCULATE THE VALUES
C           WHICH ARE USED OVER AND OVER AGAIN   ***
C
      DO 54 I=2,NODX
      DX(I)=XX(I)-XX(I-1)
      DLX(I-1)=XX(I)-XX(I-2)
   54 CONTINUE
      IF(IDRF.EQ.0) GO TO 114
      DO 113 I=1,NDAT
      PTRT(I)=2.0*PTRT(I)
      PETP(I)=2.0*PETP(I)
  113 PEVP(I)=2.0*PEVP(I)
  114 IPC=1
```

```
      DT=DELT
      NB=NA-1
      LINE=JTD/52+1
      MRDE=NRDE-1
      LRDE=NRDE+1
      NPRC=1
      OMGB=1.0-OMGA
      COIN=1.0-COIN
      PEND=PRBE(IPC)+PRDU(IPC)
C
CC    ***   CALCULATE WATER POTENTIALS AT EACH NODAL POINTS    ***
C
      CALL POTH(WW,TETA,DELW,HI,PRES,NODX)
      HE(1)=HI(1)
      DO 34 I=2,NODX
      HE(I)=HI(I)
 34   CONI=CONI+DX(I)*(WW(I)+WW(I-1))
      CONI=CONI/2.0
      CONO=CONI
C
CCC   ***   IS THERE A WATER TABLE INITIALLY ?   ***
CCC         IF THERE IS KEEP IN MIND
C
      IF(HI(NODX).LT.0.0) GO TO 20
      CALL TABLE(HI,DX,XX,NODX,WTBI,JJ)
      NTW=1
      GO TO 13
 141  WRITE(6,142) IPSW
      GO TO 143
 20   NTW=0
 13   AA=CUMT+DT
      IF(CUMT.LT.PRBE(IPC).AND.AA.GT.PRBE(IPC)) DT=PRBE(IPC)-CUMT
      IF(CUMT.LT.PEND.AND.AA.GT.PEND) DT=PEND-CUMT
      IDC=IFIX(SNGL(CUMT/24.000+1.000))
C
CC    ***   SET UP UPPER BOUNDARY CONDITIONS    ***
C
      IF(DABS(CUMT-PEND).LT.0.1D-03) GO TO 67
      IF(DABS(CUMT-PRBE(IPC)).LT.0.1D-03) GO TO 18
 15   IF(CUMT.GE.PRBE(IPC).AND.CUMT.LT.PEND) GO TO 93
      GO TO 26
 67   DT=DELT
      RFL=0.0
      RNF=0.0
      ERIN=0.0
      IPC=IPC+1
      PEND=PRBE(IPC)+PRDU(IPC)
 27   ISC=0
 26   AA=CUMT+DT
      IF(IDPF.EQ.0) GO TO 115
      IAM=IFIX(SNGL((AA+TMLG)/12.000))
      ICM=IFIX(SNGL((CUMT+TMLG)/12.000))
      IF(ICM.EQ.IAM) GO TO 110
      MRR=0
      SDT=DT
      DT=DFLOAT(IAM*12)
      DT=DT-CUMT-TMLG
 110  IF(((ICM/2)*2).EQ.ICM) GO TO 112
      IF(MRR.EQ.1) GO TO 93
      GO TO 111
 115  BB=DFLOAT(IDC*24)
      IF(AA.LE.BB) GO TO 112
      ICM=IAM+5
      SDT=DT
      DT=BB-CUMT
 112  CALL EVAPO(PTRT,PEVP,HI,HE,SINK,RDF,EVP,TRP,IDC,NRDE,ALFA,DLX)
      GO TO 93
 18   ISC=1
      DT=DELT
      RFL=PRIN(IPC)*COIN
      ERIN=RFL
      IF(RFL.GE.SATK) GO TO 66
      CALL INTER(COND,RFL,NTAB,NH,NL)
      HA=(RFL-COND(NL))/(COND(NH)-COND(NL))
      HWTT=(PRES(NH)-PRES(NL))*HA+PRES(NL)
 66   HWTT=HWET
 111  TRP=0.0
      EVP=0.0
      ETP=0.0
      MRR=1
      DO 28 I=1,NRDE
 28   SINK(I)=0.0
C
CCCC  ***   CALCULATE SOIL WATER CAPACITIES AT EACH    ***
C     ***   AND HYDRAULIC CONDUCTIVITIES BETWEEN EACH
C     ***   SUCCESSIEVE NODAL POINTS
```

```
C
 93   I=1
 132  HA=HI(I)
      CALL HYDC(HA,PRES,COND,BF,NTAB,SATK,NH,NL)
      CALL SWCAP(HA,CM,PRES,DELW,NTAB,NH,NL)
      IF(I.EQ.2) GO TO 131
      I=2
      CB=CM
      BB=BF
      GO TO 132
 131  BBB(I-1)=(BF+BB)/2.0
      BB=BF
      DO 74 I=3,NODX
      HA=HI(I)
      CALL HYDC(HA,PRES,COND,BF,NTAB,SATK,NH,NL)
      CALL SWCAP(HA,CF,PRES,DELW,NTAB,NH,NL)
      BBB(I-1)=(BF+BB)/2.0
      CC(I-1)=(CB*DX(I-1)+CF*DX(I))/(4.0*DLX(I-1))+0.75*CM
      BB=BF
      CB=CM
      CM=CF
 74   CONTINUE
C
CC    ***   NOW MAIN TRIDIAGONAL MATRIX BODY CAN BE SET UP   ***
CC          AND SOLVED OF COURSE
C
 63   CALL SOLVE(BBB,CC,HI,HF,DX,DLX,DT,SINK,EVP,ERIN,BFLUX,OMGA,
     1OMGB,NODX,NRDF,LRDF,ISC,IBC,NA,NB)
C
CC         C. NOW CECK BUNDARY CONDITIONS
C
      IF(ISC.EQ.0.OR.ISC.EQ.4) GO TO 49
      IF(ISC.EQ.2) GO TO 73
      HF(1)=HF(2)+(OMGB*(HI(2)-HI(1))+DX(2)*(ERIN-BBB(1))/BBB(1))/OMGA
      IF(HF(1).LE.HWTT.OR.HI(1).GE.HWTT) GO TO 69
      IF(HF(2).GE.HF(1)) GO TO 62
      HF(1)=HWTT
      DO 140 I=2,NODX
      IF(HF(I).LE.HWTT.OR.HI(I).GE.HWTT) GO TO 69
 140  HF(I)=HWTT
      GO TO 69
 62   IF(HF(1).LE.HWET) GO TO 69
      ISC=2
      HI(1)=HWET
      HF(1)=HWET
      GO TO 69
 49   HF(1)=HF(2)+(OMGB*(HI(2)-HI(1))-DX(2)*(EVP+BBB(1))/BBB(1))/OMGA
      GO TO 69
 73   ERIN=-BBB(1)*(OMGA*(HF(2)-HF(1))+OMGB*(HI(2)-HI(1))-DX(2))/DX(2)
 69   IF(IBC.EQ.0) GO TO 19
      HF(NODX)=HF(NA)-(OMGB*(HI(NODX)-HI(NA))+DX(NODX)*(BFLX-BBB(NA)))
     1BBB(NA)
      GO TO 91
 19   BFLX=-BBB(NA)*(OMGA*(HF(NODX)-HF(NA))+OMGB*(HI(NODX)-HI(NA))-
     1DX(NODX))/DX(NODX)
 91   CONTINUE
C
CC    ***   CALCULATE MOISTURE CONTENDS AT THE END OF TIME STEP   ***
CC    ***  IF NECCESSARY   ***
C
      CALL MOIST(HF,HWET,PRES,WF,TETA,DELW,PORE,NODX,NTAB)
      CONF=0.0
      DO 53 I=2,NODX
 53   CONF=CONF+(WF(I)+WF(I-1))*DX(I)
      IF(ITER.EQ.0.AND.ISC.EQ.0) GO TO 127
      CONF=CONF/2.0
      STCH=CONF-CONI
      ADLS=(ERIN-EVP-TRP-BFLX)*DT
      SERR=100.0*(STCH-ADLS)/(CONI+ADLS)
      IF(DABS(SERR).LE.TOL.OR.ITER.GT.2) GO TO 92
 127  ITER=ITER+1
      I=1
 135  HA=HF(I)
      CALL HYDC(HA,PRES,COND,BF,NTAB,SATK,NH,NL)
      IF(DABS(WF(I)-WW(I)).LT.0.01) GO TO 139
      CM=(WF(I)-WW(I))/(HF(I)-HI(I))
      GO TO 126
 139  CALL SWCAP(HA,CM,PRES,DELW,NTAB,NH,NL)
 126  IF(I.EQ.2) GO TO 134
      I=2
      CB=CM
      BB=BF
      GO TO 135
 134  BBB(I-1)=(BF+BB)/2.0
      BB=BF
```

```
      DO 136 I=3,NODX
      HA=HF(I)
      CALL HYDC(HA,PRES,COND,BF,NTAB,SATK,NH,NL)
      IF(DABS(WF(I)-WW(I)).LT.0.01) GO TO 137
      CF=(WF(I)-WW(I))/(HF(I)-HI(I))
      GO TO 138
  137 CALL SWCAP(HA,CF,PRES,DELW,NTAB,NH,NL)
  138 BRB(I-1)=(BF+BB)/2.0
      CC(I-1)=(CB*DX(I-1)+CF*DX(I))/(4.0*DLX(I-1))+0.75*CM
      BB=BF
      CB=CM
      CM=CF
  136 CONTINUE
      IF(ISC.EQ.0.AND.((ICM/2)*2).EQ.ICM)
     1CALL EVAPO(PTRT,PEVP,HI,HF,SINK,PDF,EVP,TRP,IDC,NRDF,ALFA,DLX)
      GO TO 63
   92 CUMT=CUMT+DT
C
C     ***   IS THERE A WATER TABLE AT THE END OF THIS TIME STEP?   ***
C           IF THERE IS OR THERE WAS AT THE BEGINNING OF
C           THIS TIME STEP CALCULATE RATE OF RECHARGE
C
      IF(HF(NODX).LT.0.0.AND.NTW.EQ.0) GO TO 81
      IF(HF(NODX).LT.0.0) GO TO 80
      CALL TABLE(HF,DX,XX,NODX,WTBF,JJ)
      IF(NTW.EQ.1) GO TO 84
      RCH=(XX(NODX)-WTBF)*EPOR/DT
      NTW=1
      WTBI=WTBF
      GO TO 83
   84 RCH=(WTBI-WTBF)*EPOR/DT
      WTBI=WTBF
      GO TO 83
   80 RCH=(WTBI-XX(NODX))*EPOR/DT
      NTW=0
      GO TO 83
   81 RCH=0.0
C
C     ***   CALCULATE RATE OF INFILTRATION AND RUNOFF   ***
C           THEN ALSO CALCULATE CUMULATIVE EVAPORATION
C           TRANSPIRATION INFILTRATION RUNOFF AND RECHARGE
C
   83 CRCH=CRCH+RCH*DT
   85 IF(ISC.EQ.0) GO TO 70
      IF(ISC.EQ.1) GO TO 71
      CRFL=CRFL+ERIN*DT
      RNF=RFL-ERIN
      CRNF=CRNF+RNF*DT
      GO TO 72
   70 CEVP=CEVP+EVP*DT
      CTRP=CTRP+TRP*DT
      ETP=TRP+EVP
      CETP=CETP+ETP*DT
      GO TO 72
   71 CRFL=CRFL+ERIN*DT
      RNF=RFL-ERIN
      CRNF=CRNF+RNF*DT
   72 CBFL=CBFL+BFLX*DT
      IF(NTW.EQ.1) GO TO 68
      WRITE(6,43) CUMT,RCH,CRCH,SERR,CRFL,CONI,CRNF,TRP,CTRP,EVP,CEVP,
     1ETP,CETP
      GO TO 75
   68 WRITE(6,43) CUMT,RCH,CRCH,SERR,CRFL,CONI,CRNF,TRP,CTRP,EVP,CEVP,
     1ETP,CETP,WTBF
   75 I=CUMT/DPRN
      IF(DT.GT.DPRN.OR.CUMT.GT.DRUN.OR.ITC.NE.0.OR.I.GE.NPRC) GO TO 52
      GO TO 94
   52 NPRC=I+1
      WRITE(6,64) CUMT
      JHI=4*JTO
      DO 60 I=1,JTO,LINE
      JHI=JHI+LINE
      IF(JHI.GT.NODX) JHI=JHI-JTO
   60 WRITE(6,61) (XX(JJJ),WF(JJJ),HF(JJJ),JJJ=I,JHI,JTO)
      WRITE(6,95)
   94 IF(CUMT.GT.DRUN.OR.(LEFTIM(DUMMY)/100.0).LT.30.0) GO TO 86
      IF(ICM.NE.IAM) DT=SDT
      IF(ITER.GT.2.AND.DT.GT.DELT) DT=DT/CDT**5
      ITER=0
      CONI=CONF
      DO 39 I=1,NODX
      WW(I)=WF(I)
   39 HI(I)=HF(I)
```

```
      DT=DT*CDT
      IF(DT.GT.12.0D0) DT=12.0D0
      GO TO 13
86    OVALE=(CONF-CONO-CPFL+CETP)*100.0/(CONO+CRFL-CETP)
      WRITE(6,150) OVALE
10    FORMAT(14I5)
11    FORMAT(7D10.4)
21    FORMAT(1H1///33H          CLIMATOLOGICAL INFORMATION//52H NTH    PETP
     1    PSVP       NTH    START     DRTN    INTEN/52H DAY  CM/DY    CM/DY
     2   RAIN    AT HR      HR     CM/HR)
23    FORMAT(I4,2F8.4,4X,I4,2F8.2,F8.4)
24    FORMAT(///4X,7H NODX =,I4,9X,7H PORE =,F7.4/4X,7H NOAT =,I4,9X
     1,7H WRES =,F7.4/4X,7H NPPP =,I4,9X,7H PLA  =,F7.4/4X,7H IDC  =,I4,
     29X,7H PNA  =,F7.4/4X,7H DELT =,F5.2,3H HR,5X,7H DPR  =,F9.4,3H CM/
     34X,7H CDT  =,F8.5,3H HR,9H   HWET =,F7.4,3H CM/4X,7H DPRN =,F5.2,
     43H HR,5X,7H SATK =,F6.2,6H CM/HR/4X,7H DPUN =,F6.0,3H HR,4X,7H BFL
     5X =,F5.2,6H CM/HR/4X,7H INTR =,F5.2,8X,7H ALFA =,D11.4)
31    FORMAT(1H1//39X,49H INITIAL CONDITION AND ROOT DISTRIBUTION FUNCTI
     1ON//5(26H   DEPTH    TETA     ROFX   )/6H     CM,4(23X,3H CM))
33    FORMAT(5(F8.1,2F8.4,2X))
41    FORMAT(1H1///23H          SOIL PROPERTIES//
     128H   TETA   POTENTIAL     HYD CON/27H     %          CM          CM/HR)
43    FORMAT(F6.2,2D12.4)
46    FORMAT(F10.3,11D11.3/10X,11D11.3/10X,11D11.3)
48    FORMAT(0PF9.2,1P2D10.2,1P11D9.2)
61    FORMAT(5(0PF8.1,F7.4,1PD11.3))
64    FORMAT(//39X,50H MOISTURE CONTENT AND WATER POTENTIAL DISTRIBUTION
     1/55X,3H AT,F8.2,7HTH HOUR/5(26H   DEPTH    WF         HF     )/
     25(26H     CM                CM     ))
78    FORMAT(/5X,21H TOTAL STORAGE CHANGE,F9.2,3H CM,10X,
     114H TOTAL LEAKEGE,F9.2,3H CM//)
95    FORMAT(/126H      CUMT     RECH       CRCH      SERR      CERN      RUNF
     1      CRNF       TRNP       CTRP      EVPR      CEVP      ETPR      CETP
     2   WTBL)
121   FORMAT(5X,67H THE SOLUTION DID NOT CONVERGE TO DESIRED ACCURACY IN
     1 30 ITERATIONS/5X,28H REDUCE YOUR SPACE INCREMENT)
650   FORMAT(I5,1P7D14.6/5X,1P8D14.6)
142   FORMAT(5X,' PROGRAM CHECK AT: ',Z8,Z8)
150   FORMAT(10X,25H OVERALL PERCENT ERROR IS,F6.2)
143   STOP
      END




      SUBROUTINE POTH(WW,TETA,DELW,HI,PRES,NODX)
      IMPLICIT REAL*8 (A-H,O-Z)
      DIMENSION WW(1000),HI(1000),TETA(100),PRES(100)
      DO 34 I=1,NODX
      J=(WW(I)-TETA(1))/DELW+1.0
      HI(I)=(PRES(J+1)-PRES(J))*(WW(I)-TETA(J))/DELW+PRES(J)
34    CONTINUE

      RETURN
      END




      SUBROUTINE MOIST(HF,HWET,PRES,WF,TETA,DELW,PORE,NODX,NTAB)
      IMPLICIT REAL*8 (A-H,O-Z)
      DIMENSION HF(1000),WF(1000),PRES(100),TETA(100)
      DO 53 I=1,NODX
      IF(HF(I).GE.HWET) GO TO 57
      IF(HF(I).LT.PRES(1)) GO TO 55
      HA=HF(I)
      CALL INTER(PRES,HA,NTAB,NH,NL)
      WF(I)=DELW*(HF(I)-PRES(NL))/(PRES(NH)-PRES(NL))+TETA(NL)
      GO TO 53
57    WF(I)=PORE
53    CONTINUE
      RETURN
55    WRITE(6,58) I
58    FORMAT('PRESURE AT THE NODE ',I2,' BELOW SATURATION')
      STOP
      END
```

```
      SUBROUTINE TABLE(HH,DX,XX,NODX,WTBI,J)
      IMPLICIT REAL*8 (A-H,O-Z)
      DIMENSION HH(100),DX(100),XX(100)
      DO 10 I=2,NODX
      J=NODX-I+1
      IF(HH(J)) 18,17,10
10    CONTINUE
      WTBI=XX(1)
      GO TO 24
18    WTBI=-DX(J+1)*HH(J)/(HH(J+1)-HH(J))+XX(J)
      GO TO 24
17    WTBI=XX(J)
24    RETURN
      END



      SUBROUTINE SOLVE(BB,CC,HI,HF,DX,DLX,DT,SINK,AEV,FLUX,BFLUX,OMGA,
     1OMGB,NODX,NPRP,MPRP,ISC,IBC,NA,NB)
      IMPLICIT REAL*8 (A-H,O-Z)
      DIMENSION BB(1000),CC(1000),DX(1000),DLX(1000),SINK(100),
     1HI(1000),HF(1000),EE(1000),FF(1000)
      INTEGER IPSW(2)
      CALL IFPCK(&141,IPSW)
      AKRB=2.0*BB(1)*DT/(DX(2)*DLX(2))
      AKRF=2.0*BB(2)*DT/(DX(3)*DLX(2))
      IF(ISC.EQ.0) GO TO 34
      IF(ISC.EQ.2) GO TO 77
      ER=AKRF*(OMGB*(HI(3)-HI(2))-DX(3))+2.0*DT*FLUX/DLX(2)+CC(2)*HI(2)-
     1SINK(2)*DT
      EL=OMGA*AKRF+CC(2)
      GO TO 35
34    ER=AKRF*(OMGB*(HI(3)-HI(2))-DX(3))-2.0*DT*AEV/DLX(2)+CC(2)*HI(2)-
     1SINK(2)*DT
      EL=OMGA*AKRF+CC(2)
      GO TO 35
141   WRITE(6,142) IPSW
142   FORMAT(5X,' PROGRAM CHECK AT: ',Z8,Z8)
      STOP
77    ER=AKRF*(OMGB*(HI(3)-HI(2))-DX(3))-AKRB*(OMGB*HI(2)-HI(1)-DX(2))+
     1CC(2)*HI(2)-SINK(2)*DT
      EL=OMGA*(AKRB+AKRF)+CC(2)
35    EE(2)=AKRF/EL
      FF(2)=ER/EL
      DO 36 I=3,NPRP
      AKRB=2.0*BB(I-1)*DT/(DX(I)*DLX(I))
      AKRF=2.0*BB(I)*DT/(DX(I+1)*DLX(I))
      ER=AKRF*(OMGB*(HI(I+1)-HI(I))-DX(I+1))-
     1AKRB*(OMGB*(HI(I)-HI(I-1))-DX(I))+CC(I)*HI(I)-SINK(I)*DT
      EL=OMGA*(AKRB+AKRF)+CC(I)
      EE(I)=OMGA*AKRF/(EL-AKRB*OMGA*EE(I-1))
      FF(I)=(ER+OMGA*AKRB*FF(I-1))/(EL-OMGA*AKRB*EE(I-1))
36    CONTINUE
      DO 42 I=MPRP,NB
      AKRB=2.0*BB(I-1)*DT/(DX(I)*DLX(I))
      AKRF=2.0*BB(I)*DT/(DX(I+1)*DLX(I))
      ER=AKRF*(OMGB*(HI(I+1)-HI(I))-DX(I+1))-
     1AKRB*(OMGB*(HI(I)-HI(I-1))-DX(I))+CC(I)*HI(I)
      EL=OMGA*(AKRB+AKRF)+CC(I)
      EE(I)=OMGA*AKRF/(EL-AKRB*OMGA*EE(I-1))
      FF(I)=(ER+OMGA*AKRB*FF(I-1))/(EL-OMGA*AKRB*EE(I-1))
42    CONTINUE
      AKRB=2.0*BB(NB)*DT/(DX(NA)*DLX(NA))
      AKRF=2.0*BB(NA)*DT/(DX(NODX)*DLX(NA))
      IF(IBC.EQ.0) GO TO 33
      ER=-2.0*DT*BFLUX/DLX(NA)-AKRB*(OMGB*(HI(NA)-HI(NB))-DX(NA))+
     1CC(NA)*HI(NA)
      EL=OMGA*AKRB+CC(NA)
      GO TO 38
33    ER=AKRF*(HI(NODX)-OMGB*HI(NA)-DX(NODX))-
     1AKRB*(OMGB*(HI(NA)-HI(NB))-DX(NA))+CC(NA)*HI(NA)
      EL=OMGA*(AKRF+AKRB)+CC(NA)
38    HF(NA)=(ER+OMGA*AKRB*FF(NB))/(EL-OMGA*AKRB*EE(NB))
37    HF(I)=FF(I)+EE(I)*HF(I+1)
      I=I-1
      IF(I.GT.1) GO TO 37
      RETURN

      END
```

```
      SUBROUTINE SWCAP(HA,CC,PPES,DELW,NTAB,NH,NL)
      IMPLICIT REAL*8 (A-H,O-Z)
      DIMENSION PRES(100)
      IF(HA.GE.0.0) GO TO 76
      CC=DELW/(PRES(NH)-PRES(NL))
      GO TO 29
76    CC=0.0
29    RETURN
      END



      SUBROUTINE HYDC(HA,PRES,COND,BB,NTAB,SATK,NH,NL)
      IMPLICIT REAL*8 (A-H,O-Z)
      DIMENSION PRES(100),COND(100)
      IF(HA.GE.0.0) GO TO 10
      CALL INTER(PRES,HA,NTAB,NH,NL)
      BB=(COND(NH)-COND(NL))*(HA-PRES(NL))/
     1(PRES(NH)-PRES(NL))+COND(NL)
      GO TO 20
10    BB=SATK
20    RETURN
      END



      SUBROUTINE INTER(YY,YF,NTAB,NH,NL)
      IMPLICIT REAL*8 (A-H,O-Z)
      DIMENSION YY(100)
      NH=NTAB
      NL=1
58    J=(NH+NL)/2
      IF(YF-YY(J)) 55,56,57
55    NH=J
      IF(NH-NL-1) 58,59,58
57    NL=J
      IF(NH-NL-1) 58,59,58
56    NL=J
      NH=J+1
59    RETURN
      END
```

```
      SUBROUTINE EVAPO(PTRT,PEVP,HI,HF,SINK,RDF,EVP,TRP,IDC,NRDF,ALFA,
     1DLX)
      IMPLICIT REAL*8 (A-H,O-Z)
      DIMENSION PTRT(100),PEVP(100),SINK(100),RDF(100),HI(1000),
     1HF(1000),DLX(1000)
      INTEGER IPSW(2)
      CALL IEPCK(&141,IPSW)
      AA=-PTRT(IDC)/ALFA
      HA=(HI(1)+HF(1))/2.0
      IF(HA.GE.0.0) GO TO 82
      ALF=AA*HA**2
      IF(HA.LT.-20000.0.OR.ALF.LT.-160.0) GO TO 86
      SINK(1)=DEXP(ALF)*PTRT(IDC)*RDF(2)
      GO TO 87
141   WRITE(6,142) IPSW
142   FORMAT(5X,' PROGRAM CHECK AT: ',Z8,Z8)
      STOP
86    SINK(1)=0.0
87    ALF=-PEVP(IDC)*HA**2/ALFA
      IF(ALF.LT.-160.0) GO TO 88
      EVP=(DEXP(ALF)*PEVP(IDC)+SINK(1)/2.0)/24.0
      GO TO 89
88    EVP=SINK(1)/48.0
      GO TO 89
82    EVP=(PTRT(IDC)*RDF(2)/2.0+PEVP(IDC))/24.0
89    TRP=0.0
      DO 38 I=2,NRDF
      HA=(HI(I)+HF(I))/2.0
      IF(HA.GE.0.0) GO TO 98
      ALF=AA*HA**2
      IF(HA.LT.-20000.0.OR.ALF.LT.-160.0) GO TO 99
      TT=DEXP(ALF)*PTRT(IDC)*(RDF(I)+RDF(I+1))/24.0
      GO TO 14
99    TT=0.0
      GO TO 14
98    TT=PTRT(IDC)*(RDF(I)+RDF(I+1))/24.0
14    TRP=TRP+TT
      SINK(I)=TT/DLX(I)
38    CONTINUE
      TRP=TRP/2.0
      RETURN
        END
```

This dissertation is accepted on behalf of the faculty of the Institute by the following committee:

Lynn W. Gelhar
Adviser

P. Huyakorn

V. L. Fore

12/19/77
Date